

## Development of Potent Mcl-1 Inhibitors: Structural Investigations on Macrocycles Originating from a DNA-Encoded Chemical Library Screen

Koen F. W. Hekking,\* Sergio Maroto, Kees van Kekem, Frank S. Haasjes, Jack C. Slootweg, Patrick G. B. Oude Alink, Ron Dirks, Malvika Sardana, Marjon G. Bolster, Brian Kuijpers, Dennis Smith, Robin Doodeman, Marcel Scheepstra, Birgit Zech, Mark Mulvihill, Louis M. Renzetti, Lee Babiss, Paolo A. Centrella, Matthew A. Clark, John W. Cuozzo, Marie-Aude Guié, Eric Sigel, Sevan Habeshian, Christopher D. Hupp, Julie Liu, Heather A. Thomson, Ying Zhang, Anthony D. Keefe,\* Gerhard Müller, and Stijn Gremmen



Cite This: <https://doi.org/10.1021/acs.jmedchem.3c02206>



Read Online

ACCESS |



Metrics & More

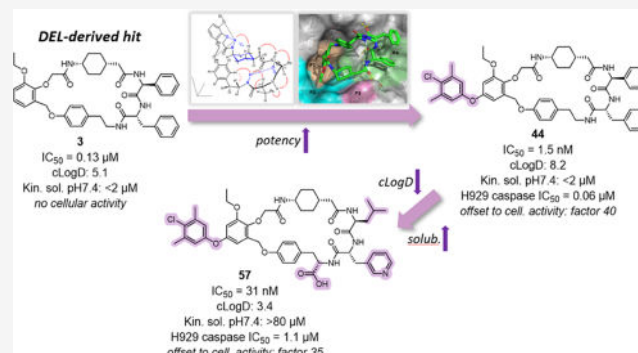


Article Recommendations



Supporting Information

**ABSTRACT:** Evasion of apoptosis is critical for the development and growth of tumors. The pro-survival protein myeloid cell leukemia 1 (Mcl-1) is an antiapoptotic member of the Bcl-2 family, associated with tumor aggressiveness, poor survival, and drug resistance. Development of Mcl-1 inhibitors implies blocking of protein–protein interactions, generally requiring a lengthy optimization process of large, complex molecules. Herein, we describe the use of DNA-encoded chemical library synthesis and screening to directly generate complex, yet conformationally privileged macrocyclic hits that serve as Mcl-1 inhibitors. By applying a conceptual combination of conformational analysis and structure-based design in combination with a robust synthetic platform allowing rapid analoging, we optimized *in vitro* potency of a lead series into the low nanomolar regime. Additionally, we demonstrate fine-tuning of the physicochemical properties of the macrocyclic compounds, resulting in the identification of lead candidates **57**/**59** with a balanced profile, which are suitable for future development toward therapeutic use.



## INTRODUCTION

Apoptosis is a highly conserved form of programmed cell death and constitutes an essential process for the elimination of dispensable and potentially dangerous cells.<sup>1,2</sup> The intrinsic apoptotic pathway is predominantly controlled by the B-cell lymphoma 2 (Bcl-2) family of proteins, which includes both antiapoptotic (e.g., Bcl-2, Bcl-xl, Mcl-1, Bcl-w) and pro-apoptotic members (e.g., BAK, BAX, BIM, BID). The dynamic interplay between these two subfamilies is essential in maintaining the apoptotic equilibrium of cells, with the  $\alpha$ -helical BH3 domain of pro-apoptotic proteins binding to a helix-shaped groove on the surface of their antiapoptotic counterparts.<sup>3</sup> In detail, cellular stress results in upregulation of BH3-only pro-apoptotic Bcl-2 proteins (e.g., BIM, BID), which associate with antiapoptotic family members preventing those from deactivating pro-apoptotic effectors (e.g., BAK, BAX), thereby driving apoptosis. Evasion of apoptosis is known to be a critical element of the development and expansion of tumors, and additionally influences resistance to diverse anticancer treatments.<sup>4</sup> To this purpose, cancer cells highly express pro-

survival members of the Bcl-2 family, and their expression has been shown to be essential, making them promising targets for cancer treatment.<sup>5,6</sup> The druggability of this class of proteins, and the potential of direct apoptosis activation as a therapeutic approach, was demonstrated by the landmark approval of the selective Bcl-2 inhibitor Venetoclax for chronic lymphocytic leukemia (CLL) in 2016.<sup>7,8</sup> Among the other antiapoptotic family members, myeloid cell leukemia differentiation protein 1 (Mcl-1) is known to act as a master regulator of apoptosis in various human tumor types.<sup>9–11</sup> Overexpression of Mcl-1 has been broadly observed in both hematological cancers<sup>12,13</sup> and solid tumors, including non-small-cell lung cancer (NSCLC)<sup>14</sup>

**Received:** November 24, 2023

**Revised:** January 12, 2024

**Accepted:** January 18, 2024



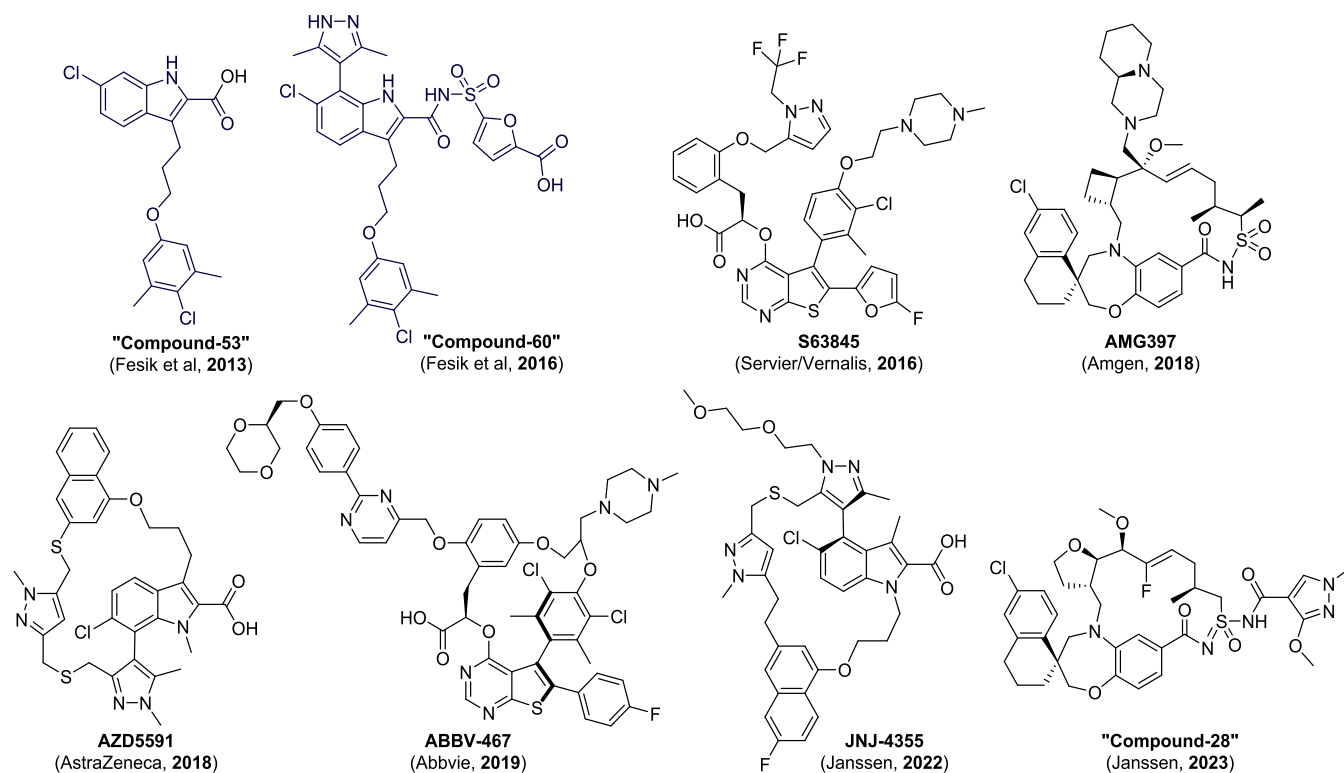


**Figure 1.** Structures of representative Mcl-1 inhibitors from different structural classes.

and breast cancer.<sup>15,16</sup> Additionally, there is evidence that Mcl-1 expression is associated with cancer relapse and drug resistance caused by, for instance, the Bcl-2 inhibitor Venetoclax.<sup>17,18</sup>

Over the past 5–10 years, a variety of potent and selective Mcl-1 inhibitors have been disclosed in the (patent) literature, some compounds reaching clinical development,<sup>19–22</sup> albeit with mixed results and certain toxicity concerns.<sup>23,24</sup> Appreciating the fact that inhibition of Mcl-1 function requires interrupting a protein–protein interaction, most of the developed inhibitors are reasonably large molecules, with many properties such as Log *P*, PSA, and MW being in the “non-Lipinski” beyond-Rule-of-Five (bRo5) area.<sup>25,26</sup> Figure 1 illustrates the chemical space of these elaborate molecules, showing a representative selection of inhibitors reported over the past decade.

The development of pharmaceutically relevant molecules was preceded by the pioneering work from the lab of Fesik, involving fragment-based drug discovery, more specifically fragment linking.<sup>27–29</sup> Initial investigations led to a potent indole carboxylic acid derivative (“Compound 53”, Figure 1), the cocrystal structure of which provided important insights into druggable pockets of the Mcl-1 protein.<sup>27</sup> Further optimization by the same group was carried out by performing a fragment screen, while saturating the primary binding site of the protein with the original compound. The resulting hits, consequently binding to other subpockets of the target protein, were subjected to a fragment-linking approach keeping the original indole scaffold. This resulted in more complex structures (e.g., “Compound-60”, Figure 1), with increased potency and improved selectivity over other members of the Bcl-2 family.<sup>29</sup>

In 2016, Servier and Vernalis reported on a compound class based on a thienopyrimidine scaffold (e.g., S63845, Figure 1).

These molecules were originally discovered by fragment screening and further optimized through several rounds of SBDD. Compound S63845 (Figure 1) was proven to be effective in a range of preclinical tumor models upon IV administration.<sup>30,31</sup> Follow-up work yielded compound S64315, which entered Phase I/II clinical development.<sup>32</sup>

Since 2017/2018, several macrocyclic inhibitors have emerged, based on several different core scaffolds. Amgen claimed a class of macrocycles based on the known thienopyrimidine scaffold, with lead compound ABBV-467 entering clinical trials in 2019.<sup>23,33</sup> AstraZeneca published AZD5991 (Figure 1), which was rationally designed from the known, open-chain indole carboxylic acid scaffold by subsequent macrocyclization.<sup>34</sup> Around the same time, Amgen reported a novel class of macrocycles containing a spirocyclic tetrahydronaphthalene moiety (e.g., AMG397, Figure 1).<sup>35,36</sup> These compounds originated from a fragment-based lead generation approach, followed by macrocyclization at a later stage. In 2020/2021, similar tetrahydronaphthalene-containing macrocyclic inhibitors were disclosed by both Gilead and Prelude Therapeutics, however with distinct differences in either the backbone structure or the decoration pattern.<sup>37,38</sup> Finally, linear DNA-encoded chemical library (DEL)-based screening hits that were subsequently macrocyclized have been described AstraZeneca and X-Chem in 2017.<sup>39</sup> Very recently, Janssen published their extensive work on two macrocyclic inhibitor series, based on the previously described indole carboxylic acid<sup>40,41</sup> and spirocyclic tetrahydronaphthalene<sup>42</sup> cores, exemplified by JNJ-4355 and “Compound 28” in Figure 1, respectively.

The large, mostly macrocyclic, compounds from Figure 1 are associated with many apparent challenges in both hit finding and hit evolution. All compounds were eventually developed from smaller, noncyclic molecules, requiring extensive

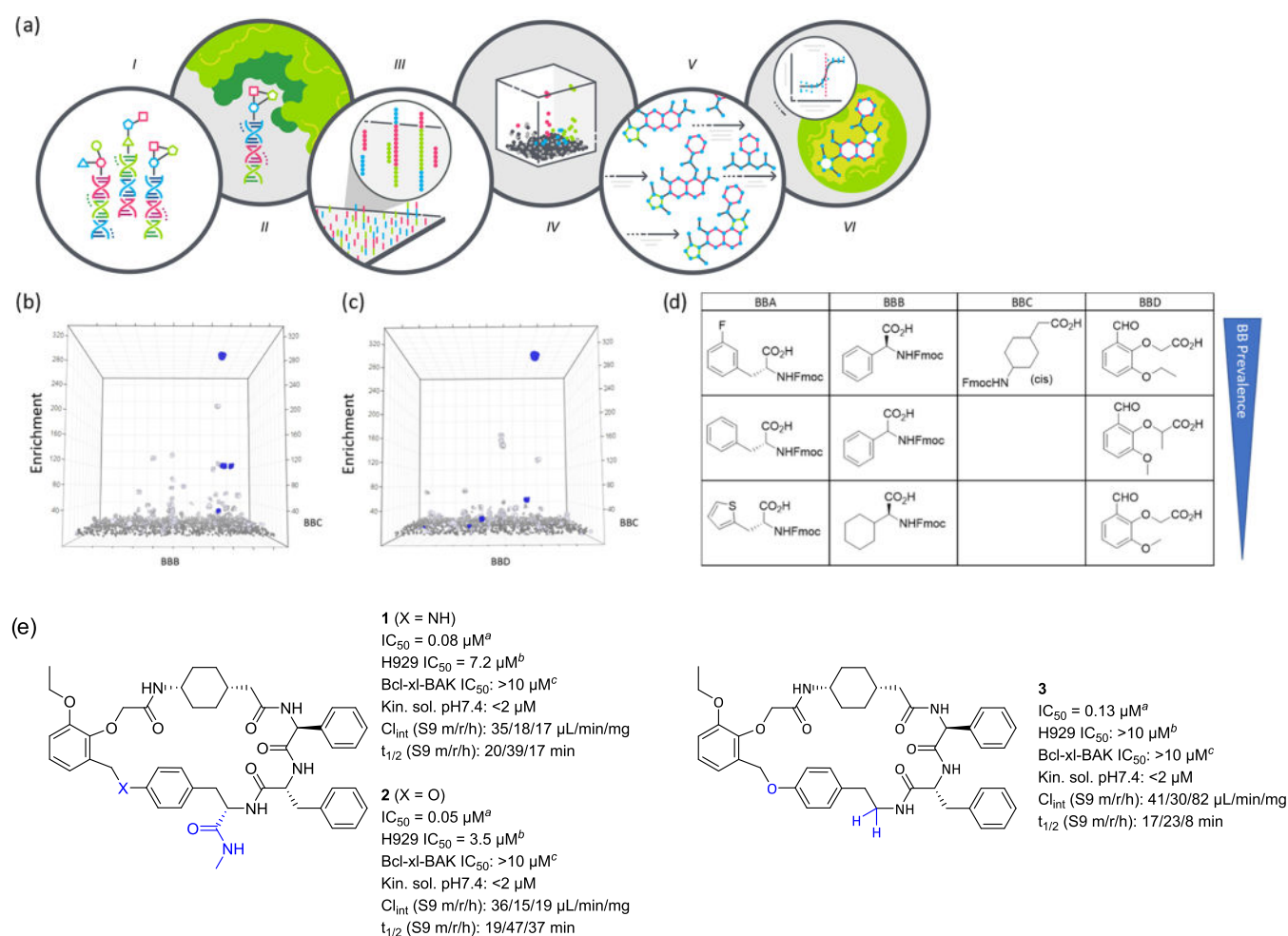


**Figure 2.** Selection output data used to discover individual DNA-Encoded Chemical Library Hits: (a) workflow representation, I: design and synthesis of DNA-encoded libraries, II: enrichment for selective binders via affinity screening, III: characterization of selection output using deep sequencing of DNA tags, IV: identification of enriched library compounds through statistical analysis, V: synthesis of representative label-free compounds, VI: assay of compounds and identification of leads; (b, c) enrichment data for individual building block pairs enriched within the 4-cycle macrocycle library against 16.6  $\mu\text{M}$  Mcl-1 (172–327). Blue clusters represent the family of compounds containing the hit; (d) “SAR” data as manifested in the selection output for the family of compounds containing the hit in which the prevalence of coenriched variable building blocks is shown at each of the four cycles of chemistry; (e) label-free hit compounds that were used to establish the series here; <sup>a</sup>IC<sub>50</sub> values determined in an Mcl-1-BAK time-resolved fluorescence resonance energy transfer (TR-FRET) assay; <sup>b</sup>IC<sub>50</sub> values determined in a Bcl-xl-BAK TR-FRET assay.

optimization processes, typical for macrocyclic synthesis.<sup>43,44</sup> On the other hand, directly identifying a large macrocyclic hit molecule from a screening campaign requires exceptionally large and diverse libraries, typically only offered by DNA-encoded chemical libraries (DEL).<sup>45–47</sup> Given our experience in optimizing hits from DEL compounds,<sup>48,49</sup> in combination with the availability of X-Chem’s macrocyclic DELs, we decided on this approach for hit-finding. By directly generating macrocyclic hits, while at the same time setting up a robust synthetic platform for efficiently preparing numerous macrocyclic variations, we were aiming to shorten the development time for such complex drug candidates. This paper describes our efforts from hit-finding to the development of an advanced lead with improved potency and physicochemical properties, including extensive conformational analyses on the precise macrocyclic three-dimensional (3D) structure.

## RESULTS AND DISCUSSION

**DNA-Encoded Chemical Library Screening.** Figure 2a depicts the general workflow for this screening campaign. A

mixture of 21 different DNA-encoded chemical libraries was combined into the single library deck that was used to screen against Mcl-1. Each library had been synthesized individually with a distinct chemical scheme and defined set of building blocks. Each of the 95 billion compounds comprising this library deck is covalently attached to, and encoded by, a unique sequence of DNA that records its split-and-pool synthetic history and permits its identification. Among the subtypes included in this library deck was a four-cycle peptidic macrocyclic library for which the synthesis had initiated with the installation of the protected trifunctional building block, 2-amino-3-(4'-aminophenyl)-propionic acid, by acylation of it onto a 5'-amine-terminated linker-oligonucleotide conjugate. The 2-amino group was then utilized as a point of chemical diversification by the successive installation of three sets of *N*-Fmoc-amino acids, each numbering more than 300, followed by a fourth chemical cycle in which formyl acids were installed. This was followed by a macrocyclization step using reductive amination chemistry, which resulted in a library of 1.5 billion four-cycle macrocyclic compounds.

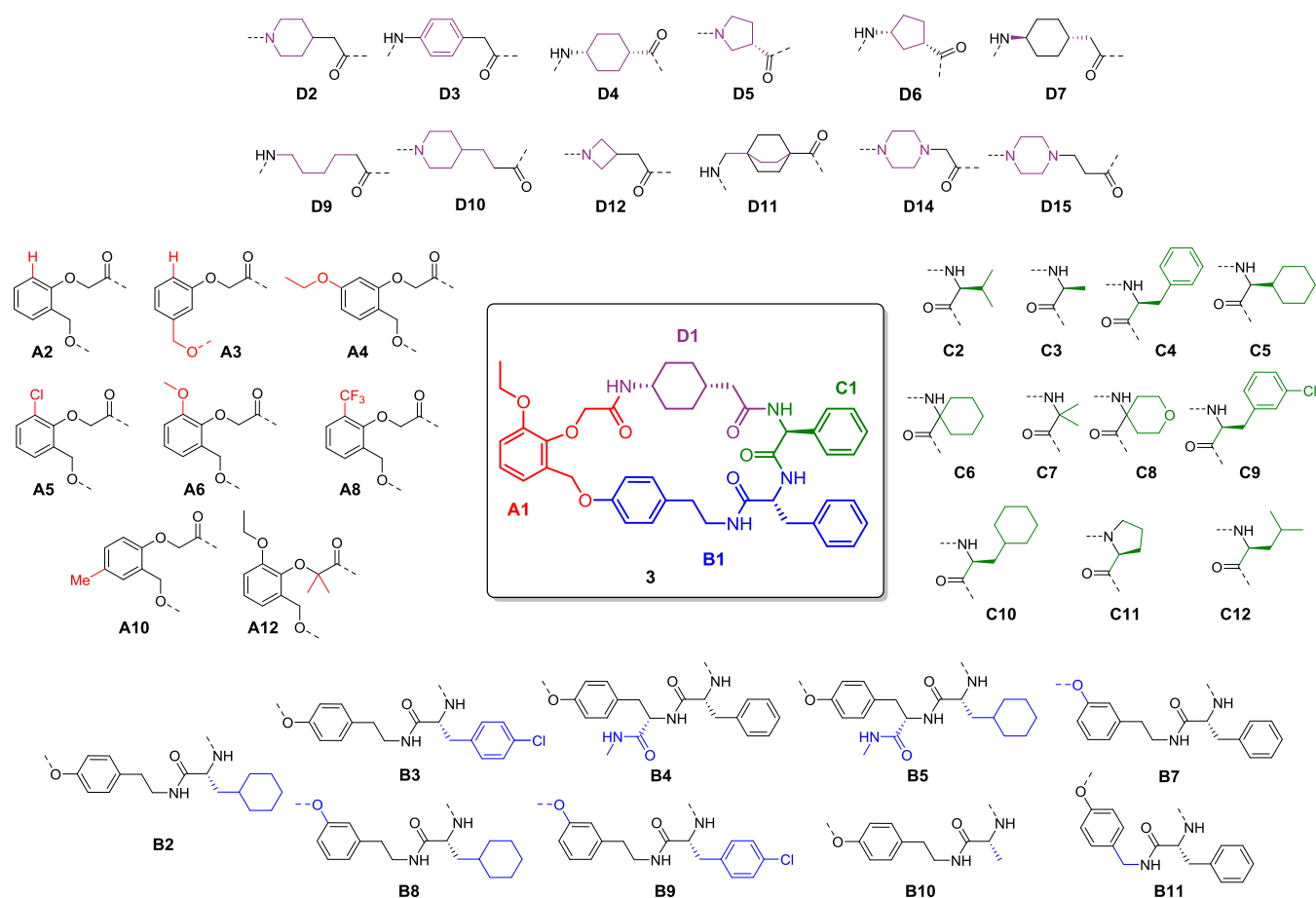


**Figure 3.** Building blocks used for all four components during combinatorial array synthesis.

Selection was initiated with the capture of a 60  $\mu$ L volume of 16.6  $\mu$ M Mcl-1 (172–327) onto a 5  $\mu$ L volume of the IMAC affinity matrix His-Select (Sigma-Aldrich, MO) entrained between two frits within a Phytip (Phynexus, CA). Uncaptured protein was washed away and then one nanomole of the library deck, dissolved in a model cytosolic buffer with additionally 1 mg/mL Sheared Salmon Sperm DNA, 0.02% Tween-20, and 1 mM DTT, was incubated with the captured target for 30 min. The matrix was then washed eight times followed by elution at 95  $^{\circ}$ C. The eluted library was subjected to a second round of selection with fresh protein to further increase the enrichment of Mcl-1 binders. A range of additional selections were conducted in parallel including Mcl-1 (172–327) with 80  $\mu$ M BIM peptide, Mcl-1 (33–327), Bcl-xl, and a no-target control (His-Select matrix only). The output of the second round of selection was PCR-amplified and submitted for Illumina sequencing. A total of 120 million single-end reads were generated across all 21 libraries and all selection conditions, averaging 1.14 million reads per library per selection condition.

Individual sequence reads were translated back into the corresponding building block and library schemes and statistical prevalence data were calculated for all building block combinations in each library across all selection conditions. Many strongly enriched building block combinations were observed across all of the libraries screened and these were identified, clustered into compound families, and profiled across all selection conditions. All of these compounds enriched against both the long and short Mcl-1 constructs and all were seen to be competitive with the BIM peptide, i.e., did

not enrich when a saturating concentration of the peptide was included in selection with Mcl-1. Most enriched compounds also enriched against the off-target Bcl-xl thereby confirming the known difficulty of finding compounds selective for Mcl-1 over Bcl-xl. Representative compounds were then prioritized for resynthesis off-DNA based on the desirability of the family SAR as it appeared in the selection output and the selectivity profile. One prioritized family was the most enriched in the macrocycle library described above. The relative enrichment levels for compounds within the selection output are shown in Figure 2b,c. These cubic plots display the building blocks present in each of two cycles of chemistry along the *x*- and *y*-axes and the enrichment of these building block pairs is plotted along the *z*-axis. The clusters in blue represent the family within which the active macrocycle (compound 1) was found. Different clusters correspond to different building block pairs, points within each cluster represent different compounds each containing the same building block pairs, i.e., are differentiated by nonplotted building blocks. The top three coenriched building blocks at each cycle within this family can be seen in Figure 2d, which shows that this family is defined by *cis*-(4-aminocyclohexyl) acetic acid at the third cycle of the library synthesis chemistry. The corresponding *trans* isomer was present in the library but did not enrich in the context of the other building blocks defining this family. The first cycle of chemistry was defined by D-phenylalanine and closely related structures, e.g., thiophene in place of phenyl, the second by L-phenylglycine and closely related structures, e.g., the corresponding racemate and the corresponding cyclohexyl



derivative and the fourth cycle by 2-(2-ethoxy-6-formylphenoxy) acetic acid and closely related structures, e.g., a methoxy derivative and the  $\alpha$ -methyl derivative. None of these building block combinations enriched against Bcl-xl. The most prevalent of the family members corresponds to the top row of Figure 2d and was enriched by approximately 50,000-fold over two rounds of affinity-mediated selection. This compound was then resynthesized off-DNA with a linker truncation point that retained the methylamide (Compound 1, Figure 2e). Compound 1 was determined to have an  $IC_{50}$  value of 80 nM for the displacement of BAK peptide binding to Mcl-1 in a TR-FRET assay. Initial follow-up compounds showed that the aniline amine could be converted into an ether and the methylamide linker stub could be removed, both resulting compounds (Figure 2e, compounds 2 and 3) were approximately equipotent with the initial hit.

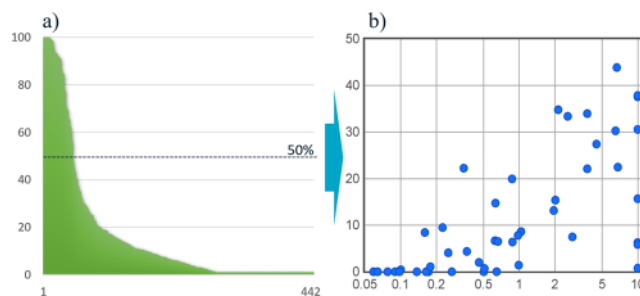
**Macrocyclic Combinatorial Array Approach.** As outlined in Figure 2e, the macrocyclic hits from the DEL screen already showed appreciable binding affinity (50–130 nM), with no detectable off-target activity against Bcl-xl, thus providing excellent starting points for further optimization. Despite their semipeptidic character, the compounds had sufficient metabolic stability for further development. Efficacy in a cellular viability assay, using H929 myeloma cells, was only moderate for 2 of the 3 hits (7.2, 3.5, and >10  $\mu$ M, respectively), and aqueous solubility was <2  $\mu$ M at pH 7.4 for all compounds. These results clearly suggested that points of improvement focus on both potency and physicochemical properties.

Because the binding mode of the compounds to the Mcl-1 protein was unknown, it was initially unclear which area of the macrocyclic molecules we needed to focus on for improvement. Structurally interrogating all areas separately would require multiple, lengthy design-make-test-analyze (DMTA) cycles to obtain sufficient useful SAR information. For this reason, we decided to continue to apply a combinatorial approach, to investigate all parts of the molecule simultaneously. The macrocyclic structure therefore needed to be dissected into fragments in a manner that would allow robust synthetic coupling procedures. Hence, four fragments were identified, while taking advantage of amide bond connections that were the same as those utilized in the synthesis of the DEL within which the hits were found. Figure 3 highlights fragments A–D, which were anticipated to represent the separate areas explicitly important for activity. Only one bond formation (A–B) did not rely on amide coupling. Detailed synthetic routes are described in the chemical synthesis paragraph (*vide infra*).

Using 3 as reference structure, we decided to limit the chosen strategy to single and double substitutions, assuming that this would provide the most essential SAR information, while maintaining a manageable array size. This limitation could theoretically yield 733 target molecules from the building blocks depicted in Figure 3. Of this set, 444 compounds were successfully synthesized, establishing an overall success rate of 61% for the entire combinatorial array. Since the original screening hits 2/3 were inherently part of the array matrix, the actual number of novel compounds was 442. It should be noted that variable amounts of epimerization of the (S)-phenylglycine in fragment C1 were observed, and in some cases, the resulting isomers were not fully removed by the parallel purification procedure. However, the isolated phenylglycine (R)-epimer was later found to be only weakly active (cmpd 18, Table 2), so the influence of epimer

contaminations on measured activity values is most likely less than the standard assay variability.

All combinatorial array compounds were submitted at a single concentration for the Mcl-1-BAK TR-FRET binding assay, the results of which are depicted in Figure 4a. The 49

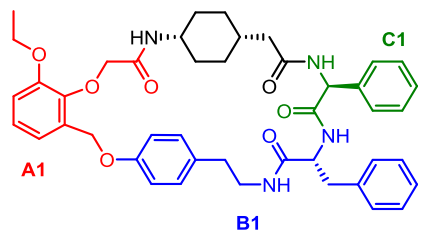


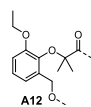
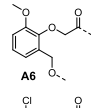
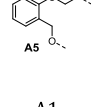
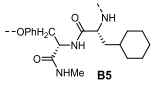
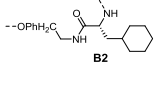
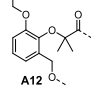
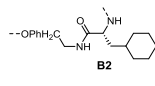
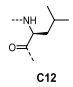
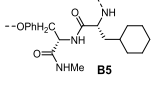
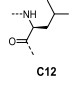
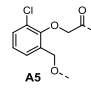
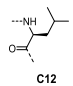
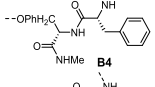
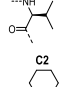
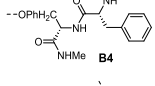
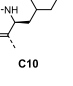
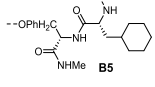
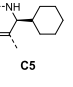
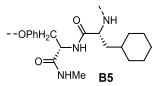
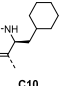
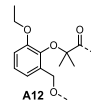
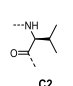
**Figure 4.** Assay results from the Mcl-1/BAK TR-FRET assay: (a) percentage inhibition at 10  $\mu$ M for the 442 new combinatorial array compounds; (b)  $IC_{50}$  values in  $\mu$ M (horizontal axis) vs percentage inhibition at 10  $\mu$ M (vertical axis) for the 49 most active compounds.

novel compounds that exhibited >50% inhibition at a 10  $\mu$ M concentration were subjected to dose–response measurement and the resulting  $IC_{50}$  values are shown in Figure 4b. The  $IC_{50}$  values were reasonably in line with percentage inhibition, with only 5 compounds classified as false positives ( $IC_{50} > 10 \mu$ M). Despite the steep SAR observed, multiple compounds exhibited activity in the range of the parent compound 3. Both single-concentration and  $IC_{50}$  values for the combinatorial array compounds can be found in the Supporting Information (Tables S1/S2). All compounds that showed an  $IC_{50}$  value lower than 300 nM are depicted in Table 1.

Several early SAR trends could be deduced from the compounds depicted in Tables 1, S1, and S2. Evidently, the ethoxy moiety in the A-fragment is not particularly crucial, since methoxy (5) and chloro (6/12) are also tolerated. Conversely, the unsubstituted A2-containing variations showed decreased activity, suggesting the need for at least some steric bulk at that position. Possibly, influencing the orientation of the *ortho* ether acetamide linker is important for stabilizing the bioactive conformation. The same explanation can also be envisioned for the fact that an  $\alpha$ -gem-dimethylacetamide has a beneficial effect (4/9 vs 3/8), perhaps by reducing the O–C–C(O) binding angle.

More variation was tolerated in the B and C regions, particularly in the peripheral substituents. This suggested that the precise backbone conformation is more important in this part of the macrocycle and that the side chains make less crucial interactions. Reintroducing the exocyclic carboxamide in the B-fragment was obviously tolerated, which was the original position of the linker to the encoding DNA (B4- and B5-containing analogues). The 1,4-substitution pattern of the phenoxy linker appeared vital because B7–9 analogues showed diminished activity. Furthermore, this amino acid segment tolerated the reasonably large lipophilic cyclohexylalanine as an analogue of phenylalanine (compounds 7–9, 11, and 15–16), while the smaller aniline (B10) analogues generally lost activity (Tables S1 and S2). The C-region phenylglycine could be replaced with several smaller, aliphatic amino acids (10–17). In contrast,  $\alpha$ -disubstituted amino acids C6–C8 were not tolerated (Tables S1 and S2), highlighting the relevance of stereochemistry.

**Table 1.** Combinatorial Array Compounds with IC<sub>50</sub> < 300 nM


Cmpd	A	B	C	IC <sub>50</sub> (μM) <sup>a</sup>
3	A1	B1	C1	0.130
4		B1	C1	0.059
5		B1	C1	0.174
6		B1	C1	0.078
7	A1		C1	0.064
8	A1		C1	0.227
9			C1	0.124
10	A1	B1		0.090
11	A1			0.098
12		B1		0.253
13	A1			0.298
14	A1			0.101
15	A1			0.179
16	A1			0.271
17		B1		0.137

<sup>a</sup>IC<sub>50</sub> values determined in an Mcl-I-BAK TR-FRET assay.

Finally, none of the D-fragment variations showed significant activity at 10 μM. This striking observation suggests that the axial–equatorial orientation of the *cis*-cyclohexyl group has a crucial role in maintaining the three-dimensional active conformation of the macrocycle.

**Specific/Targeted SAR Interrogations.** Despite its presence in natural (glyco)peptides, albeit mostly as the (*R*)-isomer,<sup>50</sup> we considered the (*S*)-phenylglycine C-fragment to be one of the more undesirable parts of the molecule. In particular, the known risk of epimerization due to increased acidity of the α-proton,<sup>51</sup> was deemed a liability. As described earlier, partial epimerization was observed during combinatorial array synthesis. Nonetheless, the phenylglycine provided a suitable variation point, particularly for introducing polarity with the goal of improving solubility.

Chirality of the amino acid fragments was expected to be important for macrocycle conformation and this was confirmed by synthesizing the pure (*R*)-phenylglycine epimer **18**, which lost >50-fold in activity. Another apparent variation was the α-methylated compound **19**, which would be insensitive to epimerization. Unfortunately, **19** was significantly less active than **3**, which was not surprising, in view of the poorly active disubstituted C-variations from our initial array (*vide supra*). We next turned our attention to varying the side chain with polar or more flexible groups. Interestingly, pyridines **20/21** showed increased activity, although improvements in solubility were minimal. The larger His/Tyr/Trp variants (**22–24**) were less favorable in terms of activity; however, we were content to observe that **22** and **23** did result in a significant boost in solubility. Finally, nonaromatic side chain variants **25–27** did not substantially improve activity, although **27** was slightly more soluble.

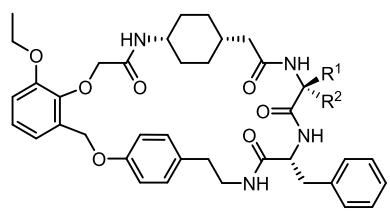
In addition to the lipophilic analogues from Table 1, more polar substituents are apparently also tolerated, at least in the phenylglycine C-area of the macrocycle. Although a suitable combination of activity and improved solubility has not yet been identified, Tables 1 and 2 clearly show that the amino acid side chains tolerate several modifications and can be employed for further optimization. The activity data for compounds **18** and **19** does, however, underline the importance of backbone conformation, particularly in the B/C region. For this reason, it was decided to investigate *N*-methylated variants as well as peptoid derivatives in this area.

Table 3 summarizes the results of the B/C-region backbone investigations. Mono-*N*-methylation was not tolerated at R<sup>3</sup> and R<sup>5</sup> (**28** and **30**, respectively), but R<sup>4</sup>-methylated **29** showed only a minor decrease in activity. Introducing the peptoid variant of phenylglycine completely abrogated activity (**31/33**), but installing only the phenylalanine peptoid appeared to be tolerated (**32**).

Interestingly, R<sup>4</sup>-methylated **29**, as well as the phenylalanine R<sup>4</sup>-peptoid derivative **32** maintain activity. This could suggest that the phenylalanine NH is not crucial for maintaining the overall active conformation of the macrocycle. With this emerging knowledge of the SAR of this compound series, as shown in Tables 1–3, more detailed structural investigations were initiated.

**Structural Investigations.** To gain insight into the SAR of the synthesized compounds, we investigated the conformational features of the free macrocyclic ligand in solution using various NMR techniques including 2D NMR (such as NOESY), variable-temperature (VT) NMR, and H/D exchange experiments. In this context, the active and inactive

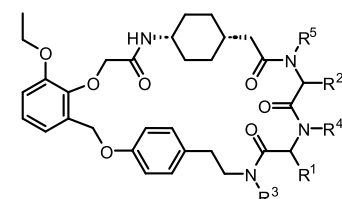
Table 2. Focused phenylglycine modifications



Cmpd	R <sup>1</sup>	R <sup>2</sup>	IC <sub>50</sub> (μM) <sup>a</sup>	Kin. sol. (μM)
3	Ph	H	0.130	<2
18	H	Ph	7.1	ND
19	Ph	Me	1.43	4
20		H	0.043	6
21		H	0.034	3
22		H	7.35	69
23		H	1.37	37
24		H	1.44	1
25		H	0.212	9
26		H	0.080	5
27		H	0.678	25

<sup>a</sup>IC<sub>50</sub> values determined in an Mcl-1-BAK TR-FRET assay; ND = not determined.

Table 3. B/C Area Backbone Modifications



cmpd	R <sup>1</sup>	R <sup>2</sup>	R <sup>3</sup>	R <sup>4</sup>	R <sup>5</sup>	IC <sub>50</sub> (μM) <sup>a</sup>
3	(R)-Bn	(S)-Ph	H	H	H	0.130
28 <sup>b</sup>	(R)-Bn	(S)-Ph	Me	H	H	21.8
29	(R)-Bn	(S)-Ph	H	Me	H	0.382
30	(R)-Bn	(S)-Ph	H	H	Me	>30
31	(R)-Bn	H	H	H	Ph	>30
32	H	(S)-Ph	H	Bn	H	0.234
33	H	H	H	Bn	Ph	>30

<sup>a</sup>IC<sub>50</sub> values determined in an Mcl-1-BAK TR-FRET assay. <sup>b</sup>4:1 mixture of phenylglycine epimers.

isomeric macrocycles **3** and **18** were analyzed in CDCl<sub>3</sub> (low dielectric solvent) and DMSO-*d*<sub>6</sub> (high dielectric solvent) to mimic lipophilic and hydrophilic conditions, respectively. The <sup>1</sup>H NMR spectra of both compounds in both solvents showed sharp proton resonances suggesting that the macrocycles adopt a single predominant conformer in solution on the NMR time scale (spectroscopic details are presented in the [Supporting Information](#)).

Analysis of the vicinal coupling constants (<sup>3</sup>J<sub>H,H</sub>) and NOEs of compound **3** in CDCl<sub>3</sub> ([Figure 5](#)) indicated that the *cis*-1,4-disubstituted cyclohexyl D-fragment adopts a preferred <sup>1</sup>C<sub>4</sub> chair conformation in which the amino group is oriented in an axial position, and the 4-substituent is equatorially positioned. This precise axial–equatorial relation, apparently crucial for the three-dimensional active conformation of the macrocycle, is stabilized by the participation of the axial NH in a strong intramolecular 5-membered hydrogen-bonded ring with the phenolic oxygen of the acetamide linker on the A-fragment, as revealed by VT NMR (Δδ/ΔT of 2.4 ppb/K) and H/D exchange (*t*<sub>1/2</sub> > 18 h) studies. NMR parameters suggested that the active macrocycle **3** adopts a major bent-shape conformation in solution as shown in [Figure 5](#).

The absolute configuration of the amino acid C-fragment also influences the shape and activity of the 27-atom macrocycle. The stereochemical difference between the phenylglycine epimers **3** and **18** results in a rearrangement of the intramolecular hydrogen-bonding network on the peptide segment with all amides in a *trans* geometry. The local conformational changes around the stereocenters propagate along the ring backbone to drastically affect the global conformation of the macrocycle, and thus its binding affinity and physicochemical properties. Indeed, the (*R*)-epimer **18** was found to be >50-fold less active than the reference (*S*)-phenylglycine compound **3** (see [Table 2](#)).

VT NMR data of **3** and **18** in CDCl<sub>3</sub> revealed distinct hydrogen-bonding patterns for the two isomers, as illustrated in [Figure 6](#). For (*S*)-epimer **3** ([Figure 6a](#)), the Phe-NH was the only amide proton that was exposed to the solvent, as evidenced by its high chemical shift/temperature coefficient of −12.8 ppb/K and fast H/D exchange. The other amide protons of the peptide segment showed lower temperature coefficients and slow H/D exchange, implying them to be involved in intramolecular hydrogen bonds. The NOE and coupling constant (<sup>3</sup>J<sub>NH-CαH</sub>) data suggested that the phenethylamine NH formed a relatively strong 7-membered hydrogen bond with the Phg-CO (γ-turn-like structure), although the cyclohexylacetamide CO could also act as a H-bond acceptor (β-turn-like structure). Conversely, for (*R*)-epimer **18** ([Figure 6b](#)), the Phe-NH had a low temperature coefficient of 0.4 ppb/K, indicating that it was not solvent-exposed but rather participated in an intramolecular hydrogen bond with the acetamide CO of C-fragment (additional γ-turn). The resulting hydrogen-bond network causes an extensive, presumably unfavorable, conformational change of the whole macrocycle in solution, almost certainly explaining the reduced biological activity observed for (*R*)-Phg isomer.

In the active conformation, the phenylalanine NH is solvent-exposed and can be modified while retaining the overall active conformation of the macrocycle. For example, the *N*-methylated derivative **29** and the Phe peptoid **32** ([Table 3](#)) show only a small decrease in binding affinity compared to the reference compound **3**. In contrast, *N*-methylations and peptoid substitutions on any other amide NH are not tolerated

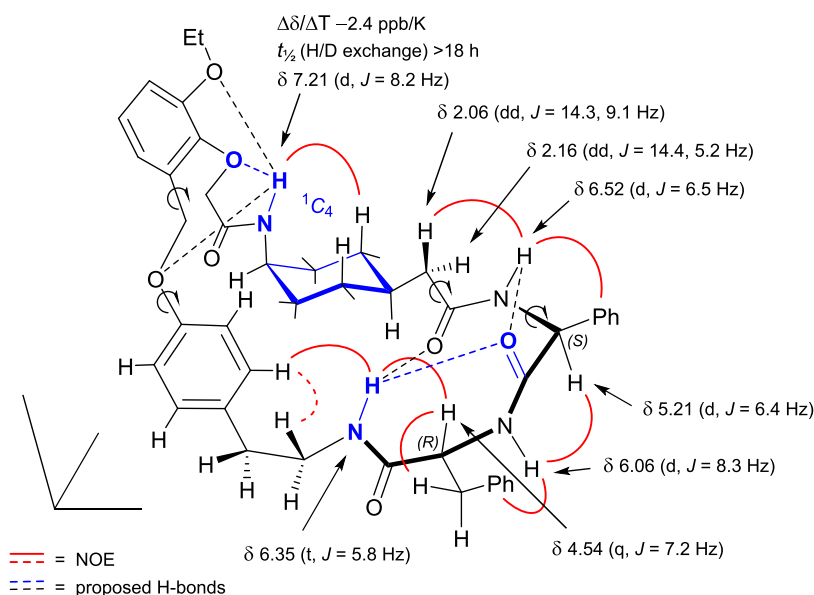


**Figure 5.** Significant spectroscopic data and elucidation of the major conformation in solution (CDCl<sub>3</sub>) of the reference compound 3. The most probable intramolecular H-bonds are indicated by blue dashed lines.

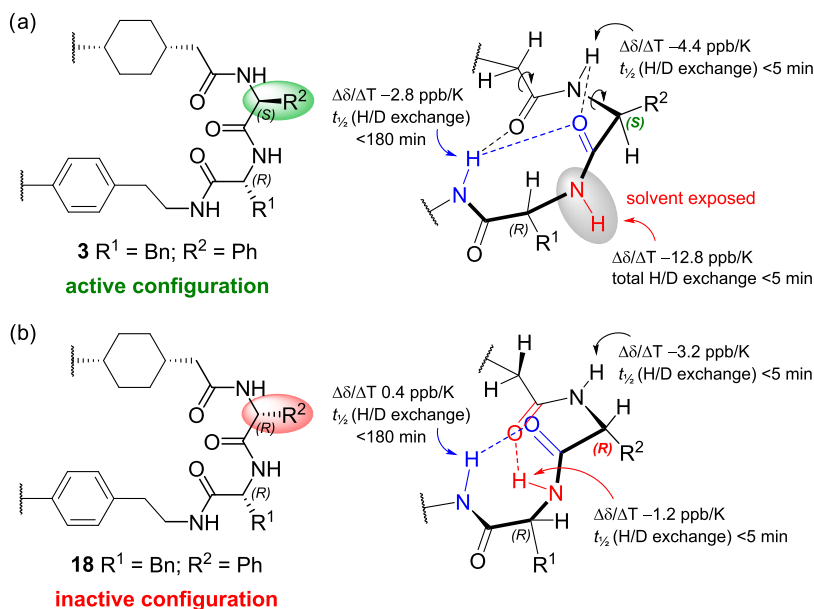


**Figure 6.** Hydrogen-bond networks proposed for the peptide chain fragment of the epimeric macrocycles 3 (a) and 18 (b) in solution (CDCl<sub>3</sub>). Temperature coefficients ( $\Delta\delta/\Delta T$ ) and H/D exchange rates ( $t_{1/2}$ ) of the NH amide groups are shown.

because they would disrupt the delicate intramolecular hydrogen bonding network (Figure 6a) that appears to stabilize the active macrocycle conformation. In summary, the NMR conformational analysis is in line with the SAR findings and highlighted the significance of the *cis*-cyclohexyl moiety (D1-fragment), the (*S*)-chirality of Phg C-fragment, and the transannular hydrogen bonding in the peptide segment, as driving forces for the conformational preorganization of the macrocycle in solution. Moreover, the NMR studies did not reveal major differences in the macrocycle backbone conformation in either CDCl<sub>3</sub> or DMSO-*d*<sub>6</sub>, potentially explaining the low aqueous solubility.

We were able to generate a single-molecule X-ray diffraction structure of compound 2 (Figure 7), which exhibits an overall topology similar to the solution-phase structure of 3. The

upward kink caused by the *cis*-cyclohexyl is apparent, and the predicted H-bond between the axial aminocyclohexyl-NH and the phenoxy-O is also observed with a distance of 2.1 Å. On the other hand, the intramolecular H-bond between the two amide bonds of the phenylalanine is not observed in the solid-state structure, in contrast to the solution-phase conformation.

Finally, we managed to obtain a protein–ligand cocrystal structure of compound 1 with Mcl-1 (1.9 Å resolution, PDB 8QSO), which shows an active conformation that is remarkably similar to the solid- and solution-phase structures described above. To illustrate this resemblance we superimposed a prospective conformational model of the macrocycle backbone based on experimental NMR constraints of 3 (depicted in Figure 5) with the bioactive ligand structure of 1 as shown in Figure 8.



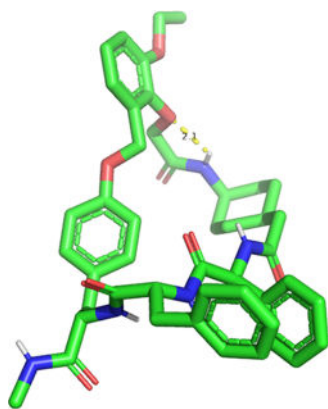


**Figure 7.** Single-molecule crystal structure of compound 2; the yellow dotted line indicates the 2.1 Å intramolecular H-bond between the axial NH and the phenoxy oxygen.

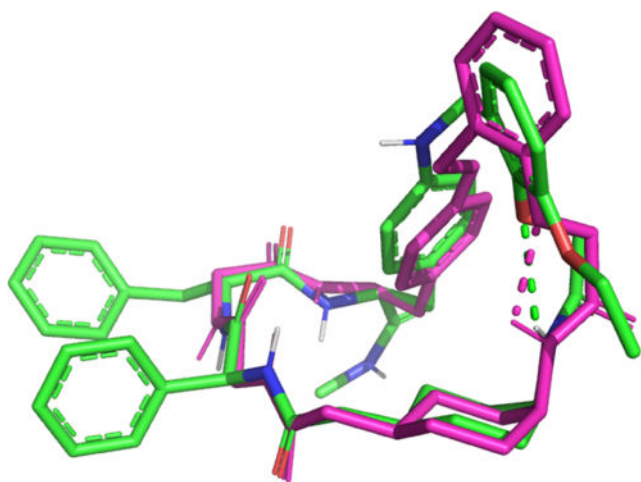


**Figure 8.** Overlay of ligand 1 from the protein–ligand crystal structure (green) with the conformational backbone model of 3 (magenta); side chains and substituents of 3 were removed for clarity; conformational model was generated with MacroModel from Schrödinger.

The overall bent-shape conformation is apparent in both structures, partially caused by the axial–equatorial orientation of the *cis*-cyclohexyl amine and its strong intramolecular hydrogen bond with the phenolic oxygen, present in both structures (dotted lines). The peptidic B/C-area of the macrocycle is also similar, with certain differences caused by intramolecular hydrogen bonds in 3 being exchanged for interactions of 1 with the protein.

In the Mcl-1 complex structure (Figure 9), compound 1 binds to the BH3-helix binding groove,<sup>52,53</sup> similarly to most reported Mcl-1 inhibitors, including those depicted in Figure 1. The macrocyclic compound occupies all of the most commonly found binding pockets, often designated as P1–4, as recently summarized in detail by Romanov-Michailidis, Hsiao et al.<sup>42</sup> The peptidic Phe-Phg segment occupies the P4-area, with the phenylalanine side chain lying on top of Gly262 and wedged against a lipophilic wall formed by Phe318/319. The phenylglycine side chain appears to partially occupy a small lipophilic den in the protein surface, formed by valines 216, 220, 265, and glycine 262, explaining why the Phg-epimer (18) lost much of its potency. The phenylglycine carbonyl forms an important H-bond interaction with Asp263, which is

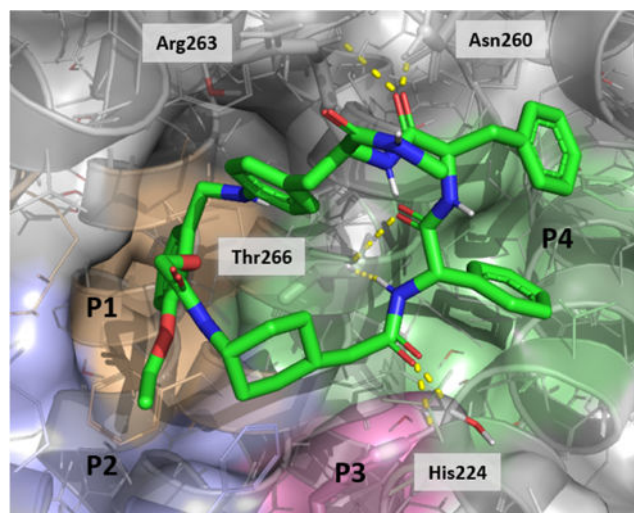


**Figure 9.** X-ray crystal structure of 1 (green) in complex with the Mcl-1 protein (PDB: 8QSO), highlighting the different pockets: P1 (wheat), P2 (light-blue), P3 (pink), and P4 (pale green); H-bonds are indicated by a yellow dotted line.

observed in nearly all reported Mcl-1 inhibitors, albeit usually in a salt bridge.<sup>42</sup> Additionally, the same carbonyl forms a much less common interaction with the side chain of Asn260. The Phg backbone finally engages in a double H-bond interaction with the adjacent Thr266. The structurally significant *cis*-aminocyclohexylacetic acid fragment is positioned in the P3 pocket with the carbonyl forming an H-bond interaction with His224, both directly and via a nearby water molecule. The structure clearly shows the effect of the *cis*-configuration, since its induced bend effectively allows deeper access into the P1 pocket. The small lipophilic P2 pocket is occupied by the ethoxy group that branches out from the A-fragment aryl group, while the aromatic part itself is positioned toward the P1 pocket. A regularly reported feature of this part of the Mcl-1 protein is the potential for forming an extended “P1’-pocket”. Many of the reported Mcl-1 inhibitors fill this induced-fit pocket;<sup>19,42</sup> however, 1 does not occupy this region and the inducible pocket appears to be collapsed. To further investigate the exact nature of the P1/P1’ pocket we superimposed the crystal structure with that of “Compound-60” (Figure 10) from Fesik and co-workers,<sup>29</sup> the molecular structure of which is depicted in Figure 1.

Figure 10a shows the overlay of the protein crystal structure of 1 with the protein from pdb 5FDR, which has the induced P1’ pocket in its open form. This clearly demonstrates that with our compound the pocket between the two  $\alpha$ -helices is not accessible. This is mainly due to the different side chain orientations of two residues, Met250 and Leu246, which are folded away when the pocket is occupied. Overlaying compound 1 with Fesik’s protein–ligand structure (Figure 10b) then demonstrated the potential of targeting the P1’ pocket from the direction of our phenoxy A-fragment. Both lipophilic interactions and a  $\pi$ – $\pi$  interaction with Phe270 are apparent in the P1’ pocket, which we used to guide further efforts.

Having acquired sufficient structural knowledge of the different aspects of the macrocyclic compound series, we felt confident enough to embark on further optimization. Both activity and physicochemical properties were the focus points, both approaches are described below.

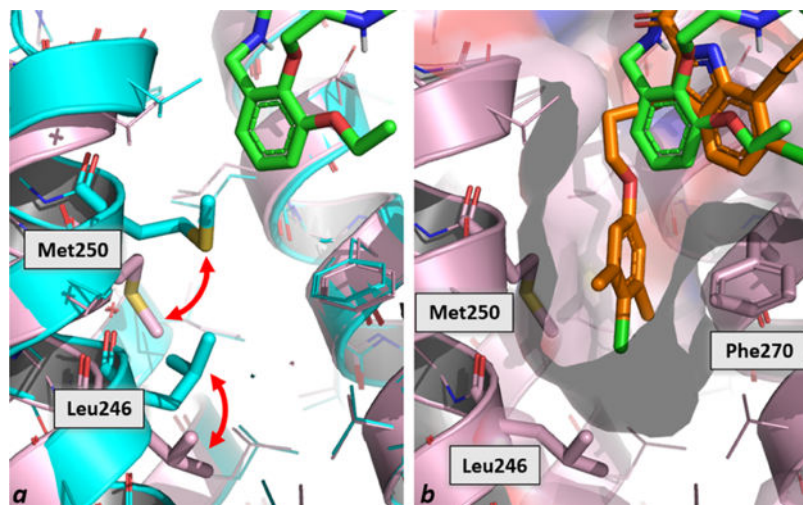


**Figure 10.** Overlay of **1** with the X-ray crystal structure of “Compound-60” from Figure 1 (PDB 5FDR); (a) comparison of the inducible P1' pocket in its closed form (from X-ray structure of **1**, PDB: 8QSO, cyan) and in the open form (PDB: 5FDR, ligand omitted, light-pink); (b) overlay of **1** (green) with “Cmpd 60” (orange) in the protein of 5FDR, showing the surface of the induced pocket.

**Lead Optimization.** Although the protein complex structure with **1** provided several guidelines for structure-based design, we gave the highest priority to addressing the P1'-pocket, assuming that this could lead to a significant increase in affinity. Based on the overlay from Figure 10b, the 4-position of the P1-pocket aryl ring was assessed to be the obvious branching position, providing the appropriate vectorial orientation. Following that design, >200 unique variations were prepared, based on the original backbone of **3**, employing a diverse set of linking methods. From three promising subseries, we highlight the most interesting compounds in Table 4. Activity of the most active compounds in a cellular context was determined, initially in a proliferation assay using multiple myeloma-derived H929 cells. However, quickly thereafter we added a caspase-based apoptosis assay to the profiling cascade, providing more biologically relevant, target-related activity data.

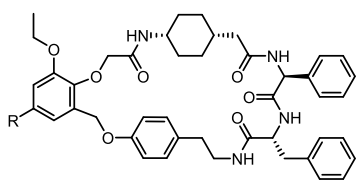
Our first approach to targeting the P1'-pocket involved the preparation of biaryl compounds. This immediately led to several compounds with moderately increased activity, four of which are shown in Table 4 (34–37). Some of these compounds also exhibited cellular efficacy, although drop-offs were relatively high (>50-fold). We were delighted to see that the significantly elongated biaryl alkynes **38–42** drastically improved activity. This subseries offered the first compounds with activities in the single-digit nanomolar range, with the most active variant being the *para-tert-butylphenyl* derivative **41** (1.8 nM). Despite the increase in biochemical IC<sub>50</sub>, an improvement in cellular activity was not observed, with IC<sub>50</sub> values still in the low micromolar range, in both the H929 proliferation and caspase assays. We hypothesized that the biaryl and biarylalkyne compounds lacked flexibility and in combination with the surprisingly rigid macrocycle (*vide supra*) reduced permeability. Introducing a somewhat more flexible aryether functionality provided a solution to this. Compounds **43–47** generally maintained low-nanomolar activity in the TR-FRET assay, but also exhibited outstanding cellular IC<sub>50</sub> values in the submicromolar range. Within this subseries, **43** and **44** are the most interesting representatives, achieving cellular IC<sub>50</sub> values below 100 nM. Additionally, the H929 caspase assay of these compounds showed very similar IC<sub>50</sub> values as the cell

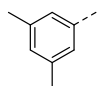
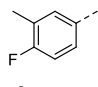
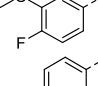
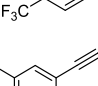
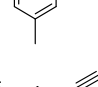
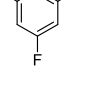
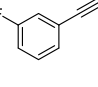
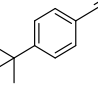
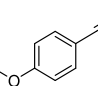
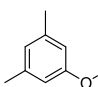
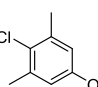
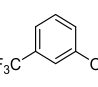
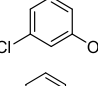
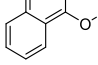
proliferation assay, suggesting that the observed antiproliferative effect is indeed target-related. It is also worth mentioning that both **43** and **44** retained full selectivity over Bcl-xl (IC<sub>50</sub> > 10 μM) and showed improved metabolic stability compared to **3** (S9 mouse *t*<sub>1/2</sub>: 30 min (**43**), >200 min (**44**)).

Although we managed to increase potency by nearly 2 log units through interrogation of the P1'-pocket, this resulted in a marked increase in cLogD, which raised from 5.1 for **3** to 8.2 for **44**. Aqueous solubility for all compounds in Table 4 was measured below 2 μM, which was not unexpected in view of the lipophilicity and the known physicochemical challenges generally associated with large macrocyclic molecules.<sup>54</sup> We had previously observed that appreciable solubility can be achieved by simply optimizing the side chains (see Table 2). Hence, we set out to balance both activity and physicochemical properties using the insight obtained so far, using our most potent compounds (**43/44**) as starting points.

Table 5 summarizes our efforts to optimize physicochemical properties while trying to maintain cellular potency. The first variants (**48–52**) focused on reducing cLogD by altering the R<sup>2</sup> and R<sup>3</sup> side-chain substituents. Phenylalanine pyridyl variants were tolerated (**48/49**), i.e., led to a modest decrease of cLogD, but did not improve solubility. Combining the more active 4-pyridyl group with two previously discovered phenylglycine replacements from Table 2 lowered lipophilicity further, but unfortunately came at the cost of cellular efficacy (**50/51**). The B-area D-proline variation was previously found to improve both solubility and passive permeability (data not shown); however, in the current context, it did not result in the expected breakthrough (**52**). As expected from the original DEL hits, changing the ether into an amine linker (X = NH) retained activity; however, it did not improve solubility (**53/54**). We already knew that reinstalling the original carboxamide linker stub would not enhance solubility (see Figure 2e). However, introducing a carboxylic acid functionality at that position significantly lowered cLogD and resulted in an excellent improvement in solubility (**55/56**). Biochemical activity was preserved, but a decrease in cellular efficacy was observed, presumably due to lower permeability compared to **48**, which was confirmed by their low PAMPA values. It should be noted that overall, PAMPA values were low to moderate. It

Table 4. Optimization of the P1'-Pocket Substituent



Cmpd	R	Mcl-1-BAK IC <sub>50</sub> (nM) <sup>a</sup>	H929 IC <sub>50</sub> (μM) <sup>b</sup>	H929 caspase IC <sub>50</sub> (μM) <sup>c</sup>
3	H	130	>10	ND
34		15	>10	ND
35		54	2.9	ND
36		50	2.1	ND
37		39	7.1	ND
38		14	3.4	>10
39		5.6	3.3	1.9
40		7.3	2.2	2.8
41		1.8	9.9	>10
42		8.0	1.4	7.4
43		1.6	0.056	0.078
44		1.5	0.041	0.060
45		12	0.18	0.19
46		22	0.33	0.41
47		12	0.17	0.22

<sup>a</sup>IC<sub>50</sub> values determined in an Mcl-1-BAK TR-FRET assay. <sup>b</sup>IC<sub>50</sub> values determined in an NCI-H929 cell viability assay. <sup>c</sup>IC<sub>50</sub> values determined in an NCI-H929 cellular Caspase 3/7 assay; ND = not determined

is known that the permeability of large bRo5-compounds (e.g., macrocycles, bivalent degraders, etc.) can be challenging to accurately measure with *in vitro* permeability assays, even when they are active in cells.<sup>26,34</sup> For this reason we were satisfied with the current data, although extrapolating robust trends from them was difficult.

Despite the improved profiles of **55** and **56**, we decided to further fine-tune the structures. Keeping the chloro as R<sup>4</sup> for its slight affinity benefit and reinstalling the ether linker to reduce the HBD count by one, required compensation for lipophilicity elsewhere, i.e., in the B-/C-area side chains. This ultimately resulted in compounds **57** and **59** that exhibited moderate but measurable passive permeability with low cLogD and high solubility. Interestingly, the carboxylic acid (R)-epimer **58** had significantly reduced solubility, compared to **57**. This is possibly related to the acid group being more in-plane with the macrocycle, compared to the out-of-plane orientation observed for the (S)-isomer in the crystal structure of **1** (Figure 9).

The cellular caspase induction activity assay value improved slightly for **59** (480 nM), but most importantly the increased permeability caused the drop-off of the TR-FRET IC<sub>50</sub> values to be reduced from 190-fold for **56** to less than 40-fold. From a development point of view, we consider **57** and **59** as suitable lead candidates with a balanced profile, having appreciable cellular efficacy, moderate passive permeability, and excellent aqueous solubility.

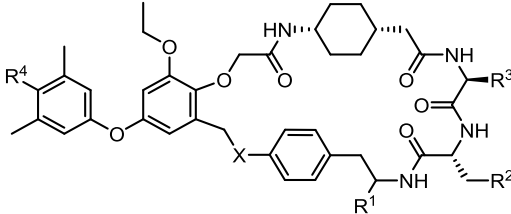
## CHEMICAL SYNTHESIS

Considering the peptidic character of the B- and C-fragments of the macrocyclic hits, our overall synthetic approach utilized C-to-N directed peptide synthesis to circumvent the risk of epimerization. For the key macrocyclization step, we opted for amide coupling at the phenoxy acetic acid position of the A-fragment, which was anticipated to be the least risky. The above rationale required that our general synthetic sequence proceeded through the ester intermediate **64**, which could be prepared via two routes (I/II, Scheme 1), the main difference being the order of events. Route I initiated with the introduction of the B-fragment amino acid on amine **60**, followed by Mitsunobu coupling of the phenol with the A-fragment benzylic alcohol **63**. Alternatively, route II started with either Mitsunobu coupling or bromination/substitution of Boc-protected **65**, followed by amide coupling with the first amino acid fragment. Classical peptide-coupling strategies then converted **64** into precursor **69** by consecutively introducing the C- and D-fragments. To circumvent purification issues with the intramolecular amine-/acid-containing macrocycle precursor, ester saponification and Boc-deprotection were performed sequentially on **69**, with no workup except concentration. Crude intermediates were immediately cyclized, resulting in the macrocyclic final products.

The two synthetic routes from Scheme 1 were used for preparing all compounds that had the general A–B–C–D makeup, including all compounds described in Tables 1–3. Route I was the method of choice for the combinatorial array approach outlined in Figure 3, synthetic details are found in the Experimental Section and the Supporting Information. Preparation of the more elaborate P1'-pocket variations



Table 5. Balancing Activity and Physicochemical Properties



Cmpd	X	R <sup>1</sup>	R <sup>2</sup>	R <sup>3</sup>	R <sup>4</sup>	cLogD	Mcl-1-BAK IC <sub>50</sub> (nM) <sup>c</sup>	H929 caspase IC <sub>50</sub> (μM) <sup>d</sup>	Kin. sol. (μM)	P (10 <sup>-6</sup> cm/s) pH 7.4 <sup>b</sup>
44	O	H	Ph	Ph	Cl	8.2	1.5	0.060	<2	ND
48	O	H		Ph	Cl	7.0	14	0.045	<2	5.5
49	O	H		Ph	Cl	7.0	5.3	0.035	<2	<1
50	O	H			Cl	5.7	9.4	1.4	<2	ND
51	O	H			Cl	4.0	5.3	>10	<2	ND
52 <sup>a</sup>	O	H		Ph	Cl	6.8	18	0.54	<2	7.3
53	NH	H	Ph	Ph	H	7.3	9.1	0.094	<2	ND
54	NH	H	Ph	Ph	Cl	7.9	5.3	0.057	<2	ND
55	NH		Ph	Ph	H	3.7	7.7	0.63	>80	2.0
56	NH		Ph	Ph	Cl	4.3	5.7	1.1	>80	<1
57	O				Cl	3.4	31	1.1	>80	5.3
58	O				Cl	3.4	16	0.41	11	1.5
59	O			Ph	Cl	3.5	13	0.48	>80	3.9

<sup>a</sup>D-Phenylalanine fragment replaced by D-proline. <sup>b</sup>Passive permeability measured with PAMPA. <sup>c</sup>IC<sub>50</sub> values determined in an Mcl-1-BAK TR-FRET assay. <sup>d</sup>IC<sub>50</sub> values determined in an NCI-H929 cellular Caspase 3/7 assay; ND = not determined.

required devising a different approach, in order to facilitate the efficient synthesis of >200 variants (Scheme 2).

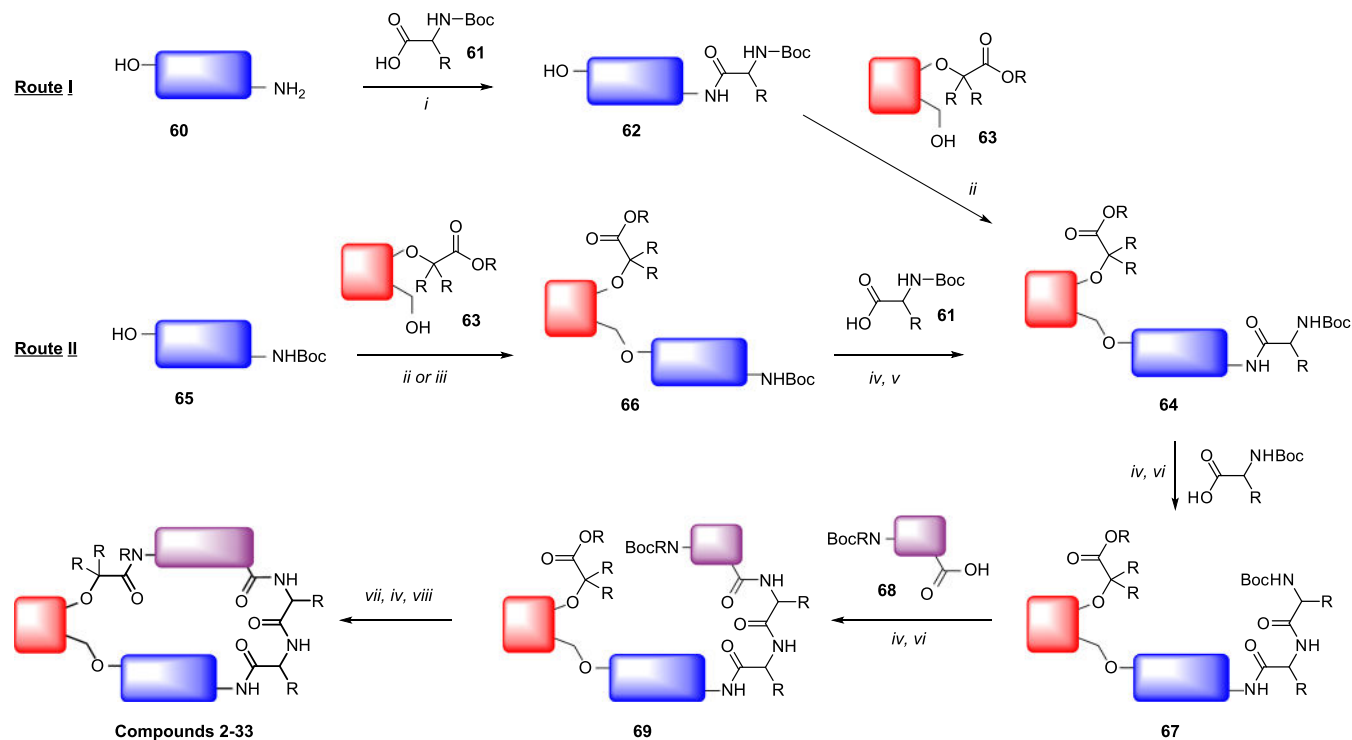
Scheme 2 depicts the slightly modified reaction sequence applied to introduce an iodo handle in the A-area and subsequently prepare the P1'-pocket variations summarized in Table 4. Starting from O-benzyl protected 4-(2-aminoethyl) phenol (70), standard peptide-coupling conditions were used to introduce the phenylalanine and phenylglycine fragments. Debenzylation of 71 under hydrogenation conditions yielded the phenol, which was coupled with the iodo bromo A-fragment bromide 72, resulting in the macrocycle precursor 73. Simultaneous Boc-deprotection and ester hydrolysis under acidic conditions, followed by macrocyclization resulted in the iodo-functionalized building block 74. This highly versatile route was carried out on a large scale, eventually yielding 4.7 g of the macrocyclic building block with an excellent overall yield of 65%. The iodo derivative 74 could ultimately be converted into the aryl, alkyne, and aryloxy products via Suzuki, Sonogashira, and Ullmann conditions, respectively.

Once the optimal P1'-pocket substituents were identified, the final optimizations from Table 5 were initiated. These compounds were either prepared via the late-stage P1'-pocket

aryloxy groups described in Scheme 2, or via the original approach from Scheme 1, using a fully functionalized A-fragment. Details are described in the Experimental Section.

Finally, the amine-linked variants 53–56, and also the original DEL-hit 1 could not be rapidly synthesized by our usual approaches, due to complications caused by the reactive NH. For these compounds, we decided to employ solid-phase peptide synthesis (SPPS), as outlined in Scheme 3. Compounds without the linker carboxylate (53/54) started from the chlorotrityl resin-bound aniline 75. The stepwise buildup of the peptidic fragment resulted in intermediate 76, which was then coupled to functionalized A-fragment benzaldehydes 77b/c to form resin-bound 78b/c. These were cleaved from the resin with diluted TFA in dichloromethane, and the resulting anilines were cyclized via reductive amination, yielding 53/54. For the carboxamide-containing products, we opted for loading onto the chlorotrityl resin through the carboxylate, i.e., compound 79, Boc-protected on the aniline. Sequential introduction of the amino acid fragments, followed by functionalized benzaldehydes 77a–c, and cleavage from the resin gave N-Boc-protected macrocyclization precursors 81a–c. Deprotection and reductive



Scheme 1. Schematic Outline Used for Array Synthesis and Tables 1–3 Compounds<sup>a</sup>

<sup>a</sup>Reagents and conditions: [i] EDCI, Oxyma Pure, Et<sub>3</sub>N, dichloromethane (DCM); [ii] P(*n*Bu)<sub>3</sub>, diisopropyl azodicarboxylate (DIAD), tetrahydrofuran (THF), 0 °C → rt; [iii] **63**, PBr<sub>3</sub>, DCM, *then* alcohol **65**, K<sub>2</sub>CO<sub>3</sub>, MeCN; [iv] HCl, dioxane; [v] amino acid, HATU, Et<sub>3</sub>N, DCM; [vi] amino acid, EDCI, Oxyma Pure, Et<sub>3</sub>N, DCM; [vii] aq. NaOH, THF; [viii] HATU, Et<sub>3</sub>N, *N,N*-dimethylformamide (DMF).

amination yielded macrocycles **55/56/82**, the latter of which was subsequently converted into methylamide **1**.

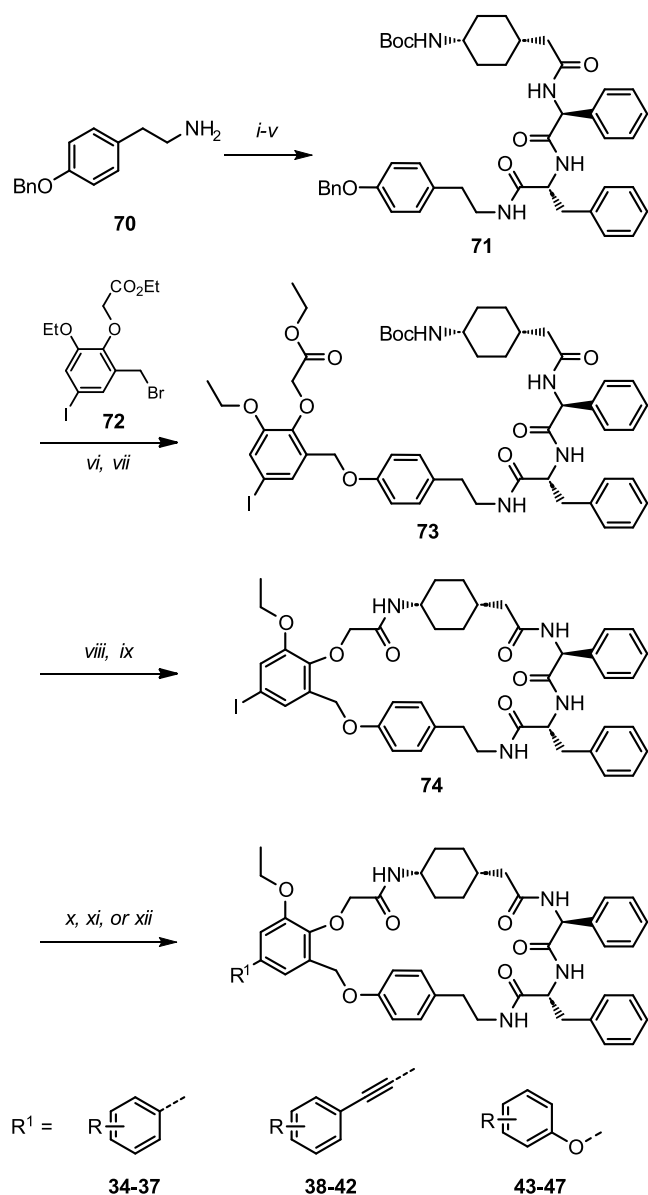
## CONCLUSIONS

Myeloid cell leukemia 1 (Mcl-1) inhibition requires the blocking of a protein–protein interaction, which can often only be achieved with the use of relatively large, (semi-) peptidic, compounds. This can make hit identification by traditional HTS challenging, and for this reason, we employed a DEL screen using a macrocyclic library. This screen delivered outstanding starting points with submicromolar activities, but with nonideal physicochemical properties. By using a combination of solution-phase conformation analysis by NMR and solid-phase conformation analysis by single-molecule X-ray crystallography, we were able to demonstrate that the three-dimensional conformation of the DEL hits was surprisingly rigid. The striking similarity between the solution-phase and the active (Mcl-1 bound) conformation was later confirmed by ligand-protein complex X-ray crystallography and indicated that the DEL hits were conformationally preorganized for Mcl-1 binding. The X-ray crystal structure was used for structure-based design, initially by addressing the inducible P1' pocket, which brought affinities into the low nanomolar range. Particularly for the somewhat flexible P1' phenoxy functionalized compounds (e.g., **43/44**) this also translated to cellular efficacies below 100 nM. However, these large and highly lipophilic macrocyclic molecules continued to exhibit nonideal physicochemical properties, including poor solubility at physiological pH. In the next stage, during which the macrocyclic backbone itself was untouched, and instead the peripheral side chains were optimized, we successfully improved physicochemical properties. Significantly reduced

cLog *D*'s (from 8.2 to 3.4–3.5) were accompanied by excellent aqueous solubility and modest permeability. Lead candidates **57** and **59** demonstrate a balanced profile and make us confident that this series of novel macrocyclic Mcl-1 inhibitors can be further optimized for therapeutic use in cancer patients. This study also successfully demonstrates how DEL screening followed by rapid analoging can provide an efficient entry to complex, semipeptidic macrocycles, including compounds highly suitable for the inhibition of protein–protein interactions.

## ■ EXPERIMENTAL SECTION

**General.** Unless otherwise noted, commercial reagents and solvents were obtained from commercial suppliers and used without further purification. Analytical TLC was performed on Merck precoated TLC glass sheets with silica gel 60 F254. Normal-phase flash column chromatography was performed on a Büchi Reveleris system, using prepacked silica gel (SiO<sub>2</sub>, 20–40 mesh) cartridges. <sup>1</sup>H and <sup>13</sup>C NMR spectra were recorded on a 400 MHz Bruker Avance DRX-400 spectrometer, and chemical shifts are reported in ppm from TMS as an internal standard. Purities of all tested compounds were confirmed to be >95% by high-performance liquid chromatography (HPLC) analysis, with the exception of compounds generated by combinatorial chemistry, where a purity cutoff of >90% was maintained. Analytical HPLC-mass spectrometry (MS) measurements were performed on an Agilent Infinity 1260 apparatus (DAD: Agilent G1315D, 220–320 nm, MSD: Agilent LC/MSD G6130B ESI, pos/neg 100–800), using a Waters XSelect C18 (50 × 2.1 mm, 3.5 μm), Waters Sunfire C18 (150 × 2.1 mm, 3.5 μm) or a Phenomenex GeminiNX C18 (150 × 4.6 mm, 3 μm) column. The mobile phase was a gradient over 6 min starting from 5% A and 95% B and finishing at 98% A and 2% B with a flow rate of 0.8 mL/min (acidic: A = 0.1% formic acid in acetonitrile, B = 0.1% formic acid in water; basic: A = 95% acetonitrile +5% 10 mM ammonium bicarbonate in water in

Scheme 2. P1'-Pocket Variations<sup>a</sup>

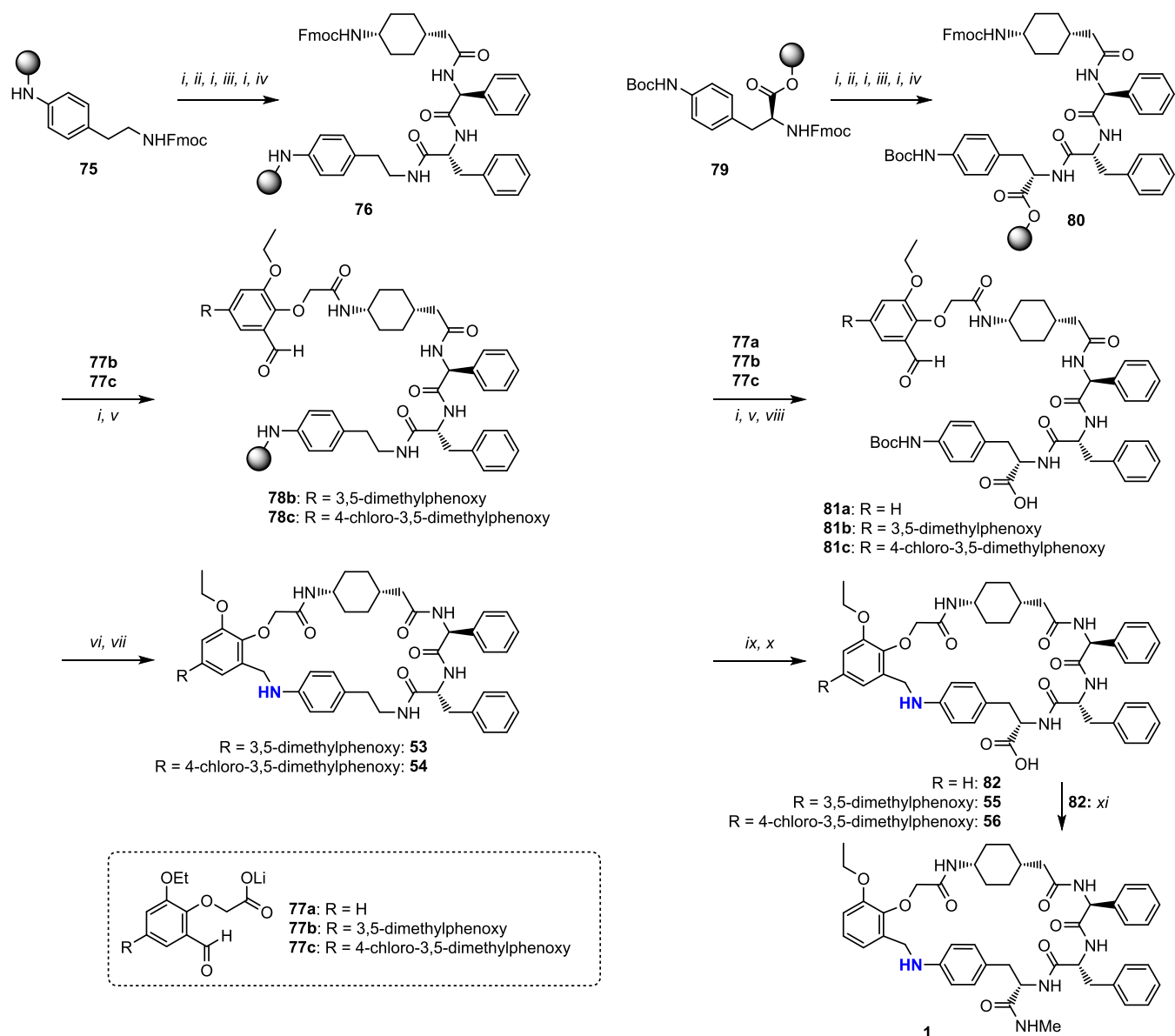
<sup>a</sup>Reagents and conditions: [i] Boc-D-phenylalanine, EDCI, HOAT, DCM; [ii] HCl, dioxane; [iii] Boc-L-phenylglycine, EDCI, Oxyma Pure, Et<sub>3</sub>N, DCM; [iv] HCl, dioxane; [v] *cis*-(4-(Boc-amino)-cyclohexyl)acetic acid, EDCI, Oxyma Pure, Et<sub>3</sub>N, DCM, 75% over 5 steps; [vi] Pd/C, H<sub>2</sub>, THF/MeOH; [vii] 72, Cs<sub>2</sub>CO<sub>3</sub>, DMF, 91% over 2 steps; [viii] aq. HCl, dioxane; 40 °C; [ix] HATU, Et<sub>3</sub>N, THF, 95% over 2 steps; [x] boronic acid or ester, PdCl<sub>2</sub>dppf, Na<sub>2</sub>CO<sub>3</sub>, DME/H<sub>2</sub>O, 100 °C; [xi] alkyne, PdCl<sub>2</sub>(PPh<sub>3</sub>)<sub>2</sub>, CuI, Et<sub>3</sub>N, THF; [xii] phenol, CuCl, 2,2,6,6-tetramethyl-3,5-heptanedione, Cs<sub>2</sub>CO<sub>3</sub>, N-methylpyrrolidone (NMP), 120 °C.

acetonitrile, B = 10 mM ammonium bicarbonate in water). Chiral SFC was performed on a Waters Prep 100 SFC UV/MS directed system (Waters 2998 Photodiode Array (PDA) Detector; Waters Acquity QDa MS detector). Preparative HPLC-MS purifications were performed on an Agilent Technologies 1290 preparative LC (DAD: 220–320 nm, MSD: Agilent G6130B Quadrupole, pos/neg 100–1200), using a Waters XSelect C18 (100 × 30 mm, 10 μm) column. High-resolution mass spectra were obtained on a Vanquish/Orbitrap Q Exactive HF (Thermo Scientific) system (ESI positive). S9 metabolic stability assays were performed by Cyprotex Ltd. (U.K.). DataWarrior<sup>55</sup> was used for SAR analysis. Chemaxon's JChem was

used for cLogP/cLogD calculations. MacroModel from Schrödinger, LLC was used to generate the conformational model using experimental constraints from the NMR data. The force field used was OPLS4 and the search method was "Mixed Torsional/Low mode MD". Protein pictures were prepared using PyMOL Molecular Graphics System, Version 2.0 Schrödinger, LLC. The syntheses of methyl and ethyl 2-(2-ethoxy-6-(hydroxymethyl)phenoxy)acetate and ethyl 2-(2-ethoxy-6-(hydroxymethyl)-4-iodophenoxy)acetate were performed according to the A-fragment procedure described in the Supporting Information (SI).

**General Combinatorial Procedure.** All compounds in the combinatorial array approached were prepared according to Route 1 from Scheme 1. The general procedure for this process as well as the analytical data for the products depicted in Table 1 are described in the Supporting Information. Furthermore, an overview of all products successfully isolated from the combinatorial approach, including their exact compositions is given in Table S1.

**Synthesis of 3 (Route 1, Scheme 1).** *N*-Boc-D-phenylalanine (1.93 g, 7.29 mmol), EDCI·HCl (1.40 g, 7.29 mmol, 1.0 equiv), Oxyma Pure (1.04 g, 7.29 mmol, 1.0 equiv), and triethylamine (2.03 mL, 14.6 mmol, 2.0 equiv) were dissolved in DCM (20 mL) and stirred for 30 min. To this mixture, 4-(2-aminoethyl)phenol (1.00 g, 7.29 mmol, 1.0 equiv) was added, and the mixture was stirred overnight at room temperature. The resulting mixture was diluted with methanol, and the organic layer was washed with saturated aqueous NaHCO<sub>3</sub> and aqueous KHCO<sub>3</sub>. The organic layer was dried over Na<sub>2</sub>SO<sub>4</sub> and concentrated *in vacuo*. The crude material was purified by silica column chromatography (2 to 75% ethyl acetate in *n*-heptane), yielding *tert*-butyl (R)-1-((4-hydroxyphenethyl)amino)-1-oxo-3-phenylpropan-2-yl)carbamate (1.55 g, 55%). HPLC purity >95%, MS (ESI) 407.4 [M + Na]<sup>+</sup>. To a solution of methyl 2-(2-ethoxy-6-(hydroxymethyl)phenoxy)acetate (0.687 g, 2.86 mmol, 1.1 equiv) in tetrahydrofuran (40 mL) were added *tert*-butyl (R)-1-((4-hydroxyphenethyl)amino)-1-oxo-3-phenylpropan-2-yl)carbamate (1.00 g, 2.60 mmol) and P(*n*-Bu)<sub>3</sub> (0.637 g, 3.12 mmol, 1.2 equiv) at 0 °C. The reaction mixture was stirred under a nitrogen atmosphere for 10 min, after which DIAD (0.631 g, 3.12 mmol, 1.2 equiv) was added. The reaction mixture was allowed to warm to room temperature and stirring was continued overnight. The resulting solution was concentrated and the residue purified by silica gel column chromatography (2 to 50% ethyl acetate in *n*-heptane) to afford methyl (R)-2-((4-(2-(2-((*tert*-butoxycarbonyl)amino)-3-phenylpropanamido)ethyl)phenoxy)methyl)-6-ethoxyphenoxy)-acetate (877 mg, 56%). HPLC purity >95%, MS (ESI) 607.3 [M + H]<sup>+</sup>. Methyl (R)-2-((4-(2-(2-((*tert*-butoxycarbonyl)amino)-3-phenylpropanamido)ethyl)phenoxy)methyl)-6-ethoxyphenoxy)-acetate (877 mg, 1.45 mmol) was treated with HCl in 1,4-dioxane (4 N, 3.60 mL, 14.4 mmol, 10 equiv), and the reaction mixture was stirred at room temperature for 2 h. Volatiles were removed *in vacuo* and the residue was co-evaporated once with chloroform. Methyl (R)-2-((4-(2-(2-(2-amino-3-phenylpropanamido)ethyl)phenoxy)methyl)-6-ethoxyphenoxy)acetate hydrochloride was obtained as a sticky solid (898 mg, quant). HPLC purity >95%, MS (ESI) 507.4 [M + H]<sup>+</sup>. Methyl (R)-2-((4-(2-(2-(2-amino-3-phenylpropanamido)ethyl)phenoxy)methyl)-6-ethoxyphenoxy)acetate hydrochloride (392 mg, 0.72 mmol) was dissolved in dichloromethane (2 mL), and the solution was washed twice with saturated aqueous NaHCO<sub>3</sub>. The organic layer was dried over anhydrous sodium sulfate and stored. (S)-2-((*tert*-Butoxycarbonyl)amino)-2-phenylacetic acid (0.18 g, 0.72 mmol, 1.0 equiv) was treated with EDCI·HCl (0.14 g, 0.72 mmol, 1.0 equiv) and Oxyma Pure (0.103 g, 0.72 mmol, 1.0 equiv) and stirred for 15 min. Both solutions were combined and the material was stirred at room temperature for 3 h. The reaction mixture was concentrated under reduced pressure and the resulting crude methyl 2-((4-(2-((R)-2-((S)-2-amino-2-phenylacetamido)-(*tert*-butoxycarbonylamino)-3-phenylpropanamido)ethyl)phenoxy)methyl)-6-ethoxyphenoxy)acetate was used without further purification in the next step. Part of the crude material (approximately 0.37 mmol) was dissolved in a solution of HCl in 1,4-dioxane (4 N, 1.87 mL, 7.46 mmol, 2 equiv), and the solution was stirred at room temperature for

Scheme 3. SPPS-Based Synthetic Route toward NH-Linked Compounds<sup>a</sup>

<sup>a</sup>Reagents and conditions: [i] piperidine, DMF; [ii] Fmoc-D-phenylalanine, HATU, *N,N'*-diisopropylcarbodiimide (DIC), DMF; [iii] Fmoc-L-phenylglycine, Oxyma Pure, DIC, DMF; [iv] *cis*-4-(Fmoc-amino)cyclohexylacetic acid, HATU, DIPEA, DMF; [v] **77a**, **b** or **c**, Oxyma Pure, DIC, DMF; [vi] TFA (2.5%) in DCM; [vii] NaBH(OAc)<sub>3</sub>, DMF/DCM; [viii] TFA (2%) in DCM; [ix] TFA, DCM; [x] NaCNBH<sub>3</sub>, CHCl<sub>3</sub>/DMF; [xi] MeNH<sub>2</sub> in EtOH, Oxyma Pure, EDCI, DMF.

45 min, after which it was concentrated *in vacuo*. The residue was taken up in dichloromethane (4 mL) and triethylamine (0.104 mL, 0.746 mmol, 2 equiv) was added. The resulting solution was stored and used as such in the next step. *N*-Boc-*cis*-1,4-aminocyclohexylacetic acid–OH (96 mg, 0.37 mmol, 1 equiv), HATU (71.5 mg, 0.37 mmol, 1 equiv), and triethylamine (0.104 mL, 0.746 mmol, 1 equiv) were suspended in dichloromethane (4 mL), and the mixture was stirred for 15 min. Both solutions were combined and the resulting mixture was stirred at room temperature overnight. The reaction mixture was washed with saturated aqueous NaHCO<sub>3</sub>, 1 N aqueous KHSO<sub>4</sub>, and brine. The organic layer was dried over Na<sub>2</sub>SO<sub>4</sub>, and solvents were evaporated *in vacuo*, resulting in methyl 2-(2-((4-(2-((*R*)-2-((*S*)-2-(2-((*cis*-4-((*tert*-butoxycarbonyl)amino)cyclohexyl)acetamido)-2-phenylacetamido)-3-phenylpropanamido)ethyl)phenoxy)methyl)-6-ethoxyphenoxy)acetate, which was used without further purification (312 mg, 89%). HPLC purity 94%, MS (ESI) 879.4 [M + H]<sup>+</sup>. Methyl 2-(2-((4-(2-((*R*)-2-((*S*)-2-(2-((*cis*-4-((*tert*-butoxycarbonyl)-

amino)cyclohexyl)acetamido)-2-phenylacetamido)-3-phenylpropanamido)ethyl)phenoxy)methyl)-6-ethoxyphenoxy)-acetate (138 mg, 0.16 mmol) was dissolved in tetrahydrofuran (4 mL) and water (1 mL) and aqueous NaOH (4 N, 0.20 mL, 0.79 mmol, 5 equiv) was added. The reaction mixture was stirred at room temperature for 2 h, concentrated *in vacuo*, the residue was suspended in HCl in 1,4-dioxane (4 N, 0.98 mL, 3.92 mmol), and stirred at room temperature for 45 min. The resulting mixture was concentrated *in vacuo*. Triethylamine (63.5 mg, 0.088 mL, 0.63 mmol, 4 equiv), Oxyma Pure (26.8 mg, 0.19 mmol, 1.2 equiv), *N,N*-dimethylformamide (1 mL) and dichloromethane (9 mL) were added. When all material had dissolved, EDCI-HCl (36.1 mg, 0.19 mmol, 1.2 equiv) was added and the mixture was stirred at room temperature for 16 h. HATU (29.8 mg, 0.079 mmol, 0.5 equiv) was added and stirring was continued for 5 h to reach full conversion. The resulting mixture was concentrated *in vacuo* and the residue was purified by preparative HPLC (ammonium formate in water/acetonitrile), affording **3** as a



white solid (37 mg, 36%).  $^1\text{H}$  NMR (400 MHz,  $\text{CDCl}_3$ ):  $\delta$  7.33–7.24 (m, 3H), 7.21 (d,  $J$  = 8.2 Hz, 1H), 7.18–7.09 (m, 5H), 7.09–7.00 (m, 3H), 6.99–6.89 (m, 6H), 6.52 (d,  $J$  = 6.5 Hz, 1H), 6.35 (t,  $J$  = 5.8 Hz, 1H), 6.06 (d,  $J$  = 8.3 Hz, 1H), 5.21 (d,  $J$  = 6.4 Hz, 1H), 5.14 (d, A of AB,  $J$  = 11.6 Hz, 1H), 5.09 (d, B of AB,  $J$  = 11.6 Hz, 1H), 4.75 (d, A of AB,  $J$  = 14.8 Hz, 1H), 4.54 (q,  $J$  = 7.2 Hz, 1H), 4.47 (d, B of AB,  $J$  = 14.8 Hz, 1H), 4.20–4.13 (m, 1H), 4.08 (q,  $J$  = 7.0 Hz, 2H), 3.53–3.35 (m, 2H), 3.02 (d,  $J$  = 6.8 Hz, 2H), 2.72 (t,  $J$  = 5.7 Hz, 2H), 2.16 (dd, A of ABX,  $J$  = 14.4, 5.2 Hz, 1H), 2.06 (dd, B of ABX,  $J$  = 14.3, 9.1 Hz, 1H), 1.94–1.81 (m, 1H), 1.81–1.70 (m, 1H), 1.66–1.49 (m, 5H), 1.46 (t,  $J$  = 6.9 Hz, 3H), 1.37–1.17 (m, 2H);  $^{13}\text{C}$  NMR (101 MHz,  $\text{DMSO}-d_6$ ):  $\delta$  171.8, 171.7, 170.3, 167.3, 157.3, 151.8, 145.8, 138.9, 138.4, 132.6, 130.9, 130.3, 129.5, 128.4, 127.5, 127.2, 126.5, 124.9, 122.0, 115.1, 114.5, 71.8, 66.1, 64.4, 56.1, 54.7, 45.0, 41.1, 40.6, 40.4, 40.2, 40.0, 39.8, 39.6, 39.4, 37.7, 33.8, 32.8, 29.0, 28.5, 27.2, 15.2; HPLC purity >95%, MS (ESI): 747.3 ( $\text{M} + \text{H}$ ) $^+$ ; HRMS:  $\text{C}_{44}\text{H}_{50}\text{N}_4\text{O}_7$  [ $\text{M} + \text{H}$ ] $^+$ , calc.  $m/z$  747.3752, found 747.3743,  $-1.27\Delta\text{ppm}$ .

The following compound was prepared via the same procedure as 3, using the appropriate starting materials:

**Compound 18.** 3.5 mg;  $^1\text{H}$  NMR (400 MHz,  $\text{CDCl}_3$ ):  $\delta$  7.43 (d,  $J$  = 7.8 Hz, 1H), 7.30–7.15 (m, 6H), 7.09 (d, AA' of AA'BB',  $J$  = 8.5 Hz, 2H), 7.06–6.96 (m, 5H), 6.90 (dd, B of ABX,  $J$  = 8.3, 1.5 Hz, 1H), 6.84 (dd, B of ABX,  $J$  = 7.6, 1.5 Hz, 1H), 6.76 (d, BB' of AA'BB',  $J$  = 7.1 Hz, 2H), 6.38 (d,  $J$  = 5.3 Hz, 1H), 5.93 (t,  $J$  = 5.5 Hz, 1H), 5.39 (d,  $J$  = 8.1 Hz, 1H), 5.26 (d, A of AB,  $J$  = 12.4 Hz, 1H), 5.17 (d, B of AB,  $J$  = 12.5 Hz, 1H), 5.07 (d,  $J$  = 5.3 Hz, 1H), 4.69 (d, A of AB,  $J$  = 15.0 Hz, 1H), 4.60 (d, B of AB,  $J$  = 15.0 Hz, 1H), 4.56 (td,  $J$  = 7.9, 5.6 Hz, 1H), 4.21–4.12 (m, 1H), 4.07 (q,  $J$  = 6.9 Hz, 2H), 3.59–3.46 (m, 1H), 3.25–3.14 (m, 1H), 3.13 (dd, A of ABX,  $J$  = 14.3, 5.7 Hz, 1H), 2.97 (dd, B of ABX,  $J$  = 14.3, 7.8 Hz, 1H), 2.82–2.62 (m, 2H), 2.18 (dd, A of ABX,  $J$  = 13.3, 5.8 Hz, 1H), 1.95 (dd, B of ABX,  $J$  = 13.4, 9.4 Hz, 1H), 1.88–1.74 (m, 2H), 1.72–1.50 (m, 5H), 1.46 (t,  $J$  = 6.9 Hz, 3H), 1.36–1.10 (m, 2H); MS (ESI): 747.3 ( $\text{M} + \text{H}$ ) $^+$ .

**Synthesis of 2 (route II, Scheme 1).** Ethyl 2-(2-ethoxy-6-(hydroxymethyl)phenoxy)acetate (3.07 g, 9.68 mmol) was dissolved in dichloromethane (150 mL) and cooled to 0 °C. Phosphorus tribromide (2.23 mL, 23.6 mmol, 2.4 equiv) was added, and the reaction mixture was stirred at room temperature for 2.5 h, after which the reaction mixture was concentrated *in vacuo*. Silica gel chromatography of the residue (0 to 30% ethyl acetate in *n*-heptane) afforded an orange oil, which was dissolved in ethyl acetate (70 mL) and washed with saturated aqueous  $\text{NaHCO}_3$  and brine (30 mL). The organic layer was dried over  $\text{Na}_2\text{SO}_4$  and concentrated *in vacuo* to afford ethyl 2-(2-(bromomethyl)-6-ethoxyphenoxy)acetate as a clear oil (3.07 g, 82%). HPLC purity >95%, MS (ESI) 317.1/319.1 [ $\text{M} + \text{H}$ ] $^+$ . To a suspension of ethyl 2-(2-(bromomethyl)-6-ethoxyphenoxy)acetate (1.37 g, 4.32 mmol) and *tert*-butyl (S)-(3-(4-hydroxyphenyl)-1-(methylamino)-1-oxopropan-2-yl)carbamate (1.27 g, 4.32 mmol, 1.0 equiv) in anhydrous acetonitrile (50 mL) was added potassium carbonate (1.19 g, 8.64 mmol, 2.0 equiv). The reaction mixture was stirred at 80 °C for 16 h, cooled to room temperature and solids were removed by filtration. The filtrate was concentrated *in vacuo* and the residue was purified by silica gel column chromatography (10 to 80% ethyl acetate in heptane) to afford ethyl (S)-2-(2-((4-(2-((*tert*-butoxycarbonyl)amino)-3-(methylamino)-3-oxopropyl)phenoxy)methyl)-6-ethoxyphenoxy)acetate as a white solid (1.67 g, 73%). HPLC purity >95%, MS (ESI) 531.2 [ $\text{M} + \text{H}$ ] $^+$ . Ethyl (S)-2-(2-((4-(2-((*tert*-butoxycarbonyl)amino)-3-(methylamino)-3-oxopropyl)phenoxy)methyl)-6-ethoxyphenoxy)acetate (1.65 g, 3.11 mmol) was dissolved in 1,4-dioxane (14 mL) and HCl in 1,4-dioxane (4 N, 7.77 mL, 31.1 mmol, 10 equiv) was added. The reaction mixture was stirred under a nitrogen atmosphere at room temperature for 3 h, after which the volatiles were removed *in vacuo* and the residue was co-evaporated with diethyl ether. Trituration in diisopropylether (20 mL) for 20 min, followed by filtration afforded ethyl (S)-2-(2-((4-(2-amino-3-(methylamino)-3-oxopropyl)phenoxy)methyl)-6-ethoxyphenoxy)acetate hydrochloride as a white solid (1.37 g, 94%). HPLC purity >95%, MS (ESI) 431.2 [ $\text{M} + \text{H}$ ] $^+$ . *N*-Boc-D-phenylalanine (344 mg, 1.30 mmol, 1.1 equiv) was dissolved

in dichloromethane (5 mL), and HATU (493 mg, 1.30 mmol, 1.1 equiv) and triethylamine (0.172 mL, 1.24 mmol, 1.1 equiv) were added. The reaction mixture was stirred at room temperature for 20 min, and the resulting solution was added slowly to a solution of ethyl (S)-2-(2-((4-(2-amino-3-(methylamino)-3-oxopropyl)phenoxy)methyl)-6-ethoxyphenoxy)acetate hydrochloride (550 mg, 1.15 mmol) and triethylamine (0.172 mL, 1.24 mmol, 1.1 equiv) in dichloromethane (5 mL). Stirring was continued for 1.5 h, after which the reaction mixture was concentrated *in vacuo*. The residue was dissolved in ethyl acetate, and the organic layer was washed with 1 N aqueous  $\text{KHSO}_4$ , saturated aqueous  $\text{NaHCO}_3$ , and brine. The organic layer was dried over  $\text{Na}_2\text{SO}_4$  and concentrated. Purification by silica gel column chromatography (10 to 100% ethyl acetate in *n*-heptane) afforded ethyl 2-(2-((4-((S)-2-((*tert*-butoxycarbonyl)amino)-3-phenylpropanamido)-3-(methylamino)-3-oxopropyl)phenoxy)methyl)-6-ethoxyphenoxy)acetate as a white solid (737 mg, 92%). HPLC purity >95%, MS (ESI) 678.3 [ $\text{M} + \text{H}$ ] $^+$ .

Conversion into the Boc-/ester-containing precursor and subsequent macrocyclization were performed following the procedures described for 3 in route I. Purification by preparative HPLC afforded 2 as a white solid (20 mg, 39%),  $^1\text{H}$  NMR (400 MHz,  $\text{CDCl}_3$ ):  $\delta$  7.35–7.24 (m, 2H), 7.17–7.04 (m, 10H), 7.00 (dd,  $J$  = 7.7, 1.5 Hz, 1H), 6.96–6.84 (m, 5H), 6.49 (d,  $J$  = 8.2 Hz, 1H), 6.40 (d,  $J$  = 5.9 Hz, 1H), 6.35 (q,  $J$  = 4.8 Hz, 1H), 5.23 (d,  $J$  = 5.9 Hz, 1H), 5.09 (d, A of AB,  $J$  = 11.2 Hz, 1H), 5.04 (d, B of AB,  $J$  = 11.1 Hz, 1H), 4.83 (d, A of AB,  $J$  = 14.7 Hz, 1H), 4.71–4.61 (m, 2H), 4.39 (d, B of AB,  $J$  = 14.9 Hz, 1H), 4.17–4.05 (m, 1H), 4.09 (q,  $J$  = 7.0 Hz, 2H), 3.16 (dd, A of ABX,  $J$  = 14.7, 7.6 Hz, 1H), 3.12 (dd, A of ABX,  $J$  = 14.4, 4.9 Hz, 1H), 3.02 (dd, B of ABX,  $J$  = 14.3, 9.4 Hz, 1H), 3.00 (dd, B of ABX,  $J$  = 14.8, 3.9 Hz, 1H), 2.72 (d,  $J$  = 4.7 Hz, 3H), 2.09 (dd, A of ABX,  $J$  = 14.7, 5.9 Hz, 1H), 2.03 (dd, B of ABX,  $J$  = 14.8, 8.6 Hz, 1H), 1.85–1.63 (m, 2H), 1.62–1.37 (m, 5H), 1.46 (t,  $J$  = 6.9 Hz, 3H), 1.32–1.15 (m, 1H), 1.15–1.01 (m, 1H);  $^{13}\text{C}$  NMR (101 MHz,  $\text{DMSO}-d_6$ ):  $\delta$  171.5, 171.1, 170.2, 167.3, 157.4, 151.7, 145.7, 139.3, 138.3, 130.8, 130.8, 130.7, 129.2, 128.6, 128.5, 127.7, 127.4, 126.5, 125.0, 121.9, 114.9, 114.4, 71.9, 66.0, 64.4, 56.8, 55.2, 55.1, 44.7, 40.6, 40.4, 40.2, 40.0, 39.8, 39.6, 37.6, 36.9, 32.7, 28.9, 28.6, 28.4, 26.8, 26.1, 15.2; HPLC purity >95%, MS (ESI): 804.5 ( $\text{M} + \text{H}$ ) $^+$ ; HRMS:  $\text{C}_{46}\text{H}_{53}\text{N}_5\text{O}_8$  [ $\text{M} + \text{H}$ ] $^+$ , calc.  $m/z$  804.3967, found 804.3959,  $-0.99\Delta\text{ppm}$ .

The following compounds were prepared via the same procedure as 2, using the appropriate starting materials:

**Compound 19.** 15.2 mg;  $^1\text{H}$  NMR (400 MHz,  $\text{CDCl}_3$ ):  $\delta$  7.37–7.22 (m, 2H), 7.22–7.04 (m, 7H), 7.03–6.97 (m, 5H), 6.92 (dd,  $J$  = 8.4, 6.6 Hz, 3H), 6.85–6.76 (m, 2H), 6.35 (t,  $J$  = 5.8 Hz, 1H), 5.51 (d,  $J$  = 7.8 Hz, 1H), 5.14 (s, 2H), 4.68 (d,  $J$  = 14.9 Hz, 1H), 4.47 (d,  $J$  = 14.9 Hz, 1H), 4.40 (td,  $J$  = 7.9, 5.5 Hz, 1H), 4.21–4.12 (m, 1H), 4.06 (q,  $J$  = 7.0 Hz, 2H), 3.59 (ddd,  $J$  = 13.4, 6.8, 3.9 Hz, 1H), 3.38 (ddd,  $J$  = 13.3, 8.9, 4.5 Hz, 1H), 3.00 (qd,  $J$  = 14.2, 6.8 Hz, 2H), 2.76 (ddd,  $J$  = 14.5, 7.1, 3.6 Hz, 1H), 2.67 (ddd,  $J$  = 14.4, 8.2, 3.8 Hz, 1H), 2.10 (dd,  $J$  = 13.7, 5.5 Hz, 1H), 2.00 (dd,  $J$  = 13.7, 8.5 Hz, 1H), 1.90–1.34 (m, 13H, partial overlap with water signal), 1.32–1.06 (m, 2H); MS (ESI): 761.5 ( $\text{M} + \text{H}$ ) $^+$ .

**Compound 20.** 12.2 mg;  $^1\text{H}$  NMR (400 MHz,  $\text{CDCl}_3$ ):  $\delta$  8.50 (dd,  $J$  = 4.8, 1.7 Hz, 1H), 8.45 (d,  $J$  = 2.4 Hz, 1H), 7.35 (dt,  $J$  = 7.9, 2.0 Hz, 1H), 7.25–7.18 (m, 1H), 7.17–7.00 (m, 7H), 7.00–6.84 (m, 7H), 6.68 (d,  $J$  = 6.8 Hz, 1H), 6.36 (t,  $J$  = 5.8 Hz, 1H), 5.37 (d,  $J$  = 6.8 Hz, 1H), 5.19–5.02 (m, 2H), 4.77 (d,  $J$  = 14.8 Hz, 1H), 4.54 (td,  $J$  = 8.6, 5.6 Hz, 1H), 4.45 (d,  $J$  = 14.8 Hz, 1H), 4.16 (br s, 1H), 4.08 (q,  $J$  = 7.0 Hz, 2H), 3.56–3.46 (m, 1H), 3.41–3.32 (m, 1H), 3.08 (dd,  $J$  = 14.2, 5.6 Hz, 1H), 2.92 (dd,  $J$  = 14.2, 8.8 Hz, 1H), 2.70 (m, 2H), 2.18 (dd,  $J$  = 14.3, 5.1 Hz, 1H), 2.07 (dd,  $J$  = 14.3, 9.4 Hz, 1H), 1.88 (br s, 1H), 1.81–1.41 (m, 8H, partial overlap with water signal), 1.27 (dd,  $J$  = 22.5, 9.9 Hz, 3H); MS (ESI): 748.4 ( $\text{M} + \text{H}$ ) $^+$ .

**Compound 21.** 12.4 mg;  $^1\text{H}$  NMR (400 MHz,  $\text{CDCl}_3$ ):  $\delta$  7.94 (d,  $J$  = 5.4 Hz, 1H), 7.24 (d,  $J$  = 8.0 Hz, 1H, partial overlap with NMR solvent peak), 7.17–7.09 (m, 3H), 7.09–6.84 (m, 10H), 6.65 (d,  $J$  = 6.8 Hz, 1H), 6.53 (d,  $J$  = 1.3 Hz, 1H), 6.48 (dd,  $J$  = 5.3, 1.6 Hz, 1H), 6.35 (t,  $J$  = 5.8 Hz, 1H), 5.27 (d,  $J$  = 6.8 Hz, 1H), 5.11 (h,  $J$  = 15.7, 15.3 Hz, 2H), 4.76 (d,  $J$  = 14.8 Hz, 1H), 4.58–4.39 (m, 2H), 4.22–



4.02 (m, 3H), 3.90 (s, 3H), 3.48 (dt,  $J = 10.1, 4.9$  Hz, 1H), 3.36 (dt,  $J = 16.6, 5.3$  Hz, 1H), 3.11 (dd,  $J = 14.2, 5.6$  Hz, 1H), 2.94 (dd,  $J = 14.2, 9.0$  Hz, 1H), 2.81–2.60 (m, 2H), 2.30–2.16 (m, 1H), 2.14–2.06 (m, 1H), 1.91 (br s, 1H), 1.86–1.42 (m, 9H, partial overlap with water signal), 1.29 (m, 2H); MS (ESI): 778.5 ( $M + H$ )<sup>+</sup>.

**Compound 22.** 18.9 mg; <sup>1</sup>H NMR (400 MHz, CDCl<sub>3</sub>):  $\delta$  7.37–7.13 (m, 6H), 7.09–6.82 (m, 6H), 6.80–6.73 (m, 4H), 6.67–6.60 (m, 2H), 5.14–4.94 (m, 2H), 4.73–4.61 (m, 2H), 4.60–4.44 (m, 1H), 4.16–4.02 (m, 3H), 3.61 (br s, 1H), 3.28–3.18 (m, 1H), 3.14–2.99 (m, 3H), 2.81–2.56 (m, 4H), 2.11–2.02 (m, 1H), 1.99–1.90 (m, 1H), 1.69–1.37 (m, 10H), 1.27–1.06 (m, 2H); MS (ESI): 751.4 ( $M + H$ )<sup>+</sup>.

**Compound 23.** 9.8 mg; <sup>1</sup>H NMR (400 MHz, CDCl<sub>3</sub>):  $\delta$  7.35–7.18 (m, 3H, partial overlap with NMR solvent peak), 7.11–7.04 (m, 4H), 6.99–6.91 (m, 4H), 6.90–6.83 (m, 4H), 6.70–6.65 (m, 2H), 6.52 (d,  $J = 8.4$  Hz, 1H), 6.20 (t,  $J = 5.9$  Hz, 1H), 5.59 (d,  $J = 7.4$  Hz, 1H), 5.06 (s, 2H), 4.70 (d,  $J = 14.8$  Hz, 1H), 4.63 (q,  $J = 7.0$  Hz, 1H), 4.53 (d,  $J = 14.9$  Hz, 1H), 4.38 (q,  $J = 7.4$  Hz, 1H), 4.10 (dq,  $J = 12.9, 6.4$  Hz, 3H), 3.50 (dq,  $J = 10.8, 5.3$  Hz, 1H), 3.32 (dq,  $J = 12.4, 5.9$  Hz, 1H), 3.10–2.71 (m, 5H), 2.66 (t,  $J = 5.6$  Hz, 2H), 1.90 (dd,  $J = 13.2, 7.3$  Hz, 1H), 1.79–1.35 (m, 10H), 1.15 (d,  $J = 13.4$  Hz, 1H), 1.03 (t,  $J = 12.1$  Hz, 1H), 0.83 (m, 1H); MS (ESI): 777.5 ( $M + H$ )<sup>+</sup>.

**Compound 24.** 15.9 mg; <sup>1</sup>H NMR (400 MHz, CDCl<sub>3</sub>):  $\delta$  8.25 (d,  $J = 2.5$  Hz, 1H), 7.62 (d,  $J = 7.8$  Hz, 1H), 7.37 (d,  $J = 8.1$  Hz, 1H), 7.25–7.19 (m, 1H), 7.19–7.09 (m, 5H), 7.05 (t,  $J = 7.9$  Hz, 1H), 6.96–6.85 (m, 5H), 6.80–6.71 (m, 4H), 6.10 (t,  $J = 6.0$  Hz, 1H), 5.95 (d,  $J = 8.2$  Hz, 1H), 5.86 (d,  $J = 7.3$  Hz, 1H), 5.07–4.97 (m, 2H), 4.76 (d,  $J = 14.9$  Hz, 1H), 4.60–4.45 (m, 3H), 4.15–4.05 (m, 3H), 3.52–3.42 (m, 1H), 3.28–3.11 (m, 2H), 3.07–2.95 (m, 2H), 2.71–2.56 (m, 2H), 2.50 (dd,  $J = 13.8, 5.7$  Hz, 1H), 1.96–1.58 (m, 5H, partial overlap with water signal), 1.58–1.40 (m, 6H), 1.40–1.29 (m, 1H), 1.01 (m, 2H); MS (ESI): 800.4 ( $M + H$ )<sup>+</sup>.

**Compound 25.** 8.0 mg; <sup>1</sup>H NMR (400 MHz, CDCl<sub>3</sub>):  $\delta$  7.36–7.19 (m, 4H), 7.19–7.11 (m, 2H), 7.09–6.98 (m, 3H), 6.97–6.82 (m, 4H), 6.58–6.43 (m, 2H), 6.27 (d,  $J = 7.9$  Hz, 1H), 5.19–5.06 (m, 2H), 4.79–4.46 (m, 3H), 4.23 (q,  $J = 5.9$  Hz, 1H), 4.20–4.13 (m, 1H), 4.09 (q,  $J = 7.0$  Hz, 2H), 3.74 (m, 1H), 3.53–3.35 (m, 2H), 3.34–3.16 (m, 2H), 3.06 (td,  $J = 13.8, 8.4$  Hz, 1H), 2.78 (m, 2H), 2.33 (t,  $J = 6.7$  Hz, 2H), 2.09–1.80 (m, 7H), 1.77–1.41 (m, 10H), 1.67–1.37 (m, 16H), 1.33–1.04 (m, 2H); MS (ESI): 745.5 ( $M + H$ )<sup>+</sup>.

**Compound 26.** 13.4 mg; <sup>1</sup>H NMR (400 MHz, CDCl<sub>3</sub>):  $\delta$  7.35–7.16 (m, 6H), 7.08–6.82 (m, 8H), 6.35 (t,  $J = 5.8$  Hz, 1H), 6.29 (d,  $J = 7.3$  Hz, 1H), 5.09 (q,  $J = 11.6$  Hz, 2H), 4.76–4.65 (m, 2H), 4.56–4.47 (m, 2H), 4.17 (dt,  $J = 8.3, 4.0$  Hz, 1H), 4.08 (q,  $J = 6.9$  Hz, 2H), 3.52–3.38 (m, 2H), 3.27 (dd,  $J = 14.4, 5.1$  Hz, 1H), 3.05–2.90 (m, 2H), 2.88 (s, 3H), 2.76–2.62 (m, 2H), 2.56 (dt,  $J = 14.7, 7.6$  Hz, 1H), 2.13–1.81 (m, 4H), 1.80–1.39 (m, 5H, partial overlap with water signal), 1.36–1.07 (m, 3H); MS (ESI): 777.3 ( $M + H$ )<sup>+</sup>.

**Compound 27.** 23.5 mg; <sup>1</sup>H NMR (400 MHz, CDCl<sub>3</sub>):  $\delta$  7.47 (d,  $J = 8.4$  Hz, 1H), 7.38–7.14 (m, 5H), 7.10–6.72 (m, 7H), 6.49 (d,  $J = 8.3$  Hz, 1H), 6.32–6.16 (m, 1H major), 5.97–5.80 (m, 1H), 5.15–5.05 (m, 2H), 4.76–4.55 (m, 3H), 4.33 (dd,  $J = 6.9, 3.1$  Hz, 1H), 4.28–4.20 (m, 1H), 4.07 (q,  $J = 7.0$  Hz, 2H), 3.83 (qd,  $J = 6.3, 3.0$  Hz, 1H), 3.69 (m, 1H), 3.30 (dd,  $J = 14.0, 6.8$  Hz, 1H), 3.26–3.10 (m, 4H), 3.02 (dd,  $J = 14.0, 5.2$  Hz, 1H), 2.69–2.51 (m, 2H), 2.23–2.06 (m, 2H), 2.03–1.92 (m,  $J = 13.2, 6.2$  Hz, 1H), 1.85–1.53 (m, 6H, partial overlap with water signal), 1.51–1.28 (m, 5H), 0.78 (d,  $J = 6.3$  Hz, 3H); MS (ESI): 729.4 ( $M + H$ )<sup>+</sup>.

**Compound 28 (4:1 Mixture of Diastereoisomers).** 24 mg; <sup>1</sup>H NMR (400 MHz, DMSO-*d*<sub>6</sub>):  $\delta$  9.23–9.09 (m, 1H, major), 8.71 (d,  $J = 8.2$  Hz, 1H, minor), 8.52–8.43 (m, 1H, major), 8.26–8.18 (m, 1H, minor), 7.34–6.93 (m, 14H, major + minor), 6.94–6.81 (m, 3H, major + minor), 5.82 (d,  $J = 9.2$  Hz, 1H, minor), 5.71 (d,  $J = 9.1$  Hz, 1H, major), 5.52–5.32 (m, 1H, minor), 5.25–5.06 (m, 1H, major + minor), 4.99 (q,  $J = 9.7$  Hz, 2H, major + minor), 4.80 (d,  $J = 6.7$  Hz, 1H, major), 4.64 (d,  $J = 13.9$  Hz, 1H, major), 4.60–4.35 (m, 2H, minor), 4.21 (d,  $J = 13.9$  Hz, 1H, major), 4.09 (dq,  $J = 10.3, 7.0$  Hz, 3H, major), 3.76 (s, 2H, minor), 3.65 (br s, 1H, major + minor), 3.62–3.47 (m, 1H, major + minor), 3.26–3.11 (m, 1H, major +

minor), 2.98 (dd,  $J = 13.6, 6.0$  Hz, 1H, major + minor), 2.85 (s, 3H, major + minor), 2.74–2.54 (m, major + minor), 2.34–2.09 (m, 1H, major, 2H minor), 1.97 (d,  $J = 13.2$  Hz, 1H, minor), 1.87 (dd,  $J = 14.9, 2.9$  Hz, 1H, major), 1.75 (br s, 1H, major), 1.64–1.07 (m, 8H, major + minor), 1.02–0.82 (m, 2H major, 3H minor), 0.59 (br s, 1H, major); MS (ESI): 761.4 ( $M + H$ )<sup>+</sup>.

**Compound 29.** 4.2 mg; <sup>1</sup>H NMR (400 MHz, CDCl<sub>3</sub>):  $\delta$  7.33–6.84 (m, 18H), 6.68 (d,  $J = 6.5$  Hz, 1H), 6.33–6.17 (m, 1H), 5.65 (d,  $J = 8.2$  Hz, 1H), 5.48–5.37 (m, 1H), 5.25–5.96 (m, 3H), 4.75–4.58 (m, 2H), 4.15 (m, 1H), 4.08 (q,  $J = 6.9$  Hz, 2H), 3.57–3.35 (m, 2H), 3.29–3.13 (m, 1H), 3.08–2.74 (m, 4H), 2.57 (s, 3H), 2.19–2.10 (m, 1H), 2.05 (m, 1H), 1.89–1.35 (m, 7H), 1.46 (t,  $J = 7.0$  Hz, 3H), 1.31–1.09 (m, 2H); MS (ESI): 761.4 ( $M + H$ )<sup>+</sup>.

**Compound 30.** 30 mg; <sup>1</sup>H NMR (400 MHz, DMSO-*d*<sub>6</sub>):  $\delta$  8.79 (d,  $J = 8.8$  Hz, 1H), 7.96 (t,  $J = 5.8$  Hz, 1H), 7.44 (d,  $J = 8.4$  Hz, 1H), 7.25–7.13 (m, 9H), 7.11–7.00 (m, 6H), 6.85 (d,  $J = 8.6$  Hz, 2H), 6.69 (d,  $J = 7.5$  Hz, 2H), 6.27 (s, 1H), 5.14 (d,  $J = 10.9$  Hz, 1H), 4.99 (d,  $J = 10.9$  Hz, 1H), 4.71–4.64 (m, 1H), 4.59 (d,  $J = 14.0$  Hz, 1H), 4.18 (d,  $J = 14.1$  Hz, 1H), 4.08 (q,  $J = 6.9$  Hz, 2H), 3.76 (br s, 1H), 3.61–3.46 (m, 1H), 2.99 (dd,  $J = 13.9, 4.2$  Hz, 1H), 2.96–2.86 (m, 1H), 2.75 (s, 3H), 2.68–2.55 (m, 3H), 2.16 (dd,  $J = 15.5, 4.0$  Hz, 1H), 1.96–1.85 (m, 1H), 1.63–1.40 (m, 4H), 1.38–1.32 (m, 5H), 1.29–1.00 (m, 5H); MS (ESI): 761.4 ( $M + H$ )<sup>+</sup>.

**Compound 31.** 102 mg; <sup>1</sup>H NMR (400 MHz, DMSO-*d*<sub>6</sub>):  $\delta$  8.33 (d,  $J = 7.9$  Hz, 1H), 8.01 (dd,  $J = 6.7, 4.7$  Hz, 1H), 7.53 (d,  $J = 8.0$  Hz, 1H), 7.33–7.15 (m, 12H), 7.09–7.00 (m, 3H), 6.88 (d,  $J = 8.2$  Hz, 2H), 5.02 (dd, 2H), 4.39 (s, 3H), 4.13–4.00 (m, 4H), 3.79 (br s, 1H), 3.51 (d,  $J = 10.0$  Hz, 1H), 2.95 (dd,  $J = 13.8, 4.8$  Hz, 2H), 2.80–2.60 (m, 3H), 2.09–1.96 (m, 2H), 1.77–1.43 (m, 4H), 1.41–1.31 (m, 6H), 1.21–0.99 (m, 2H); MS (ESI): 747.4 ( $M + H$ )<sup>+</sup>.

**Compound 32.** 130 mg; <sup>1</sup>H NMR (400 MHz, DMSO-*d*<sub>6</sub>, mixture of conformers):  $\delta$  8.35 (d,  $J = 6.9$  Hz, 0.6H), 8.08 (m, 0.4H), 7.71–7.62 (m, 0.6H), 7.49 (d,  $J = 8.0$  Hz, 0.4H), 7.42–7.16 (m, 10H), 7.16–6.99 (m, 5H), 6.93 (dd,  $J = 8.6, 6.3$  Hz, 2H), 5.91–5.84 (m, 1H), 5.22–4.99 (m, 2H), 4.65–4.37 (m, 3H), 4.30 (dd,  $J = 13.9, 2.8$  Hz, 1H), 4.13–4.03 (m, 2H), 3.90 (br s, 1H), 3.80 (br s, 1H), 3.74–3.55 (m, 1H), 3.50 (m, 0.5H), 3.27 (dd,  $J = 13.0, 6.4$  Hz, 0.5H), 3.15 (m, 1H), 2.71–2.61 (m, 2H), 2.41–2.27 (m, 1.5H), 2.03 (dd,  $J = 13.3, 5.2$  Hz, 0.5H), 1.89 (br s, 1H), 1.72–1.25 (m, 10H); MS (ESI): 747.4 ( $M + H$ )<sup>+</sup>.

**Compound 33.** 61 mg; <sup>1</sup>H NMR (400 MHz, DMSO-*d*<sub>6</sub>, mixture of conformers):  $\delta$  8.11 (m, 0.35H), 7.89 (t,  $J = 5.9$  Hz, 0.65H), 7.61 (d,  $J = 8.1$  Hz, 1H), 7.40–7.23 (m, 11H), 7.18–7.02 (m, 4H), 6.91 (dd,  $J = 6.9, 5.0$  Hz, 2H), 5.12–5.02 (s, 0.7H), 5.02 (s, 1.3H), 4.72–4.35 (m, 6H), 4.20 (br s, 0.7H), 4.06 (q,  $J = 6.9$  Hz, 2H), 3.92–3.69 (m, 3.3H), 3.24 (br s, 2H), 2.83 (m, 0.35H), 2.74–2.68 (m, 1.65H), 2.07–1.98 (m, 1H), 1.83 (br s, 1H), 1.72–1.51 (m, 3H), 1.51–1.39 (m, 4H), 1.39–1.26 (m, 4H), 1.24–1.04 (m, 2H); MS (ESI): 747.4 ( $M + H$ )<sup>+</sup>.

**Synthesis of Building Block 74.** Under a nitrogen atmosphere, 2-(4-benzyloxyphenyl)ethanamine (70, 46.9 g, 206 mmol), 1-hydroxy-7-azabenzotriazole (2.87 g, 20.6 mmol, 0.1 equiv), and EDCI-HCl (44.4 g, 227 mmol, 1.1 equiv) were added to a solution of Boc-D-phenylalanine (61.4 g, 227 mmol, 1.1 equiv) in dichloromethane (700 mL) at 0 °C. The reaction was stirred at 0 °C for 1 h and allowed to warm to room temperature. The reaction mixture was successively washed with water, 0.1 M aqueous HCl, saturated aqueous NaHCO<sub>3</sub>, and brine. The organic layer was dried over Na<sub>2</sub>SO<sub>4</sub>, filtered, and concentrated under reduced pressure. Trituration of the resulting solid with diethyl ether afforded *tert*-butyl (R)-(1-((4-(benzyloxy)phenethyl)amino)-1-oxo-3-phenylpropan-2-yl)carbamate as a white solid (102 g, quant), HPLC purity >95%, MS (ESI) 497.2 [ $M + Na$ ]<sup>+</sup>. To a solution of *tert*-butyl (R)-(1-((4-(benzyloxy)phenethyl)amino)-1-oxo-3-phenylpropan-2-yl)carbamate (50 g, 105 mmol) in 1,4-dioxane (400 mL) was added HCl in dioxane (4 N, 395 mL, 1580 mmol, 15 equiv), and the mixture was stirred at room temperature under an argon atmosphere for 1 h. The volatiles were removed *in vacuo*, the residue was triturated with Et<sub>2</sub>O and dried affording (R)-2-amino-N-(4-(benzyloxy)phenethyl)-3-phenylpropanamide hydrochloride (44.3 g, quant), HPLC purity

>95%, MS (ESI) 375.2  $[M + H]^+$ . Under an argon atmosphere, EDCI-HCl (22.7 g, 116 mmol, 1.1 equiv) and Oxyma Pure (17.0 g, 116 mmol, 1.1 equiv) were added to a solution of *N*-Boc-1-phenylglycine (31.4 g, 121 mmol, 1.15 equiv) in dichloromethane (250 mL) at 0 °C, and the mixture was stirred at room temperature for 30 min. The resulting solution was added to a cooled (0 °C) solution of (R)-2-amino-*N*-(4-(benzyloxy)phenethyl)-3-phenylpropanamide hydrochloride (43.3 g, 105 mmol) and triethylamine (15.6 mL, 111 mmol, 1.05 equiv) in dichloromethane (250 mL). The reaction mixture was stirred at 0 °C for 1 h and slowly warmed to room temperature. The resulting mixture was washed with 0.1 N aqueous HCl, saturated  $\text{NaHCO}_3$ , and brine. The organic layer was dried over  $\text{Na}_2\text{SO}_4$ , filtered, and concentrated to afford a yellow solid. Trituration with  $\text{Et}_2\text{O}$  afforded *tert*-butyl ((S)-2-(((R)-1-((4-(benzyloxy)phenethyl)amino)-1-oxo-3-phenylpropan-2-yl)amino)-2-oxo-1-phenylethyl)carbamate as an off-white solid (49.9 g, 78%), HPLC purity >95%, MS (ESI) 608.4  $[M + H]^+$ . HCl in 1,4-dioxane (4 N, 308 mL, 1.23 mol, 15 equiv) was added to a solution of *tert*-butyl ((S)-2-(((R)-1-((4-(benzyloxy)phenethyl)amino)-1-oxo-3-phenylpropan-2-yl)amino)-2-oxo-1-phenylethyl)carbamate (49.9 g, 82 mmol) in 1,4-dioxane (300 mL), and the solution was stirred at room temperature under an argon atmosphere for 1 h. The volatiles were removed *in vacuo*, and the residue was triturated with  $\text{Et}_2\text{O}$  and dried affording (R)-2-((S)-2-amino-2-phenylacetamido)-*N*-(4-(benzyloxy)phenethyl)-3-phenylpropanamide hydrochloride (56.7 g, quant), HPLC purity >95%, MS (ESI) 508.2  $[M + H]^+$ . Under a nitrogen atmosphere, EDCI-HCl (17.7 g, 90 mmol, 1.1 equiv) and 1-hydroxy-7-azabenzotriazole (1.14 g, 8.22 mmol, 0.1 equiv) were added to a solution of (R)-2-((S)-2-amino-2-phenylacetamido)-*N*-(4-(benzyloxy)phenethyl)-3-phenylpropanamide hydrochloride (44.7 g, 82 mmol), triethylamine (12.2 mL, 86 mmol, 1.05 equiv), and *cis*-4-((*tert*-butoxycarbonyl)amino)cyclohexylacetic acid (25.6 g, 94 mmol, 1.15 equiv) in dichloromethane (4 mL) at 0 °C. The mixture was stirred for 2 h, while slowly warming to room temperature. The resulting mixture was washed with water, 0.1 N aqueous HCl, saturated aqueous  $\text{NaHCO}_3$ , and brine. The organic layer was dried over  $\text{Na}_2\text{SO}_4$ , filtered, and concentrated to provide a yellow solid. Trituration in  $\text{Et}_2\text{O}$  afforded *tert*-butyl *cis*-4-(2-(((S)-2-(((R)-1-((4-(benzyloxy)phenethyl)amino)-1-oxo-3-phenylpropan-2-yl)amino)-2-oxo-1-phenylethyl)amino)-2-oxoethyl)cyclohexyl)carbamate as a white solid (71, 59.5 g, 97%), HPLC purity >95%, MS (ESI) 747.5  $[M + H]^+$ . To a solution of *tert*-butyl *cis*-4-(2-(((S)-2-(((R)-1-((4-(benzyloxy)phenethyl)amino)-1-oxo-3-phenylpropan-2-yl)amino)-2-oxo-1-phenylethyl)amino)-2-oxoethyl)cyclohexyl)carbamate (59.4 g, 80 mmol) in tetrahydrofuran (250 mL) and methanol (750 mL) was added palladium on activated carbon (10%, 8.47 g, 7.96 mmol, 0.1 equiv). The reaction mixture was stirred at room temperature under a hydrogen atmosphere (1 bar) for 18 h filtered through a pad of Celite and the filter cake rinsed with methanol. The combined filtrates were concentrated *in vacuo* to provide *tert*-butyl *cis*-4-(2-(((S)-2-(((R)-1-((4-hydroxyphenethyl)amino)-1-oxo-3-phenylpropan-2-yl)amino)-2-oxo-1-phenylethyl)amino)-2-oxoethyl)cyclohexyl)carbamate as a crystalline white solid (50.7 g, 97%), HPLC purity >95%, MS (ESI) 657.5  $[M + H]^+$ . Cesium carbonate (4.56 g, 13.9 mmol, 1.3 equiv) and ethyl 2-(2-(bromomethyl)-6-ethoxy-4-iodophenoxy)acetate (72, 6.14 g, 13.9 mmol; prepared via bromination of ethyl 2-(2-ethoxy-6-(hydroxymethyl)-4-iodophenoxy)acetate as described in the synthesis of 2, *vide supra*) were added to a solution of *tert*-butyl *cis*-4-(2-(((S)-2-(((R)-1-((4-hydroxyphenethyl)amino)-1-oxo-3-phenylpropan-2-yl)amino)-2-oxo-1-phenylethyl)amino)-2-oxoethyl)cyclohexyl)carbamate (7.00 g, 10.7 mmol, 1.3 equiv) in *N,N*-dimethylformamide (75 mL), and the resulting suspension was stirred at room temperature under an argon atmosphere for 4 h. The resulting mixture was diluted with ethyl acetate and washed with water and brine. The organic layer was dried over  $\text{Na}_2\text{SO}_4$ , filtered, and concentrated. Trituration of the residue with diethyl ether afforded *tert*-butyl 2-(2-((4-(2-((R)-2-((S)-2-(2-(*cis*-4-((*tert*-butoxycarbonyl)amino)cyclohexyl)acetamido)-2-phenylacetamido)-3-phenylpropanamido)ethyl)phenoxy)methyl)-6-ethoxy-4-iodophenoxy)acetate as a white solid (73, 10.2 g, 94%), HPLC purity

>95%, MS (ESI) 1019.2  $[M + H]^+$ . Aqueous hydrochloric acid (5%, 50 mL, 70.1 mmol, 14 equiv) was added to a solution of ethyl 2-(2-((4-(2-((R)-2-((S)-2-(2-(*cis*-4-((*tert*-butoxycarbonyl)amino)cyclohexyl)acetamido)-2-phenylacetamido)-3-phenylpropanamido)ethyl)phenoxy)methyl)-6-ethoxy-4-iodophenoxy)acetate (5.0 g, 4.91 mmol) in 1,4-dioxane (200 mL), and the mixture was stirred at 40 °C under an argon atmosphere for 48 h. After that, HCl in 1,4-dioxane (4 N, 25 mL, 100 mmol, 20 equiv) was added and the reaction mixture was heated at 40 °C for 2 h. The resulting mixture was concentrated *in vacuo*, and the residue was co-evaporated once with acetonitrile (100 mL) to provide 2-(2-((4-(2-((R)-2-((S)-2-(2-(*cis*-4-aminocyclohexyl)acetamido)-2-phenylacetamido)-3-phenylpropanamido)ethyl)phenoxy)methyl)-6-ethoxy-4-iodophenoxy)acetic acid hydrochloride as an off-white solid (4.55 g, quant).  $^1\text{H}$  NMR (400 MHz,  $\text{DMSO}-d_6$ ):  $\delta$  12.84 (s, 1H), 8.65 (d,  $J$  = 8.3 Hz, 1H), 8.50 (d,  $J$  = 7.5 Hz, 1H), 8.12 (t,  $J$  = 5.7 Hz, 1H), 7.88 (s, 3H), 7.30 (q,  $J$  = 2.1 Hz, 2H), 7.27–7.16 (m, 6H), 7.16–7.03 (m, 6H), 7.00–6.83 (m, 2H), 5.50 (d,  $J$  = 7.5 Hz, 1H), 5.15 (s, 2H), 4.65 (s, 2H), 4.41–4.27 (m, 1H), 4.07 (q,  $J$  = 7.0 Hz, 2H), 3.25 (tq,  $J$  = 13.2, 7.4, 6.8 Hz, 2H), 3.13 (d,  $J$  = 6.0 Hz, 1H), 2.94 (dd,  $J$  = 13.8, 4.2 Hz, 1H), 2.79–2.62 (m, 2H), 2.25–2.15 (m, 2H), 1.90 (d,  $J$  = 3.2 Hz, 1H), 1.61 (q,  $J$  = 6.0 Hz, 4H), 1.52–1.27 (m, 7H). Triethylamine (1.52 mL, 10.8 mmol, 2.2 equiv) and HATU (2.09 g, 5.40 mmol, 1.1 equiv) were added to a solution of 2-(2-((4-(2-((R)-2-((S)-2-(2-(*cis*-4-aminocyclohexyl)acetamido)-2-phenylacetamido)-3-phenylpropanamido)ethyl)phenoxy)methyl)-6-ethoxy-4-iodophenoxy)acetic acid hydrochloride (4.55 g, 4.91 mmol) in *N,N*-dimethylformamide (850 mL), and the mixture was stirred at room temperature under argon for 1 h. The resulting mixture was concentrated under reduced pressure at 50–60 °C to a few milliliters of the initial volume. The residual yellow oil was treated with water and the resulting precipitate was collected by filtration, successively washed with water and diethyl ether, and dried *in vacuo* to provide the macrocyclized building block 74 as a white solid (4.73 g, 95%), HPLC purity >90%, MS (ESI) 874.4  $[M + H]^+$ .  $^1\text{H}$  NMR (400 MHz,  $\text{CDCl}_3$ ):  $\delta$  7.34–7.07 (m, 7H), 7.04 (d,  $J$  = 8.4 Hz, 2H), 6.91 (ddd,  $J$  = 11.6, 6.8, 1.9 Hz, 4H), 6.57 (d,  $J$  = 6.6 Hz, 1H), 6.35 (d,  $J$  = 6.0 Hz, 1H), 6.10 (d,  $J$  = 8.2 Hz, 1H), 5.22 (d,  $J$  = 6.6 Hz, 1H), 5.10–4.96 (m, 2H), 4.71 (d,  $J$  = 14.7 Hz, 1H), 4.61–4.48 (m, 1H), 4.43 (d,  $J$  = 14.7 Hz, 1H), 4.14 (d,  $J$  = 7.7 Hz, 1H), 4.05 (q,  $J$  = 7.0 Hz, 2H), 3.57–3.46 (m, 1H), 3.39 (dd,  $J$  = 13.6, 5.9 Hz, 1H), 3.01 (dd,  $J$  = 6.9, 3.0 Hz, 2H), 2.73 (t,  $J$  = 5.8 Hz, 2H), 2.24–2.01 (m, 2H), 1.79 (d,  $J$  = 49.2 Hz, 2H), 1.56 (d,  $J$  = 19.3 Hz, 2H, partial overlap with water signal), 1.42 (dt,  $J$  = 25.2, 7.1 Hz, 6H), 1.25 (dd,  $J$  = 17.7, 8.2 Hz, 2H).

**Synthesis of 34.** A solution of iodide 74 (40 mg, 0.046 mmol), 3,5-dimethylphenylboronic acid (7.56 mg, 0.050 mmol, 1.25 equiv), and sodium carbonate (14.6 mg, 0.14 mmol, 3 equiv) in 1,2-dimethoxyethane (1 mL) and water (0.25 mL) was flushed with argon for 10 min. Next,  $\text{PdCl}_2(\text{dppf})$  (1.68 mg, 2.3  $\mu\text{mol}$ , 0.05 equiv) was added and the mixture was heated to 100 °C for 1 h. After cooling to room temperature, the reaction mixture was filtered over Celite and the filter cake was rinsed with methanol and water. The filtrate was concentrated *in vacuo*, the residue was dissolved in ethyl acetate (25 mL) and washed with brine (10 mL). The organic layer was dried over  $\text{Na}_2\text{SO}_4$  and concentrated under reduced pressure. The crude material was purified using preparative HPLC (ammonium formate in water/acetonitrile) to afford 34 as an off-white foam after lyophilization (11 mg, 16%).  $^1\text{H}$  NMR (400 MHz,  $\text{DMSO}-d_6$ ):  $\delta$  8.91 (d,  $J$  = 8.8 Hz, 1H), 8.43 (d,  $J$  = 8.1 Hz, 1H), 8.18–8.09 (m, 1H), 7.36 (d,  $J$  = 8.1 Hz, 1H), 7.33–7.02 (m, 16H), 6.99–6.87 (m, 3H), 5.65 (d,  $J$  = 8.2 Hz, 1H), 5.25–5.06 (m, 3H), 4.61 (d,  $J$  = 14.0 Hz, 1H), 4.32–4.25 (m, 1H), 4.21 (q,  $J$  = 7.0 Hz, 2H), 3.76 (br s, 1H), 3.60–3.46 (m, 1H), 2.93 (d,  $J$  = 11.5 Hz, 2H), 2.81–2.69 (m, 2H), 2.64–2.55 (m, 2H), 2.33 (s, 6H), 2.09–1.95 (m, 1H), 1.79 (br s, 1H), 1.67–1.09 (m, 11H); HPLC purity >95%, MS (ESI): 851.6  $(M + H)^+$ .

The following compounds were prepared from 74 via the same procedure as 34, using the appropriate starting materials:

**Compound 35.** 9 mg;  $^1\text{H}$  NMR (400 MHz,  $\text{DMSO}-d_6$ ):  $\delta$  8.90 (d,  $J$  = 8.8 Hz, 1H), 8.42 (d,  $J$  = 8.1 Hz, 1H), 8.12 (t,  $J$  = 5.8 Hz, 1H), 7.61 (dd,  $J$  = 7.5, 2.5 Hz, 1H), 7.51 (ddd,  $J$  = 8.0, 5.0, 2.4 Hz, 1H), 7.35 (d,  $J$  = 8.0 Hz, 1H), 7.34–7.28 (m, 2H), 7.24–7.01 (m, 12H), 6.96–6.88 (m, 2H), 5.64 (d,  $J$  = 8.1 Hz, 1H), 5.19–5.03 (m, 2H), 4.60 (d,  $J$  = 14.0 Hz, 1H), 4.47–4.35 (m, 1H), 4.33–4.13 (m, 3H), 3.76 (s, 1H), 3.51 (dq,  $J$  = 10.9, 5.3 Hz, 1H), 2.93 (dt,  $J$  = 13.5, 3.8 Hz, 2H), 2.76 (ddd,  $J$  = 16.7, 12.0, 7.7 Hz, 2H), 2.69–2.55 (m, 1H), 2.39 (dd,  $J$  = 13.5, 10.8 Hz, 1H), 2.30 (s, 3H), 2.09–1.98 (m, 1H), 1.80 (s, 1H), 1.67–1.05 (m, 12H); MS (ESI): 855.4 ( $M + H$ ) $^+$ .

**Compound 36.** 13 mg;  $^1\text{H}$  NMR (400 MHz,  $\text{CDCl}_3$ ):  $\delta$  7.53 (d,  $J$  = 7.6 Hz, 1H), 7.31–6.90 (m, 19H), 6.65 (dd,  $J$  = 16.2, 7.7 Hz, 2H), 6.52–6.41 (m, 1H), 5.32 (d,  $J$  = 6.8 Hz, 1H), 5.15–5.06 (m, 2H), 4.80 (d,  $J$  = 14.8 Hz, 1H), 4.64–4.52 (m, 2H), 4.46 (d,  $J$  = 14.8 Hz, 1H), 4.23–4.09 (m, 3H), 3.93 (d,  $J$  = 3.9 Hz, 3H), 3.48–3.34 (m, 2H), 3.14–2.94 (m, 2H), 2.75–2.64 (m, 2H), 2.24–2.04 (m, 2H), 1.97–1.83 (m, 2H), 1.80–1.41 (m, 7H), 1.35–1.16 (m, 3H); MS (ESI): 871.4 ( $M + H$ ) $^+$ .

**Compound 37.** 13 mg;  $^1\text{H}$  NMR (400 MHz,  $\text{DMSO}-d_6$ ):  $\delta$  8.89 (d,  $J$  = 8.8 Hz, 1H), 8.41 (d,  $J$  = 8.2 Hz, 1H), 8.12 (m, 1H), 8.00–7.78 (m, 4H), 7.49–7.35 (m, 3H), 7.31–7.02 (m, 11H), 6.95 (m, 2H), 5.64 (d,  $J$  = 8.0 Hz, 1H), 5.27–5.07 (m, 2H), 4.63 (d,  $J$  = 14.0 Hz, 1H), 4.53–4.17 (m, 5H), 3.77 (bs, 1H), 3.52 (m, 1H), 3.07–2.90 (m, 2H), 2.85–2.70 (m, 2H), 2.70–2.53 (m, 2H), 2.39 (t,  $J$  = 12.2 Hz, 1H), 2.08–1.96 (m, 2H), 1.81 (bs, 1H), 1.60–1.14 (m, 10H); MS (ESI): 891.4 ( $M + H$ ) $^+$ .

**Synthesis of 38.** A solution of **74** (70 mg, 0.080 mmol), 1-ethynyl-3,5-dimethylbenzene (31.3 mg, 0.24 mmol, 3 equiv), triethylamine (0.045 mL, 0.32 mmol, 4 equiv), and copper(I) iodide (3.06 mg, 0.016 mmol) in tetrahydrofuran (2 mL) was flushed with argon for 15 min. Bis(triphenylphosphine)palladium(II) dichloride (5.74 mg, 8.02  $\mu\text{mol}$ ) was added, and the reaction mixture was stirred at room temperature for 16 h under an argon atmosphere. Ethyl acetate/methanol (1:1) was added, and the resulting mixture was filtered over Celite and rinsed with warm ethyl acetate/methanol. The combined filtrates were concentrated *in vacuo* and the crude product was purified by preparative HPLC (ammonium formate in water/acetonitrile) to afford **38** as an off-white solid after lyophilization (22 mg, 32%).  $^1\text{H}$  NMR (400 MHz,  $\text{CDCl}_3$ ):  $\delta$  7.31–7.19 (m, 3H), 7.18–7.09 (m, 9H), 7.06–7.01 (m, 3H), 6.98 (s, 1H), 6.96–6.89 (m, 4H), 6.60 (d,  $J$  = 6.7 Hz, 1H), 6.47–6.38 (m, 2H), 5.28 (d,  $J$  = 6.8 Hz, 1H), 5.10 (d, A of AB,  $J$  = 11.8 Hz, 1H), 5.06 (d, B of AB,  $J$  = 11.7 Hz, 1H), 4.77 (d, A of AB,  $J$  = 14.7 Hz, 1H), 4.54 (td,  $J$  = 8.2, 5.6 Hz, 1H), 4.48 (d, B of AB,  $J$  = 14.8 Hz, 1H), 4.22–4.10 (m, 1H), 4.10 (q,  $J$  = 7.0 Hz, 2H), 3.55–3.30 (m, 2H), 3.05 (dd, A of ABX,  $J$  = 14.2, 5.7 Hz, 1H), 2.98 (dd, B of ABX,  $J$  = 14.2, 8.1 Hz, 1H), 2.71 (t,  $J$  = 5.7 Hz, 2H), 2.31 (s, 6H), 2.17 (dd, A of ABX,  $J$  = 14.4, 5.3 Hz, 1H), 2.09 (dd, B of ABX,  $J$  = 14.5, 9.0 Hz, 1H), 1.94–1.81 (m, 1H), 1.81–1.71 (m, 1H), 1.71–1.40 (m, 5H), 1.47 (t,  $J$  = 6.9 Hz, 3H), 1.35–1.16 (m, 2H); HPLC purity >95%, MS (ESI): 875.6 ( $M + H$ ) $^+$ .

The following compounds were prepared from **74** via the same procedure as **38**, using the appropriate starting materials:

**Compound 39.** 27 mg;  $^1\text{H}$  NMR (400 MHz,  $\text{CDCl}_3$ ):  $\delta$  7.31–7.20 (m, 3H), 7.19–7.07 (m, 7H), 7.07–6.98 (m, 5H), 6.96–6.89 (m, 4H), 6.81 (tt,  $J$  = 8.8, 2.3 Hz, 1H), 6.60 (d,  $J$  = 6.7 Hz, 1H), 6.41 (t,  $J$  = 5.8 Hz, 1H), 6.36 (d,  $J$  = 8.3 Hz, 1H), 5.28 (d,  $J$  = 6.7 Hz, 1H), 5.10 (d, A of AB,  $J$  = 12.1 Hz, 1H), 5.07 (d, B of AB,  $J$  = 12.3 Hz, 1H), 4.79 (d, A of AB,  $J$  = 14.8 Hz, 1H), 4.55 (td,  $J$  = 8.1, 5.8 Hz, 1H), 4.49 (d, B of AB,  $J$  = 14.8 Hz, 1H), 4.19–4.05 (m, 1H), 4.11 (q,  $J$  = 7.0 Hz, 2H), 3.54–3.43 (m, A of ABXYZ, 1H), 3.39 (dq, B of ABXYZ,  $J$  = 13.5, 5.6 Hz, 1H), 3.04 (dd, A of ABX,  $J$  = 14.2, 5.9 Hz, 1H), 2.98 (dd, B of ABX,  $J$  = 14.1, 7.9 Hz, 1H), 2.71 (t,  $J$  = 5.7 Hz, 2H), 2.18 (dd, A of ABX,  $J$  = 14.1, 5.6 Hz, 1H), 2.09 (dd, B of ABX,  $J$  = 14.5, 8.9 Hz, 1H), 1.95–1.81 (m, 1H), 1.81–1.70 (m, 1H), 1.70–1.42 (m, 5H), 1.48 (t,  $J$  = 7.0 Hz, 3H), 1.35–1.16 (m, 2H); MS (ESI): 883.5 ( $M + H$ ) $^+$ .

**Compound 40.** 23 mg;  $^1\text{H}$  NMR (400 MHz,  $\text{CDCl}_3$ ):  $\delta$  7.35–6.98 (m, 18H), 6.96–6.87 (m, 4H), 6.59 (d,  $J$  = 6.7 Hz, 1H), 6.45–6.34 (m, 2H), 5.27 (d,  $J$  = 6.6 Hz, 1H), 5.11 (d, A of AB,  $J$  = 11.9 Hz, 1H), 5.07 (d, B of AB,  $J$  = 11.6 Hz, 1H), 4.78 (d, A of AB,  $J$  = 14.8 Hz,

1H), 4.55 (td,  $J$  = 8.0, 5.5 Hz, 1H), 4.49 (d, B of AB,  $J$  = 14.7 Hz, 1H), 4.19–4.05 (m, 1H), 4.11 (q,  $J$  = 6.8 Hz, 2H), 2.54–2.33 (m, 2H), 3.05 (dd, A of ABX,  $J$  = 14.2, 5.7 Hz, 1H), 2.99 (dd, B of ABX,  $J$  = 14.1, 8.0 Hz, 1H), 2.71 (t,  $J$  = 5.7 Hz, 2H), 2.18 (dd, A of ABX,  $J$  = 14.5, 5.2 Hz, 1H), 2.09 (dd, B of ABX,  $J$  = 14.3, 9.0 Hz, 1H), 1.94–1.81 (m, 1H), 1.81–1.70 (m, 1H), 1.70–1.41 (m, 5H), 1.47 (t,  $J$  = 7.0 Hz, 3H), 1.35–1.16 (m, 2H); MS (ESI): 865.6 ( $M + H$ ) $^+$ .

**Compound 41.** 14 mg;  $^1\text{H}$  NMR (400 MHz,  $\text{CDCl}_3$ ):  $\delta$  7.45 (d, AA' of AA'BB',  $J$  = 8.4 Hz, 2H), 7.37 (d, BB' of AA'BB',  $J$  = 8.5 Hz, 2H), 7.33–7.22 (m, 4H), 7.21–7.09 (m, 7H), 7.08–7.01 (m, 3H), 6.96–6.87 (m, 4H), 6.49 (d,  $J$  = 6.4 Hz, 1H), 6.29 (t,  $J$  = 5.8 Hz, 1H), 5.82 (d,  $J$  = 8.2 Hz, 1H), 5.17 (d,  $J$  = 6.4 Hz, 1H), 5.13 (d, A of AB,  $J$  = 11.9 Hz, 1H), 5.08 (d, B of AB,  $J$  = 11.7 Hz, 1H), 4.75 (d, A of AB,  $J$  = 14.8 Hz, 1H), 4.54 (q,  $J$  = 7.0 Hz, 1H), 4.50 (d, B of AB,  $J$  = 14.8 Hz, 1H), 4.21–4.13 (m, 1H), 4.11 (q,  $J$  = 6.9 Hz, 2H), 3.55–3.37 (m, 2H), 3.06–2.97 (m, 2H), 2.74 (t,  $J$  = 5.6 Hz, 2H), 2.16 (dd, A of ABX,  $J$  = 14.5, 5.5 Hz, 1H), 2.07 (dd, B of ABX,  $J$  = 14.5, 8.9 Hz, 1H), 1.92–1.81 (m, 1H), 1.81–1.71 (m, 1H), 1.66–1.42 (m, 5H), 1.47 (t,  $J$  = 7.0 Hz, 3H), 1.36–1.20 (m, 2H), 1.33 (s, 9H); MS (ESI): 903.4 ( $M + H$ ) $^+$ .

**Compound 42.** 19 mg;  $^1\text{H}$  NMR (400 MHz,  $\text{CDCl}_3$ ):  $\delta$  7.45 (d, AA' of AA'XX',  $J$  = 8.7 Hz, 2H), 7.33–7.22 (m, 4H), 7.20–7.08 (m, 7H), 7.07–7.00 (m, 3H), 6.97–6.90 (m, 4H), 6.88 (d, XX' of AA'XX',  $J$  = 8.8 Hz, 2H), 6.50 (d,  $J$  = 6.4 Hz, 1H), 6.30 (t,  $J$  = 5.8 Hz, 1H), 5.86 (d,  $J$  = 8.3 Hz, 1H), 5.18 (d,  $J$  = 6.3 Hz, 1H), 5.12 (d, A of AB,  $J$  = 11.9 Hz, 1H), 5.08 (d, B of AB,  $J$  = 11.9 Hz, 1H), 4.75 (d, A of AB,  $J$  = 14.8 Hz, 1H), 4.54 (q,  $J$  = 7.1 Hz, 1H), 4.50 (d, B of AB,  $J$  = 14.7 Hz, 1H), 4.21–4.13 (m, 1H), 4.10 (q,  $J$  = 6.9 Hz, 2H), 3.83 (s, 3H), 3.56–3.36 (m, 2H), 3.02 (d,  $J$  = 6.9 Hz, 2H), 2.73 (t,  $J$  = 5.7 Hz, 2H), 2.16 (dd, A of ABX,  $J$  = 14.5, 5.4 Hz, 1H), 2.07 (dd, B of ABX,  $J$  = 14.5, 8.8 Hz, 1H), 1.92–1.81 (m, 1H), 1.81–1.71 (m, 1H), 1.66–1.42 (m, 5H), 1.47 (t,  $J$  = 7.0 Hz, 3H), 1.36–1.20 (m, 2H); MS (ESI): 877.6 ( $M + H$ ) $^+$ .

**Synthesis of 44.** An oven-dried reaction tube containing **74** (100 mg, 0.115 mmol), 4-chloro-3,5-dimethylphenol (35.9 mg, 0.23 mmol, 2.0 equiv), cesium carbonate (74.7 mg, 0.23 mmol, 2.0 equiv), and copper(I) chloride (5.67 mg, 0.057 mmol, 0.5 equiv) was flushed with argon for 5 min. *N*-Methyl-2-pyrrolidinone (1 mL) and 2,2,6,6-tetramethyl-3,5-heptanedione (2.39  $\mu\text{L}$ , 0.011 mmol, 0.1 equiv) were added, and the reaction was stirred overnight under argon atmosphere at 120  $^\circ\text{C}$ . The resulting mixture was allowed to cool to room temperature and filtered through Celite, the filter cake was washed with EtOAc/MeOH, and the combined filtrates were concentrated *in vacuo*. The residue was dissolved in EtOAc and washed with 1 N aqueous HCl, 1 N aqueous NaOH, and brine. The organic layer was dried over  $\text{Na}_2\text{SO}_4$  and concentrated, and the residue was purified by preparative HPLC (ammonium formate in water/acetonitrile), to afford **44** as a white solid after lyophilization (17 mg, 16%).  $^1\text{H}$  NMR (400 MHz,  $\text{CDCl}_3$ ):  $\delta$  7.34–7.21 (m, 3H), 7.21–7.07 (m, 6H), 7.01 (d, AA' of AA'BB',  $J$  = 8.5 Hz, 2H), 6.95–6.85 (m, 2H), 6.88 (d, BB' of AA'BB',  $J$  = 8.5 Hz, 2H), 6.69 (s, 2H), 6.59 (s, 2H), 6.49 (d,  $J$  = 6.2 Hz, 1H), 6.25 (t,  $J$  = 5.7 Hz, 1H), 5.75 (d,  $J$  = 8.3 Hz, 1H), 5.16 (d,  $J$  = 6.4 Hz, 1H), 5.09 (d, A of AB,  $J$  = 11.8 Hz, 1H), 5.04 (d, B of AB,  $J$  = 11.8 Hz, 1H), 4.69 (d, A of AB,  $J$  = 14.8 Hz, 1H), 4.53 (q,  $J$  = 7.3 Hz, 1H), 4.45 (d, B of AB,  $J$  = 14.8 Hz, 1H), 4.21–4.12 (m, 1H), 4.01 (q,  $J$  = 7.1 Hz, 2H), 3.56–3.33 (m, 2H), 3.07–2.95 (m, 2H), 2.73 (t,  $J$  = 5.8 Hz, 2H), 2.34 (s, 6H), 2.16 (dd, A of ABX,  $J$  = 14.4, 5.0 Hz, 1H), 2.06 (dd, B of ABX,  $J$  = 14.5, 9.2 Hz, 1H), 1.92–1.71 (m, 2H), 1.69–1.39 (m, 5H), 1.44 (t,  $J$  = 7.0 Hz, 3H), 1.37–1.20 (m, 2H);  $^{13}\text{C}$  NMR (101 MHz,  $\text{DMSO}-d_6$ ):  $\delta$  171.8, 171.7, 170.3, 167.3, 157.1, 155.4, 153.0, 152.8, 141.8, 138.9, 138.4, 137.8, 132.8, 131.8, 130.3, 129.5, 128.4, 128.3, 127.6, 127.2, 126.5, 118.7, 115.2, 111.3, 105.9, 71.9, 65.9, 64.7, 56.2, 54.8, 44.9, 41.1, 40.6, 40.4, 40.2, 40.0, 39.8, 39.6, 39.4, 37.6, 33.8, 32.9, 29.4, 29.0, 28.5, 27.2, 20.9, 15.0; HPLC purity >95%, MS (ESI): 901.4 ( $M + H$ ) $^+$ ; HRMS:  $\text{C}_{22}\text{H}_{25}\text{ClN}_4\text{O}_8$  [ $M + H$ ] $^+$ , calc.  $m/z$  901.3938, found 901.3925,  $-1.36\Delta\text{ppm}$ .

The following compounds were prepared from **74** via the same procedure as **44**, using the appropriate starting materials:

**Compound 43.** 37 mg;  $^1\text{H}$  NMR (400 MHz,  $\text{CDCl}_3$ ):  $\delta$  7.33–7.22 (m, 3H), 7.20–7.10 (m, 6H), 7.01 (d, AA' of AA'BB',  $J$  = 8.4 Hz,



2H), 6.95–6.88 (m, 2H), 6.88 (d, BB' of AA'BB',  $J = 8.5$  Hz, 2H), 6.75 (s, 1H), 6.60 (s, 2H), 6.58 (s, 2H), 6.51 (d,  $J = 6.3$  Hz, 1H), 6.28 (t,  $J = 5.3$  Hz, 1H), 5.90 (d,  $J = 8.2$  Hz, 1H), 5.18 (d,  $J = 6.4$  Hz, 1H), 5.08 (d, A of AB,  $J = 11.7$  Hz, 1H), 5.03 (d, B of AB,  $J = 11.7$  Hz, 1H), 4.70 (d, A of AB,  $J = 14.7$  Hz, 1H), 4.53 (q,  $J = 7.1$  Hz, 1H), 4.45 (d, B of AB,  $J = 14.8$  Hz, 1H), 4.20–4.12 (m, 1H), 4.01 (q,  $J = 6.9$  Hz, 2H), 3.54–3.35 (m, 2H), 3.01 (d,  $J = 6.8$  Hz, 2H), 2.72 (t,  $J = 5.7$  Hz, 2H), 2.28 (s, 6H), 2.16 (dd, A of ABX,  $J = 14.4$ , 5.2 Hz, 1H), 2.06 (dd, B of ABX,  $J = 14.4$ , 9.0 Hz, 1H), 1.93–1.81 (m, 1H), 1.81–1.71 (m, 1H), 1.71–1.47 (m, 5H), 1.43 (t,  $J = 7.0$  Hz, 3H), 1.36–1.19 (m, 2H);  $^{13}\text{C}$  NMR (101 MHz, DMSO- $d_6$ ):  $\delta$  171.8, 171.7, 170.3, 167.3, 157.4, 157.1, 153.2, 152.7, 141.6, 139.8, 138.8, 138.4, 132.8, 131.7, 130.3, 129.5, 128.4, 127.6, 127.2, 126.5, 125.3, 116.2, 115.2, 111.4, 105.9, 71.9, 66.0, 64.6, 56.2, 54.8, 44.9, 41.1, 40.9, 37.6, 33.8, 33.0, 28.5, 27.2, 21.4, 15.0; MS (ESI): 867.5 ( $M + H$ ) $^+$ ; HRMS:  $\text{C}_{52}\text{H}_{58}\text{N}_4\text{O}_8$  [ $M + H$ ] $^+$ , calc.  $m/z$  867.4327, found 867.4316,  $-1.29\Delta\text{ppm}$ .

**Compound 45.** 5.4 mg;  $^1\text{H}$  NMR (400 MHz,  $\text{CDCl}_3$ ):  $\delta$  7.43 (t,  $J = 8.0$  Hz, 1H), 7.35 (d,  $J = 7.8$  Hz, 1H), 7.26 (s, 2H, partial overlap with solvent signal), 7.22–7.08 (m, 9H), 7.01 (dd,  $J = 9.0$ , 2.6 Hz, 2H), 6.95–6.86 (m, 4H), 6.71–6.57 (m, 2H), 6.51 (d,  $J = 6.3$  Hz, 1H), 6.24 (br s, 1H), 5.76 (d,  $J = 8.1$  Hz, 1H), 5.16 (d,  $J = 6.3$  Hz, 1H), 5.14–5.04 (m, 2H), 4.72 (d,  $J = 14.7$  Hz, 1H), 4.61–4.37 (m, 2H), 4.18 (bs, 1H), 4.02 (q,  $J = 6.9$  Hz, 2H), 3.46 (ddd,  $J = 36.2$ , 13.4, 6.5 Hz, 2H), 3.06–2.91 (m, 2H), 2.73 (t,  $J = 5.8$  Hz, 2H), 2.17 (dd,  $J = 14.3$ , 5.3 Hz, 1H), 2.07 (dd,  $J = 14.5$ , 9.0 Hz, 1H), 1.92–1.73 (m, 2H), 1.64–1.54 (m, 5H), 1.45 (t,  $J = 7.0$  Hz, 4H), 1.31 (d,  $J = 11.8$  Hz, 2H); MS (ESI): 907.5 ( $M + H$ ) $^+$ .

**Compound 46.** 13 mg;  $^1\text{H}$  NMR (400 MHz,  $\text{CDCl}_3$ ):  $\delta$  7.26 (s, 4H, partial overlap with solvent signal), 7.20–7.05 (m, 7H), 7.02 (dd,  $J = 8.0$ , 5.8 Hz, 2H), 6.95–6.83 (m, 6H), 6.68–6.57 (m, 2H), 6.52 (d,  $J = 6.4$  Hz, 1H), 6.26 (t,  $J = 5.8$  Hz, 1H), 5.81 (d,  $J = 8.2$  Hz, 1H), 5.17 (d,  $J = 6.5$  Hz, 1H), 5.15–5.01 (m, 2H), 4.71 (d,  $J = 14.7$  Hz, 1H), 4.57–4.43 (m, 2H), 4.18 (bs, 1H), 4.02 (q,  $J = 6.9$  Hz, 2H), 3.46 (ddt,  $J = 32.9$ , 13.4, 6.3 Hz, 2H), 3.04–2.93 (m, 2H), 2.73 (t,  $J = 5.8$  Hz, 2H), 2.22–2.14 (m, 1H), 2.07 (dd,  $J = 14.3$ , 8.8 Hz, 1H), 1.93–1.71 (m, 2H), 1.57 (m, 5H), 1.44 (t,  $J = 6.9$  Hz, 3H), 1.36–1.22 (m, 2H); MS (ESI): 873.4 ( $M + H$ ) $^+$ .

**Compound 47.** 18 mg;  $^1\text{H}$  NMR (400 MHz,  $\text{CDCl}_3$ ):  $\delta$  8.19 (d,  $J = 8.2$  Hz, 1H), 7.89 (d,  $J = 7.9$  Hz, 1H), 7.63 (d,  $J = 8.3$  Hz, 1H), 7.60–7.46 (m, 2H), 7.37 (t,  $J = 7.9$  Hz, 1H), 7.26 (s, 5H, partial overlap with solvent signal), 7.22–7.08 (m, 6H), 7.04–6.96 (m, 2H), 6.96–6.81 (m, 5H), 6.70 (d,  $J = 2.8$  Hz, 1H), 6.65 (d,  $J = 2.7$  Hz, 1H), 6.53 (d,  $J = 6.3$  Hz, 1H), 6.28 (d,  $J = 6.0$  Hz, 1H), 5.86 (d,  $J = 8.2$  Hz, 1H), 5.18 (d,  $J = 6.3$  Hz, 1H), 5.04 (q,  $J = 11.7$  Hz, 2H), 4.72 (d,  $J = 14.7$  Hz, 1H), 4.59–4.40 (m, 2H), 4.17 (bs, 1H), 4.00 (q,  $J = 7.0$  Hz, 2H), 3.55–3.35 (m, 2H), 3.07–2.93 (m, 2H), 2.73 (t,  $J = 5.8$  Hz, 2H), 2.17 (dd,  $J = 14.5$ , 5.2 Hz, 1H), 2.12–1.96 (m, 1H), 1.81 (d,  $J = 41.6$  Hz, 2H), 1.69–1.46 (m, 5H), 1.42 (t,  $J = 7.0$  Hz, 3H), 1.36–1.18 (m, 2H); MS (ESI): 889.4 ( $M + H$ ) $^+$ .

The following compounds were prepared via a synthetic route analogous to **44** via intermediate **74**, starting from 2-(4-benzoyloxyphenyl)ethanamine (**70**) and the appropriate amino acid starting materials:

**Compound 48.** 15 mg;  $^1\text{H}$  NMR (400 MHz, DMSO- $d_6$ ):  $\delta$  8.93 (d,  $J = 8.9$  Hz, 1H), 8.43 (d,  $J = 8.2$  Hz, 1H), 8.36 (s, 1H), 8.31 (d,  $J = 4.8$  Hz, 1H), 8.12 (t,  $J = 5.6$  Hz, 1H), 7.44 (dt,  $J = 7.8$ , 1.9 Hz, 1H), 7.35 (d,  $J = 8.1$  Hz, 1H), 7.26–7.11 (m, 5H), 7.10–6.97 (m, 3H), 6.92–6.84 (m, 4H), 6.82 (d,  $J = 2.8$  Hz, 1H), 6.67 (d,  $J = 2.8$  Hz, 1H), 5.62 (d,  $J = 8.0$  Hz, 1H), 5.05 (q,  $J = 11.4$  Hz, 2H), 4.55 (d,  $J = 13.9$  Hz, 1H), 4.51–4.39 (m, 1H), 4.25 (d,  $J = 14.0$  Hz, 1H), 4.06 (q,  $J = 7.0$  Hz, 2H), 3.77 (bs, 1H), 3.64–3.46 (m, 1H), 2.94 (td,  $J = 13.3$ , 12.8, 6.6 Hz, 2H), 2.83–2.67 (m, 2H), 2.60 (dt,  $J = 8.9$ , 4.6 Hz, 1H), 2.30 (s, 7H), 2.05–1.85 (m, 1H), 1.77 (d,  $J = 15.5$  Hz, 1H), 1.61–1.08 (m, 12H); MS (ESI): 902.4 ( $M + H$ ) $^+$ .

**Compound 49.** 45 mg;  $^1\text{H}$  NMR (400 MHz,  $\text{CDCl}_3$ ):  $\delta$  8.30 (br s, 2H), 7.26 (s, 3H), 7.17 (d,  $J = 8.2$  Hz, 1H), 7.13–7.01 (m, 4H), 6.96–6.77 (m, 4H), 6.70 (s, 2H), 6.59 (s, 2H), 6.51 (d,  $J = 6.4$  Hz, 1H), 6.45 (t,  $J = 5.7$  Hz, 1H), 6.22 (d,  $J = 8.3$  Hz, 1H), 5.21 (d,  $J = 6.4$  Hz, 1H), 5.13–4.98 (m, 2H), 4.72 (d,  $J = 14.6$  Hz, 1H), 4.58 (td,  $J =$

9.0, 5.1 Hz, 1H), 4.44 (d,  $J = 14.7$  Hz, 1H), 4.17 (bs, 1H), 4.01 (q,  $J = 7.0$  Hz, 2H), 3.58–3.35 (m, 2H), 3.12 (dd,  $J = 14.5$ , 5.1 Hz, 1H), 2.89 (dd,  $J = 14.4$ , 9.4 Hz, 1H), 2.79–2.67 (m, 2H), 2.34 (s, 6H), 2.18 (dd,  $J = 14.3$ , 5.2 Hz, 1H), 2.06 (dd,  $J = 14.5$ , 9.1 Hz, 1H), 1.94–1.49 (m, 7H, partial overlap water signal), 1.44 (t,  $J = 7.0$  Hz, 3H), 1.26 (dd,  $J = 18.1$ , 10.5 Hz, 2H); MS (ESI): 902.4 ( $M + H$ ) $^+$ .

**Compound 50.** 22 mg;  $^1\text{H}$  NMR (400 MHz,  $\text{CDCl}_3$ ):  $\delta$  8.58–8.48 (m, 2H), 7.33 (d,  $J = 8.3$  Hz, 1H), 7.16–7.09 (m, 2H), 6.91 (d,  $J = 8.5$  Hz, 2H), 6.84 (d,  $J = 8.5$  Hz, 2H), 6.67 (s, 2H), 6.58 (d,  $J = 2.7$  Hz, 1H), 6.52 (d,  $J = 2.7$  Hz, 1H), 6.47 (d,  $J = 8.3$  Hz, 1H), 6.23 (t,  $J = 5.8$  Hz, 1H), 5.99 (d,  $J = 6.5$  Hz, 1H), 5.06 (d,  $J = 2.9$  Hz, 2H), 4.79–4.62 (m, 2H), 4.50 (d,  $J = 14.8$  Hz, 1H), 4.30 (dd,  $J = 6.4$ , 3.4 Hz, 1H), 4.24 (bs, 1H), 4.00 (q,  $J = 6.9$  Hz, 2H), 3.84–3.74 (m, 1H), 3.59 (bs, 1H), 3.37 (bs, 1H), 3.25 (s, 3H), 3.18–3.05 (m, 2H), 2.68 (dt,  $J = 8.1$ , 4.0 Hz, 2H), 2.33 (s, 6H), 2.14–2.04 (m, 2H), 1.92 (s, 1H), 1.82 (d,  $J = 13.1$  Hz, 1H), 1.71–1.54 (m, 5H, partial overlap with water signal), 1.44 (t,  $J = 7.0$  Hz, 3H), 1.40–1.24 (m, 2H), 0.74 (d,  $J = 6.4$  Hz, 3H); MS (ESI): 884.4 ( $M + H$ ) $^+$ .

**Compound 51.** 6.7 mg;  $^1\text{H}$  NMR (400 MHz,  $\text{CDCl}_3$ ):  $\delta$  8.72–8.33 (m, 2H), 7.22 (d,  $J = 8.2$  Hz, 1H), 7.20–7.15 (m, 2H), 7.02–6.96 (m, 2H), 6.86 (d,  $J = 8.6$  Hz, 2H), 6.78 (d,  $J = 8.6$  Hz, 1H), 6.67 (s, 2H), 6.58 (d,  $J = 2.7$  Hz, 1H), 6.50 (d,  $J = 2.8$  Hz, 1H), 6.35 (t,  $J = 5.7$  Hz, 1H), 6.21 (d,  $J = 6.8$  Hz, 1H), 5.04 (q,  $J = 11.8$  Hz, 2H), 4.79–4.64 (m, 2H), 4.57–4.42 (m, 2H), 4.19 (bs, 1H), 4.01 (q,  $J = 7.0$  Hz, 2H), 3.58–3.38 (m, 1H), 3.33 (dd,  $J = 14.5$ , 5.0 Hz, 1H), 3.17–3.06 (m, 1H), 3.01–2.90 (m, 4H), 2.82–2.56 (m, 2H), 2.32 (s, 6H), 2.16 (dd,  $J = 14.4$ , 8.5 Hz, 1H), 2.07–1.91 (qd,  $J = 15.7$ , 14.1, 8.5 Hz, 3H), 1.88–1.73 (m, 2H), 1.66–1.47 (m, 7H), 1.44 (t,  $J = 7.0$  Hz, 3H), 1.32–1.08 (m, 2H); MS (ESI): 932.5 ( $M + H$ ) $^+$ .

**Compound 52 (7:3 Mixture of Diastereoisomers).** 10 mg;  $^1\text{H}$  NMR (400 MHz,  $\text{CDCl}_3$ ):  $\delta$  7.40–7.29 (m, 4H, major and minor), 7.29–7.10 (m, 4H, major and minor), 7.01–6.89 (m, 3H, major and minor), 6.83–6.76 (m, 1H, minor), 6.75–6.65 (m, 2H, major and 1H minor), 6.64–6.60 (m, 1H, major and minor), 6.58 (d,  $J = 2.8$  Hz, 1H, major), 6.54 (d,  $J = 2.6$  Hz, 1H, major and minor), 6.51 (d,  $J = 2.7$  Hz, 1H, minor), 5.55 (d,  $J = 7.0$  Hz, 1H, major), 5.45 (d,  $J = 7.1$  Hz, 1H, minor), 5.20 (d, A of AB,  $J = 13.2$  Hz, 1H, minor), 5.15 (d, B of AB,  $J = 13.3$  Hz, 1H, minor), 5.13 (d, A of AB,  $J = 11.9$  Hz, 1H, major), 5.03 (d, B of AB,  $J = 11.9$  Hz, 1H, major), 4.67 (d, A of AB,  $J = 14.8$  Hz, 1H, major), 4.62 (d, A of AB,  $J = 14.9$  Hz, 1H, minor), 4.63–4.59 (d,  $J = 7.5$  Hz, 1H, minor), 4.57 (d,  $J = 7.9$  Hz, 1H, major), 4.52 (d, B of AB,  $J = 14.8$  Hz, 1H, major and minor), 4.20–4.08 (m, 1H, major and minor), 4.01 (q,  $J = 6.8$  Hz, 1H, major), 3.99 (q,  $J = 6.9$  Hz, 1H, minor), 3.78–3.62 (m, 1H, major and minor), 3.62–3.54 (m, 1H, major), 3.43–3.28 (m, 1H, major and minor), 3.21–3.11 (m, 1H, minor), 3.06 (td,  $J = 9.4$ , 7.3 Hz, 1H, major), 2.98–2.90 (m, 1H, minor), 2.85–2.60 (m, 2H, major and minor), 2.44 (dd,  $J = 12.7$ , 6.3 Hz, 1H, major), 2.38–2.27 (m, 1H, minor), 2.33 (s, 6H, major), 2.31 (s, 6H, minor), 2.20–2.10 (m, 1H, major and minor), 2.07–1.38 (m, 11H, major and minor), 1.44 (t,  $J = 6.9$  Hz, 3H, major and minor), 1.36–1.20 (m, 2H, major and minor), 1.16–1.02 (m, 1H, major and minor); MS (ESI): 851.5 ( $M + H$ ) $^+$ .

**Solid-Phase Synthesis of 53.** To a solution of Fmoc-OSU (8.43 g, 25 mmol) in dichloromethane (100 mL) was slowly added a solution of 4-(2-aminoethyl)aniline (3.58 g, 26.3 mmol, 1.05 equiv) and triethylamine (3.48 mL, 25.0 mmol, 1.0 equiv) in dichloromethane (100 mL) and the resulting reaction was stirred at room temperature overnight. *n*-Heptane was added to the mixture until precipitation appeared, which was removed by filtration. This procedure was repeated twice with the resulting mother liquors. Next, the remaining solvents were removed *in vacuo*, the residue recrystallized from DCM/*n*-heptane, and the resulting solids were isolated by filtration and dried *in vacuo* at 40 °C to afford Fmoc-(4-aminophenethyl)amine (6.35 g, 17.7 mmol, 71%). MS (ESI): 359.2 ( $M + H$ ) $^+$ . The solid-phase peptide synthesis reaction was performed in 6 batches of 1.00 mmol. 2-Chlorotrityl resin (1.2 mmol/gram) (5.0 g, 6.00 mmol) was swelled and washed with dichloromethane (60 mL). A solution of Fmoc-(4-aminophenethyl)amine (2.15 g, 6.00 mmol) and diisopropylethylamine (1.05 mL, 6.00 mmol) in dichloromethane (60 mL) was added to the resin, and the mixture



was shaken for 45 min. The solution was removed, and the resin was washed with dichloromethane (3 × 60 mL). A mixture of dichloromethane (50 mL)/methanol (6 mL)/diisopropylethylamine (3 mL, 17.2 mmol) was added to the resin, and the mixture was shaken for 20 min. The resin was washed with dichloromethane and diethyl ether and subsequently dried *in vacuo*. The product on resin (75) was used without further purification. Resin-bound Fmoc-(4-aminophenethyl)amine (75, 2.15 g, 6 mmol) was washed with *N,N*-dimethylformamide (10 mL). Piperidine (20% in DMF, 10 mL, 20.3 mmol) was added, and the mixture was shaken for 10 min. The solution was removed, again piperidine (20% in DMF, 10 mL, 20.3 mmol) was added, and the mixture was shaken for 10 min. The solvent was removed, and the resin was washed with *N,N*-dimethylformamide. In a separate vial, a solution of Fmoc-D-phenylalanine (4.65 g, 12.0 mmol) and HATU (4.56 g, 12.0 mmol) in *N,N*-dimethylformamide (10 mL) was prepared and diisopropylethylamine (2.09 mL, 12.0 mmol) was added. The solution was added to the washed resin, and the mixture was shaken at room temperature for 2 h, resulting in a dark red resin suspension. The resin was washed with *N,N*-dimethylformamide. A test cleavage with TFA confirmed the formation of the desired product Fmoc-(R)-1-((4-aminophenethyl)amino)-1-oxo-3-phenylpropan-2-yl)amine by HPLC-MS, MS (ESI): 506.2 (M + H)<sup>+</sup>. Resin Fmoc-(R)-1-((4-aminophenethyl)amino)-1-oxo-3-phenylpropan-2-yl)amine (3.03 g, 6 mmol) was washed with *N,N*-dimethylformamide. Piperidine (20% in DMF, 10 mL, 20.3 mmol) was added, and the mixture was shaken for 10 min. The solution was removed, again piperidine (20% in DMF, 10 mL, 20.3 mmol) was added, and the mixture was shaken for 10 min. The solvent was removed, and the resin was washed with *N,N*-dimethylformamide. In a separate vial, a solution of Fmoc-L-phenylglycine (4.48 g, 12.0 mmol) and Oxyma Pure (1.88 g, 13.2 mmol) in *N,N*-dimethylformamide was prepared and *N,N'*-diisopropylcarbodiimide (1.87 mL, 12.0 mmol) was added, resulting in a yellow solution. The solution was added to the washed resin, and the mixture was shaken at room temperature overnight. The resin was washed with *N,N*-dimethylformamide. A test cleavage with TFA confirmed formation of the desired product Fmoc-((S)-2-(((R)-1-((4-aminophenethyl)amino)-1-oxo-3-phenylpropan-2-yl)amino)-2-oxo-1-phenylethyl)amine by HPLC-MS, MS (ESI): 639.3 (M + H)<sup>+</sup>. Resin-bound Fmoc-((S)-2-(((R)-1-((4-aminophenethyl)amino)-1-oxo-3-phenylpropan-2-yl)amino)-2-oxo-1-phenylethyl)amine (3.83 g, 6.0 mmol) was washed with *N,N*-dimethylformamide. Piperidine (20% in DMF, 10 mL, 20.3 mmol) was added, and the mixture was shaken for 10 min. The solution was removed, again piperidine (20% in DMF, 10 mL, 20.3 mmol) was added, and the mixture was shaken for 10 min. The solvent was removed, and the resin was washed with *N,N*-dimethylformamide. In a separate vial, a solution of Fmoc-*cis*-4-aminocyclohexane acetic acid (4.55 g, 12.0 mmol) and HATU (4.56 g, 12.0 mmol) in *N,N*-dimethylformamide (10 mL) was prepared and diisopropylethylamine (2.09 mL, 12.0 mmol) was added, resulting in a yellow solution. The solution was added to the washed resin, and the mixture was shaken at room temperature for 2 h, resulting in a dark red resin suspension. The resin was washed with *N,N*-dimethylformamide, and the resulting resin-bound Fmoc-(*cis*-4-(2-(((S)-2-(((R)-1-((4-aminophenethyl)amino)-1-oxo-3-phenylpropan-2-yl)amino)-2-oxo-1-phenylethyl)amino)-2-oxoethyl)cyclohexyl)amine (76) was stored for further use. A test cleavage with TFA confirmed the formation of the desired product Fmoc-(*cis*-4-(2-(((S)-2-(((R)-1-((4-aminophenethyl)amino)-1-oxo-3-phenylpropan-2-yl)amino)-2-oxo-1-phenylethyl)amino)-2-oxoethyl)cyclohexyl)amine by HPLC-MS, MS (ESI): 778.4 (M + H)<sup>+</sup>. Part of the resin-bound Fmoc-(*cis*-4-(2-(((S)-2-(((R)-1-((4-aminophenethyl)amino)-1-oxo-3-phenylpropan-2-yl)amino)-2-oxo-1-phenylethyl)amino)-2-oxoethyl)cyclohexyl)amine (76, 79 mg, 0.1 mmol) was washed/swelled in dichloromethane (1.5 mL) and subsequently washed with *N,N*-dimethylformamide (1.5 mL). The resin was Fmoc-deprotected with a solution of piperidine in *N,N*-dimethylformamide (20%, 1.5 mL, 3.04 mmol) and subsequently washed with *N,N*-dimethylformamide (1.5 mL). In a separate vial, lithium 2-(4-(3,5-dimethylphenoxy)-2-ethoxy-6-formylphenoxy)acetate (77b, 113 mg, 0.32 mmol)

and Oxyma Pure (68.2 mg, 0.48 mmol) were dissolved in *N,N*-dimethylformamide (5 mL) and stirred for 10 min. Next, *N,N'*-diisopropylcarbodiimide (0.070 mL, 0.45 mmol) was added, the solution was stirred for 10 min and subsequently added to the washed resin, and the resulting mixture was shaken at room temperature for 2 h. The resin was washed with *N,N*-dimethylformamide (1.5 mL) and dichloromethane (1.5 mL), dried, and stored. The resulting resin-bound (R)-N-(4-aminophenethyl)-2-((S)-2-(2-(*cis*-4-(2-(4-(3,5-dimethylphenoxy)-2-ethoxy-6-formylphenoxy)acetamido)cyclohexyl)-acetamido)-2-phenylacetamido)-3-phenylpropanamide (78b) was not analyzed further but used directly in the next step. The resin-bound precursor (78b, approximately 0.1 mmol) was suspended in dichloromethane (4.5 mL), a solution of TFA in dichloromethane (2.5%, 4.0 mL, 1.31 mmol) was added, and the mixture was shaken at room temperature for 15 min. The yellow solution was collected, the resin was extracted with DCM (4 mL) and DCM/DMF (1:1, 4 mL), and the obtained solutions were pooled. To the combined organic solvents was added sodium triacetoxyborohydride (106 mg, 0.50 mmol) and the reaction mixture was stirred at room temperature for 2 h. The resulting mixture was concentrated *in vacuo*, the residue redissolved in dichloromethane (5 mL) and washed with 1 N aqueous NaOH. The organic was concentrated *in vacuo*, and the residue was purified by preparative HPLC (formic acid in water/acetonitrile), affording macrocyclic compound 53 as a white solid after lyophilization (60 mg, 69% yield from 76). <sup>1</sup>H NMR (400 MHz, CDCl<sub>3</sub>): δ 7.34–7.23 (m, 3H), 7.20–7.07 (m, 6H), 6.97–6.88 (m, 4H), 6.73 (s, 1H), 6.61–6.54 (m, 5H), 6.52 (d, B of AB, *J* = 2.7 Hz, 1H), 6.48 (d, *J* = 6.7 Hz, 1H), 6.33 (t, *J* = 5.8 Hz, 1H), 6.14 (d, *J* = 8.4 Hz, 1H), 5.23 (d, *J* = 6.6 Hz, 1H), 4.65 (d, A of AB, *J* = 14.9 Hz, 1H), 4.58 (q, *J* = 6.9 Hz, 1H), 4.44 (d, B of AB, *J* = 14.9 Hz, 1H), 4.31 (s, 2H), 4.20–4.10 (m, 1H), 4.00 (q, *J* = 6.9 Hz, 2H), 3.42 (q, *J* = 5.8 Hz, 2H), 3.02 (d, *J* = 6.7 Hz, 2H), 2.72–2.59 (m, 2H), 2.26 (s, 6H), 2.12–2.00 (m, 2H), 1.90–1.75 (m, 2H), 1.72–1.47 (m, 5H), 1.43 (t, *J* = 6.9 Hz, 3H), 1.34–1.17 (m, 2H); HPLC purity >95%, MS (ESI): 866.6 (M + H)<sup>+</sup>.

The following compound was prepared via the same procedure as 53, using 77c instead of 77b:

**Compound 54.** 32 mg; <sup>1</sup>H NMR (400 MHz, CDCl<sub>3</sub>): δ 7.35–7.23 (m, 3H), 7.21–7.07 (m, 6H), 6.97–6.87 (m, 4H), 6.67 (s, 2H), 6.56 (d, BB' of AA'BB', *J* = 8.5 Hz, 2H), 6.53 (d, A of AB, *J* = 2.8 Hz, 1H), 6.49 (d, B of AB, *J* = 2.7 Hz, 1H), 6.43 (d, *J* = 6.5 Hz, 1H), 6.28 (t, *J* = 5.8 Hz, 1H), 5.89 (d, *J* = 8.3 Hz, 1H), 5.19 (d, *J* = 6.5 Hz, 1H), 4.64 (d, A of AB, *J* = 14.8 Hz, 1H), 4.58 (q, *J* = 7.3 Hz, 1H), 4.45 (d, B of AB, *J* = 14.8 Hz, 1H), 4.32 (s, 2H), 4.20–4.11 (m, 1H), 4.00 (q, *J* = 7.0 Hz, 2H), 3.43 (q, *J* = 5.8 Hz, 2H), 3.05 (dd, A of ABX, *J* = 13.9, 7.0 Hz, 1H), 3.00 (dd, B of ABX, *J* = 13.9, 5.8 Hz, 1H), 2.73–2.60 (m, 2H), 2.31 (s, 6H), 2.06 (d, *J* = 6.9 Hz, 2H), 1.90–1.75 (m, 2H), 1.77–1.48 (m, 5H), 1.43 (t, *J* = 6.9 Hz, 3H), 1.34–1.18 (m, 2H); MS (ESI): 900.5 (M + H)<sup>+</sup>.

**Synthesis of Carboxylate Building Block 77c.** To a cooled (0 °C) solution of 3-ethoxy-2-hydroxy-5-iodobenzaldehyde (10 g, 34 mmol) in dichloromethane (65 mL) was added *N,N*-diisopropylethylamine (10.7 mL, 61.6 mmol, 1.8 equiv), followed by a dropwise addition of MOM-Cl (3.64 mL, 47.9 mmol, 1.4 equiv). Stirring was continued at 0 °C for 30 min, after which the mixture was allowed to warm to room temperature overnight. The reaction was quenched with water and extracted twice with DCM. The combined organic layers were washed with brine, dried over Na<sub>2</sub>SO<sub>4</sub>, and concentrated to yield 3-ethoxy-5-iodo-2-(methoxymethoxy)benzaldehyde (11.1 g, 33.0 mmol, 96%) as pale-yellow solid. MS (ESI): 359.0 (M+Na)<sup>+</sup>. The resulting MOM-protected phenol (2 g, 5.95 mmol), 4-chloro-3,5-dimethylphenol (2.33 g, 14.9 mmol, 2.5 equiv), copper(I) iodide (0.113 g, 0.595 mmol, 1 equiv), 3,4,7,8-tetramethyl-1,10-phenanthroline (0.281 g, 1.19 mmol, 0.2 equiv), and cesium carbonate (4.85 g, 14.9 mmol, 2.5 equiv) were mixed with toluene (25 mL), and the reaction mixture was stirred for 20 h at 95 °C. After cooling to room temperature, the reaction mixture was passed through a plug of silica, eluted with EtOAc, and concentrated *in vacuo*. The residue was purified via reversed-phase column chromatography eluting with 5 to 100% MeCN in water, yielding 5-(4-chloro-3,5-dimethylphenoxy)-3-

ethoxy-2-(methoxymethoxy)benzaldehyde (386 mg, 17%) as an off-white solid.  $^1\text{H}$  NMR (400 MHz,  $\text{CDCl}_3$ ):  $\delta$  10.41 (s, 1H), 6.87 (dd,  $J$  = 24.7, 2.9 Hz, 2H), 6.73 (s, 2H), 5.22 (s, 2H), 4.06 (q,  $J$  = 6.7 Hz, 2H), 3.59 (s, 3H), 2.35 (s, 6H), 1.47 (t,  $J$  = 6.9 Hz, 3H); MS (ESI): 387.0 ( $\text{M} + \text{Na}$ ) $^+$ . Hydrochloric acid (6 M) (630  $\mu\text{L}$ , 3.79 mmol, 10 equiv) was added to a solution of 5-(4-chloro-3,5-dimethylphenoxy)-3-ethoxy-2-(methoxymethoxy)benzaldehyde (138 mg, 0.379 mmol) in tetrahydrofuran (630  $\mu\text{L}$ ), and the reaction was stirred overnight at room temperature. The resulting mixture was partitioned between water and  $\text{Et}_2\text{O}$ , layers were separated, and the aqueous layer was extracted twice with  $\text{Et}_2\text{O}$ . The combined organic layers were washed with water, sat. aq.  $\text{NaHCO}_3$ , and brine, dried over  $\text{Na}_2\text{SO}_4$ , filtered, and concentrated to yield MOM-deprotected 5-(4-chloro-3,5-dimethylphenoxy)-3-ethoxy-2-hydroxybenzaldehyde (126 mg, quant.) as slightly yellow solid. MS (ESI): 343.0 ( $\text{M} + \text{Na}$ ) $^+$ . To a solution of 5-(4-chloro-3,5-dimethylphenoxy)-3-ethoxy-2-hydroxybenzaldehyde (126 mg, 0.393 mmol) in  $N,N$ -dimethylformamide (2 mL) were added cesium carbonate (141 mg, 0.432 mmol, 1.1 equiv) and ethyl bromoacetate (0.048 mL, 0.432 mmol, 1.1 equiv), and the reaction was stirred at room temperature for 1.5 h. The reaction mixture was partitioned between water/brine and  $\text{EtOAc}$ , layers were separated, and the aqueous layer was extracted twice with  $\text{EtOAc}$ . The combined organic layers were washed with brine, dried over  $\text{Na}_2\text{SO}_4$ , and concentrated to yield ethyl 2-(4-(4-chloro-3,5-dimethylphenoxy)-2-ethoxy-6-formylphenoxy)acetate (150 mg, 94%) as an orange solid. MS (ESI): 407.0 ( $\text{M} + \text{H}$ ) $^+$ . Aqueous lithium hydroxide (1 N, 0.41 mL, 0.41 mmol) was added to a stirred solution of ethyl 2-(4-(4-chloro-3,5-dimethylphenoxy)-2-ethoxy-6-formylphenoxy)acetate (150 mg, 0.369 mmol) in tetrahydrofuran (2 mL), and the reaction was stirred at room temperature for 1 h. The volatiles were evaporated and the residue was stripped with MeCN to give 2-(4-(4-chloro-3,5-dimethylphenoxy)-2-ethoxy-6-formylphenoxy)acetic acid as its lithium salt (160 mg, quant.). MS (ESI): 379.0 ( $\text{M} + \text{H}$ ) $^+$ .

**Synthesis of Carboxylate Building Blocks 77a/c.** 2-(4-(3,5-Dimethylphenoxy)-2-ethoxy-6-formylphenoxy)acetic acid lithium salt (77b) was prepared analogous to 77c, using 3,5-dimethylphenol instead of 4-chloro-3,5-dimethylphenol. MS (ESI): 345.1 ( $\text{M} + \text{H}$ ) $^+$ . 2-(2-Ethoxy-6-formylphenoxy)acetic acid lithium salt (77a) was prepared similarly from the unsubstituted 3-ethoxy-2-hydroxybenzaldehyde, without the need of an *O*-protection/Ullman/deprotection sequence. MS (ESI): 225.0 ( $\text{M} + \text{H}$ ) $^+$ .

**Solid-Phase Synthesis of 1.** Chlorotriyl resin (6.01 g, 3.90 mmol) was added to a 25 mL syringe with filter and swelled in predried dichloromethane (30 mL) for 5 min, after which the resin was washed with dichloromethane (30 mL) and dried. Boc-4-amino-Fmoc-Phe-OH (1.96 g, 3.90 mmol) and diisopropylethylamine (1.39 mL, 7.80 mmol) were dissolved in dichloromethane (30 mL) and added to the resin. The resulting mixture was shaken at room temperature for 30 min, after which the solution was removed by filtration and the resin was washed with dichloromethane (30 mL). The resin was capped by adding a solution of dichloromethane/methanol/diisopropylethylamine (17:2:1, 20 mL) and subsequent shaking for 30 min. The resulting resin-bound (S)-2-(Fmoc-amino)-3-(4-((*tert*-butoxycarbonyl)amino)phenyl)propanoic acid (79) was washed with dichloromethane (30 mL) and  $N,N$ -dimethylformamide (30 mL) and used as such. Fmoc-deprotection was performed with piperidine in  $N,N$ -dimethylformamide (20%, 30 mL), and the resin was washed with  $N,N$ -dimethylformamide (30 mL). Fmoc-D-Phe-OH (1.51 g, 3.9 mmol), HATU (1.48 g, 3.90 mmol), and diisopropylethylamine (7.80 mmol, 1.39 mL) were dissolved in  $N,N$ -dimethylformamide (30 mL). This solution was added to the resin, and the reaction was shaken at room temperature for 2 h. The solution was removed by filtration, and resin-bound (S)-2-((R)-2-(Fmoc-amino)-3-phenylpropanamido)-3-(4-((*tert*-butoxycarbonyl)amino)phenyl)propanoic acid was washed with  $N,N$ -dimethylformamide (30 mL). Fmoc-deprotection was performed with piperidine in  $N,N$ -dimethylformamide (20%, 30 mL), and the resin was washed with  $N,N$ -dimethylformamide (30 mL). Fmoc-Phg-OH (1.46 g, 3.90 mmol) and Oxyma Pure (0.577 g, 4.06 mmol) were dissolved in  $N,N$ -dimethylformamide (30 mL). When dissolved,  $N,N'$ -diisopropylcar-

bodiimide (0.492 g, 3.90 mmol) was added, the solution was added to the resin, and the reaction was shaken at room temperature for 2 h. The solution was removed by filtration and resin-bound (5S,8R,11S)-8-benzyl-11-(4-((*tert*-butoxycarbonyl)amino)benzyl)-1-(9H-fluoren-9-yl)-3,6,9-trioxo-5-phenyl-2-oxa-4,7,10-triazadodecan-12-oic acid was washed with  $N,N$ -dimethylformamide (30 mL). Fmoc-deprotection was performed with piperidine in  $N,N$ -dimethylformamide (20%, 8.0 mL), and the resin was washed with  $N,N$ -dimethylformamide (8.0 mL). Fmoc-*cis*-4-aminocyclohexane acetic acid (1.48 g, 3.90 mmol), HATU (1.48 g, 3.90 mmol), and diisopropylethylamine (7.80 mmol, 1.39 mL) were dissolved in  $N,N$ -dimethylformamide (30 mL), the solution was added to the resin, and the reaction was shaken at room temperature for 2 h. The resulting resin-bound (S)-2-((R)-2-((S)-2-(2-(*cis*-4-(Fmoc-amino)cyclohexyl)acetamido)-2-phenylacetamido)-3-phenylpropanamido)-3-(4-((*tert*-butoxycarbonyl)amino)phenyl)propanoic acid (80) was washed with  $N,N$ -dimethylformamide (30 mL) and dichloromethane (30 mL), dried, and stored at room temperature. A test cleavage with TFA showed formation of the expected, Boc-deprotected product (S)-2-((R)-2-((S)-2-(*cis*-4-(Fmoc-amino)cyclohexyl)acetamido)-2-phenylacetamido)-3-phenylpropanamido)-3-(4-aminophenyl)propanoic acid by HPLC-MS, MS (ESI): 822.4 ( $\text{M} + \text{H}$ ) $^+$ . Fmoc-deprotection of 80 was performed with piperidine in  $N,N$ -dimethylformamide (20%, 8 mL), and the resin was washed with  $N,N$ -dimethylformamide (8 mL). Next, 77a (0.437 g, 1.95 mmol), HATU (0.741 g, 1.95 mmol), and diisopropylethylamine (3.90 mmol, 0.69 mL) were dissolved in  $N,N$ -dimethylformamide (8 mL). The solution was added to the resin, the reaction was shaken at room temperature for 48 h and the resulting resin was washed with  $N,N$ -dimethylformamide (8 mL). Additional amounts of 77a (0.25 equiv), HATU (0.25 equiv), and diisopropylethylamine (0.5 equiv) in  $N,N$ -dimethylformamide (8 mL) were added, and the mixture was shaken for an additional 16 h. Next, the compound was cleaved from the resin by adding a solution of TFA in dichloromethane (2%, 8.0 mL) and shaking the mixture for 30 min. The solution was collected by filtration, and this procedure was repeated twice. Combined solvents were evaporated *in vacuo*, and the residue was co-evaporated with chloroform to afford Boc-protected macrocyclization precursor 81a as an oil (1.02 g, 29%), HPLC purity 85%; MS (ESI): 906.4 ( $\text{M} + \text{H}$ ) $^+$ . Compound 81a (1.02 g, 1.13 mmol) was dissolved in dichloromethane (5.0 mL), trifluoroacetic acid (2.0 mL, 26.0 mmol, 23 equiv) was added, and the reaction was stirred at room temperature for 1.5 h. The resulting solution was concentrated *in vacuo*, the residue was co-evaporated with chloroform, and redissolved in  $N,N$ -dimethylformamide (5 mL) and chloroform (60 mL). Sodium cyanoborohydride (0.283 g, 4.50 mmol, 4 equiv) was added and the solution was stirred for 30 min. The reaction mixture was concentrated *in vacuo* to afford macrocyclic compound 82 (889 mg, 99%) as a solid, which was used without further purification. HPLC purity 90%, MS (ESI): 790.4 ( $\text{M} + \text{H}$ ) $^+$ . Compound 82 (889 mg, 1.13 mmol) was dissolved in  $N,N$ -dimethylformamide (15 mL) and Oxyma Pure (192 mg, 1.35 mmol, 1.2 equiv) was added. Next, EDCI-HCl (237 mg, 1.24 mmol, 1.1 equiv) and an ethanolic methylamine solution (8N, 0.56 mL, 4.5 mmol, 4 equiv) were added, and the reaction mixture was stirred for 1 h at room temperature. Additional amounts of Oxyma Pure (192 mg, 1.35 mmol, 1.2 equiv), EDCI-HCl (237 mg, 1.24 mmol, 1.1 equiv), and ethanolic methylamine solution (8N, 0.56 mL, 4.5 mmol, 4 equiv) were added to the mixture, and stirring was continued overnight. Since HPLC analysis indicated 50% conversion, the same aliquots of EDCI-HCl and ethanolic methylamine solution (8N) were added multiple times followed by stirring overnight, until 85% conversion was reached according to HPLC. The reaction mixture was concentrated *in vacuo*, and the residue was purified by acidic preparative HPLC (formic acid in water/acetonitrile) and again by basic preparative HPLC (ammonium formate in water/acetonitrile) to afford compound 1 as a white solid after lyophilization (56 mg, 7%).  $^1\text{H}$  NMR (400 MHz,  $\text{DMSO}-d_6$ ):  $\delta$  8.50 (d,  $J$  = 8.9 Hz, 1H), 8.27 (d,  $J$  = 7.2 Hz, 1H), 7.79 (d,  $J$  = 6.6 Hz, 2H), 7.41 (d,  $J$  = 7.9 Hz, 1H), 7.24 (dd,  $J$  = 5.1, 2.0 Hz, 3H), 7.15 (dd,  $J$  = 6.9, 2.8 Hz, 2H), 7.10–7.01 (m, 4H), 6.97 (ddd,  $J$  = 10.1, 7.5, 1.5 Hz, 4H), 6.85 (d,  $J$  = 8.1 Hz, 2H), 6.54 (d,  $J$  = 8.2 Hz, 2H), 5.65

(*t*, *J* = 5.7 Hz, 1H), 5.50 (d, *J* = 7.1 Hz, 1H), 4.59 (d, *J* = 14.1 Hz, 1H), 4.24 (tdd, *J* = 28.7, 13.6, 7.5 Hz, 5H), 4.06 (q, *J* = 6.9 Hz, 2H), 3.82 (br s, 1H), 3.10–2.96 (m, 1H), 2.88–2.69 (m, 2H), 2.68–2.55 (m, 4H), 2.42–2.27 (m, 1H), 1.92 (dd, *J* = 13.9, 5.0 Hz, 1H), 1.78 (br s, 1H), 1.62 (br s, 1H), 1.56–1.12 (m, 8H); HPLC purity >95%,  $[M + H]^+ = 803.4$ .

The following compounds were prepared via the same procedure as **1**, using **77b/c** instead of **77a**, and stopping at the carboxylic acid stage, followed by purification by preparative HPLC (formic acid in water/acetonitrile):

**Compound 55.** 14 mg;  $^1\text{H}$  NMR (400 MHz,  $\text{CDCl}_3$ ):  $\delta$  8.91 (s, 1H), 7.34 (d, *J* = 9.4 Hz, 1H), 7.30–7.15 (m, 6H), 7.13–7.03 (m, 7H), 6.71 (d, *J* = 6.6 Hz, 3H), 6.56–6.51 (m, 3H), 6.48 (d, *J* = 2.7 Hz, 1H), 6.23 (d, *J* = 6.7 Hz, 1H), 5.66 (d, *J* = 6.8 Hz, 1H), 4.73 (bs, 2H), 4.54–4.42 (m, 4H), 4.29 (s, 1H), 4.01 (q, *J* = 6.9 Hz, 2H), 3.30 (d, *J* = 14.1 Hz, 1H), 3.20 (dd, *J* = 13.7, 6.8 Hz, 1H), 2.93–2.72 (m, 2H), 2.24 (s, 6H), 2.18–2.10 (m, 1H), 2.04–1.78 (m, 5H), 1.72–1.52 (m, 2H), 1.45 (t, *J* = 6.9 Hz, 3H), 1.26 (t, *J* = 13.8 Hz, 2H); MS (ESI): 910.4 ( $M + H$ ) $^+$ .

**Compound 56.** 22 mg;  $^1\text{H}$  NMR (400 MHz,  $\text{CDCl}_3$ ):  $\delta$  12.68 (br s, 1H), 8.69 (d, *J* = 8.9 Hz, 1H), 8.14 (d, *J* = 7.8 Hz, 1H), 7.89 (d, *J* = 7.6 Hz, 1H), 7.40 (d, *J* = 7.8 Hz, 1H), 7.19 (q, *J* = 4.0, 3.2 Hz, 3H), 7.17–7.11 (m, 3H), 7.11–7.00 (m, 5H), 6.84 (d, *J* = 8.2 Hz, 2H), 6.79 (s, 2H), 6.70 (d, *J* = 2.8 Hz, 1H), 6.59 (d, *J* = 2.8 Hz, 1H), 6.52 (d, *J* = 8.2 Hz, 2H), 5.70 (br s, 1H), 5.55 (d, *J* = 7.8 Hz, 1H), 4.57 (d, *J* = 14.2 Hz, 1H), 4.39–4.13 (m, 5H), 4.02 (q, *J* = 7.0 Hz, 2H), 3.84 (br s, 1H), 3.08–2.80 (m, 3H), 2.63 (dd, *J* = 14.2, 11.5 Hz, 1H), 2.37–2.16 (m, 7H), 1.93 (dd, *J* = 13.6, 4.9 Hz, 1H), 1.77 (br s, 1H), 1.63 (br s, 1H), 1.57–1.11 (m, 8H); MS (ESI): 944.4 ( $M + H$ ) $^+$ .

**Synthesis of Compounds 57/58/59.** The methyl esters of these compounds were synthesized and purified analogous to the procedures for **2** (route II, Scheme 1), using the appropriated A/B/C/D-fragments. The final ester saponifications were carried out at room temperature in THF/ $\text{H}_2\text{O}$  (1:1), using 1.1 equiv of 0.5 N aqueous LiOH. Standard acid–base extraction with EtOAc as the organic solvent, followed by lyophilization provided the final products.

**Compound 57.** 61 mg;  $^1\text{H}$  NMR (400 MHz,  $\text{DMSO}-d_6$ ):  $\delta$  12.73 (br s, 1H), 8.50 (d, *J* = 8.9 Hz, 1H), 8.45 (br s, 1H), 8.39 (br s, 1H), 8.03 (d, *J* = 7.5 Hz, 1H), 7.76 (d, *J* = 8.0 Hz, 1H), 7.66 (d, *J* = 7.9 Hz, 1H), 7.32 (d, *J* = 8.0 Hz, 1H), 7.30–7.22 (m, 1H), 7.04 (d, *J* = 8.3 Hz, 2H), 6.90–6.75 (m, 5H), 6.67 (d, *J* = 2.8 Hz, 1H), 5.12–4.91 (m, 2H), 4.55 (d, *J* = 13.8 Hz, 1H), 4.47 (ddd, *J* = 12.1, 8.8, 3.6 Hz, 1H), 4.41–4.30 (m, 1H), 4.21 (d, *J* = 13.9 Hz, 1H), 4.19–4.11 (m, 1H), 4.04 (q, *J* = 7.0 Hz, 2H), 3.76 (br s, 1H), 3.20–3.06 (m, 1H), 3.06–2.91 (m, 2H), 2.75–2.64 (m, 1H), 2.29 (s, 6H), 2.22–2.10 (m, 1H), 1.98–1.87 (m, 1H), 1.73 (br s, 1H), 1.60–1.36 (m, 4H), 1.33 (t, *J* = 6.9 Hz, 3H), 1.30–0.93 (m, 9H), 0.70 (t, *J* = 6.2 Hz, 6H);  $^{13}\text{C}$  NMR (101 MHz,  $\text{DMSO}-d_6$ ):  $\delta$  172.7, 171.5, 167.3, 157.1, 155.4, 153.0, 152.7, 150.8, 148.0, 141.8, 137.8, 137.0, 134.2, 131.7, 130.8, 128.3, 123.6, 118.7, 115.0, 111.1, 105.7, 72.0, 65.9, 64.6, 54.5, 54.4, 51.3, 44.6, 42.0, 40.6, 40.4, 40.3, 40.2, 40.0, 39.8, 39.6, 39.4, 34.9, 28.5, 24.4, 23.1, 22.5, 20.8, 15.0; MS (ESI): 926.5 ( $M + H$ ) $^+$ ; HRMS:  $\text{C}_{50}\text{H}_{60}\text{ClN}_5\text{O}_{10}$  [ $M + H$ ] $^+$ , calc. *m/z* 926.4101, found 926.4096,  $-0.64\Delta\text{ppm}$ .

**Compound 58.** 19 mg;  $^1\text{H}$  NMR (400 MHz,  $\text{DMSO}-d_6$ ):  $\delta$  12.91 (br s, 1H), 8.52 (br s, 1H), 8.43 (br s, 1H), 8.40 (d, *J* = 8.7 Hz, 1H), 8.30 (d, *J* = 8.4 Hz, 1H), 7.85–7.71 (m, 2H), 7.37–7.30 (m, 1H), 7.26 (d, *J* = 8.1 Hz, 1H), 7.08 (d, *J* = 8.3 Hz, 2H), 6.94–6.74 (m, 5H), 6.66 (d, *J* = 2.7 Hz, 1H), 5.09–4.90 (m, 2H), 4.72 (ddd, *J* = 12.4, 8.8, 3.8 Hz, 1H), 4.57 (d, *J* = 13.8 Hz, 1H), 4.45–4.29 (m, 2H), 4.22 (d, *J* = 13.9 Hz, 1H), 4.06 (q, *J* = 7.0 Hz, 2H), 3.74 (br s, *J* = 8.7 Hz, 1H), 3.11–2.96 (m, 2H), 2.91–2.71 (m, 2H), 2.30 (s, 6H), 2.15–2.02 (m, 1H), 1.96–1.85 (m, 1H), 1.71 (br s, 1H), 1.58–1.37 (m, 4H), 1.34 (t, 3H), 1.29–0.89 (m, 11H), 0.71 (s, 6H); MS (ESI): 926.5 ( $M + H$ ) $^+$ .

**Compound 59.** 57 mg;  $^1\text{H}$  NMR (400 MHz,  $\text{DMSO}-d_6$ ):  $\delta$  12.74 (br s, 1H), 8.77 (d, *J* = 8.9 Hz, 1H), 8.37 (d, *J* = 8.4 Hz, 1H), 8.34–8.26 (m, 2H), 8.22 (d, *J* = 7.8 Hz, 1H), 7.39 (d, *J* = 8.0 Hz, 1H), 7.30 (d, *J* = 8.0 Hz, 1H), 7.22–7.09 (m, 5H), 7.09–6.96 (m, 3H), 6.92–

6.84 (m, 4H), 6.82 (d, *J* = 2.8 Hz, 1H), 6.70 (d, *J* = 2.8 Hz, 1H), 5.66 (d, *J* = 8.2 Hz, 1H), 5.07 (d, *J* = 11.0 Hz, 1H), 4.96 (d, *J* = 11.0 Hz, 1H), 4.59 (d, *J* = 13.9 Hz, 1H), 4.41 (t, *J* = 10.9 Hz, 1H), 4.18 (d, *J* = 13.9 Hz, 1H), 4.15–3.99 (m, 3H), 3.78 (s, 1H), 3.08–2.97 (m, 3H), 2.71 (d, *J* = 12.7 Hz, 1H), 2.40 (t, *J* = 12.1 Hz, 1H), 2.29 (s, 6H), 2.00–1.88 (m, 1H), 1.77 (br s, 1H), 1.60–1.42 (m, 3H), 1.36–1.30 (m, 4H), 1.30–1.03 (m, 7H); MS (ESI): 946.4 ( $M + H$ ) $^+$ ;  $^{13}\text{C}$  NMR (101 MHz,  $\text{DMSO}-d_6$ ):  $\delta$  172.8, 171.4, 171.3, 170.5, 167.2, 157.4, 155.4, 153.0, 152.8, 141.8, 139.3, 137.8, 136.7, 131.7, 131.0, 130.8, 128.5, 128.3, 127.6, 127.1, 118.7, 115.1, 111.4, 105.9, 71.9, 66.0, 64.7, 56.1, 54.9, 54.3, 44.5, 41.5, 40.6, 40.4, 40.2, 40.0, 39.8, 39.6, 39.3, 35.1, 34.7, 33.0, 29.5, 29.0, 28.6, 28.4, 26.9, 20.9, 15.0; HRMS:  $\text{C}_{52}\text{H}_{56}\text{ClN}_5\text{O}_{10}$  [ $M + H$ ] $^+$ , calc. *m/z* 946.3788, found 946.3787,  $-0.17\Delta\text{ppm}$ .

**Mcl-1 (172–327)-BAK TR-FRET Peptide Binding Assay.** In a 96-well HalfArea white plate (Corning #3642) were mixed screening compound (5  $\mu\text{L}$  in 10% DMSO) and Mcl-1 (20  $\mu\text{L}$  in reaction buffer). Control wells contain 10% DMSO and reaction buffer. After a 15 min incubation period at 30  $^\circ\text{C}$ , BAK peptide (20  $\mu\text{L}$  in reaction buffer) was added and the plates were incubated for 30 min at 30  $^\circ\text{C}$ . To control wells, only reaction buffer was added. SA-Eu/APC-anti-HIS detection mixture (5  $\mu\text{L}$ ) was added (to control wells, only SA-Eu was added). The plates were incubated for 30 min at 30  $^\circ\text{C}$  and subsequently for 30 min at 4  $^\circ\text{C}$ . The plates were analyzed in a Victor<sup>2</sup> plate reader (PerkinElmer) using a 665/615 nm TR-FRET fluorescence detection protocol. Materials: reaction buffer: 50 mM HEPES pH 7.5/100 mM NaCl/1 mM DTT/0.02% (w/v) bovine serum albumin (BSA); recombinant Mcl-1: HIS-Mcl-1 (172–327), assay concentration 25 nM; BAK peptide: BIOTIN-AHX-GQVGRQLAIIGDDINR-amide, assay concentration 17 nM; TR-FRET reagents: SA-Eu: PerkinElmer Eu–W1024 Streptavidin #AD0062, assay concentration 1 nM; anti-HIS APC antibody: PerkinElmer SureLight Allophycocyanin-anti-6His antibody #AD0059H, assay concentration 17 nM.

**Bcl-xl (1–212)-BAK TR-FRET Peptide Binding Assay.** In a 96-well HalfArea white plate (Corning #3642) were mixed screening compound (5  $\mu\text{L}$  in 10% DMSO) and Bcl-xl (20  $\mu\text{L}$  in reaction buffer). Control wells contain 10% DMSO and reaction buffer. After a 15 min incubation period at 30  $^\circ\text{C}$ , BAK peptide (20  $\mu\text{L}$  in reaction buffer) was added and the plates were incubated for 30 min at 30  $^\circ\text{C}$ . To control wells, only reaction buffer was added. SA-Eu/APC-anti-HIS detection mixture (5  $\mu\text{L}$ ) was added (to control wells only SA-Eu was added). The plates were incubated for 30 min at 30  $^\circ\text{C}$  and subsequently for 30 min at 4  $^\circ\text{C}$ . The plates were analyzed in a Victor<sup>2</sup> plate reader (PerkinElmer) using a 665/615 nm TR-FRET fluorescence detection protocol. Materials: reaction buffer: 50 mM HEPES pH 7.5/100 mM NaCl/1 mM DTT/0.02% (w/v) BSA; recombinant Bcl-xl: Bcl-xl (1–212, N-term GST, C-term HIS), assay concentration 17 nM; BAK peptide: BIOTIN-AHX-GQVGRQLAIIGDDINR-amide, assay concentration 17 nM; TR-FRET reagents: SA-Eu: PerkinElmer Eu–W1024 Streptavidin #AD0062, assay concentration 1 nM; anti-HIS APC antibody: PerkinElmer SureLight Allophycocyanin-anti-6His antibody #AD0059H, assay concentration 17 nM.

**NCI-H929 Viability Assay.** NCI-H929 cells were cultured in RPMI1640 supplemented with 10% FCS and Pen/Strep. For the assays, 2500 cells were seeded in 50  $\mu\text{L}$  in white cell culture-treated flat and clear-bottom 384-well plates and incubated at 37  $^\circ\text{C}$  overnight before screening compounds were added. Stock solutions of screening compounds in DMSO were used. Screening compound treatment of cells was performed by nanodrop-dispensing using a Tecan Dispenser. Compounds were usually tested at a concentration range from  $10^{-5}$  to  $10^{-9}$ . After incubation for 72 h at 37  $^\circ\text{C}$  at 5%  $\text{CO}_2$ , cell plates were equilibrated to room temperature for 1 h, CellTiterGlo reagent (Promega) was added and luminescence was measured after 1 h. Raw data were converted into percent cell viability relative to the high control (0.1% DMSO) and low control ( $1 \times 10^{-5}$  M Staurosporine), which were set to 100 and 0%, respectively. EC<sub>50</sub> calculation was performed using GraphPad Prism software with a



variable-slope sigmoidal response fitting model using 0% viability as bottom constraint and 100% viability as top constraint.

**NCI-H929 Caspase 3/7 Assay.** NCI-H929 cells were cultured in RPMI1640 supplemented with 10% FCS and Pen/Strep. The cells were seeded in 50  $\mu$ L (2500/well) in white cell culture-treated flat and clear-bottom 384-well plates and incubated at 37 °C overnight before compounds were added. Screening compound treatment of cells was performed by nanodrop-dispensing using a Tecan Dispenser. Compounds were usually tested at a concentration range from  $10^{-5}$  to  $10^{-9}$ . After incubation for 6 h at 37 °C at 5% CO<sub>2</sub>, cell plates were equilibrated to room temperature for 1 h, Caspase-Glo 3/7 reagent (Promega) was added, and luminescence was measured 1 h later using a luminometer. Raw data were converted into percent caspase 3/7-related apoptosis relative to the high control ( $1 \times 10^{-5}$  M Staurosporine) and low control (0.1% DMSO), which were set to 100 and 0%, respectively. IC<sub>50</sub> calculation was performed using GraphPad Prism software with a variable-slope sigmoidal response fitting model using 0% viability as bottom constraint and 100% viability as top constraint.

**Kinetic Solubility Assay.** Test compounds were dissolved in DMSO to a concentration of 10 mM and further diluted to 100  $\mu$ M in buffer (10 mM PBS, pH 7.4) in a 96-well plate at a final DMSO concentration of 1%. Incubations were performed in triplicate. The plates were shaken for 24 h at room temperature in an Eppendorf Thermomixer. After incubation, the plates were centrifuged for 20 min at 3700 rpm. From the supernatant, 150  $\mu$ L was transferred to a new 96-well plate and 50  $\mu$ L of DMSO was added to ensure continued dissolution. Samples were measured on LC-UV at injection volumes of 1 and 4  $\mu$ L. The peak area of incubated samples was determined and compared to the peak area obtained using calibration curves of the test compounds in DMSO. Results of control incubations were compared with historical data as a quality control.

**PAMPA Permeability Assay.** PAMPA studies were conducted using the PAMPA Explorer kit (pION, Inc.). Stock solutions of all compounds were prepared in dimethyl sulfoxide (DMSO) (10 mM). Each stock solution was diluted to 50  $\mu$ M in pH 7.4 Prisma HT buffer (pION) and 200  $\mu$ L were added to each well of the donor plate (3 to 6 repeats). The poly(vinylidene fluoride) (PVDF, 0.45  $\mu$ M) filter membrane on the acceptor plate was coated with 5  $\mu$ L of the gastrointestinal tract (GIT-0) lipid formulation (pION), and to each well of the acceptor plate, 200  $\mu$ L of acceptor sink buffer (ASB, pION) was added. The acceptor filter plate was carefully placed on top of the donor plate to form a "sandwich." The sandwich was incubated at 25 °C for 4 h, without stirring. UV-vis spectra of the solutions in the blank, reference, acceptor, and donor plates were measured using a microplate reader (Molecular Devices Spectramax Plus 384). For each compound,  $P(10^{-6}$  cm/s) values were calculated using the PAMPA Explorer software v. 3.6 (pION).

**Small-Molecule X-ray Diffraction of 2.** Single crystals of 2 were obtained by gradually cooling of a warm EtOH solution. For single-crystal X-ray diffraction, a transparent, rod-like single crystal was taken out of the mother liquid, immediately coated with high-viscosity oil, cut to size, and mounted on a Mitagen Microloop and shock frozen to 150 K using liquid nitrogen flow. Intensity data were collected at 150 K. The measurement was performed on a Bruker D8 Quest, with Mo K $\alpha$  radiation, using  $\varphi$  scans and  $\omega$  scans. The structure was solved by dual-space methods using SHELXT and refined by least-squares methods to  $R_1 = 0.0349$  for 13508 reflections with  $I_o > 2.0 \sigma(I_o)$ . Crystal data: C<sub>46</sub>H<sub>53</sub>N<sub>3</sub>O<sub>8</sub>, C<sub>2</sub>H<sub>6</sub>O, 3(H<sub>2</sub>O), monoclinic, space group P2<sub>1</sub> (#4),  $a = 13.4561(7)$  Å,  $b = 13.2522(8)$  Å,  $c = 13.7415(8)$  Å,  $\beta = 97.954(2)^\circ$ ,  $V = 2426.9(2)$  Å<sup>3</sup> and  $Z = 2$ . The positions of the hydrogen atoms could initially be determined using a difference Fourier map. Hydrogens were subsequently, when possible, replaced by hydrogens at calculated positions and refined riding on the parent atoms. On the completed model, Bijvoet analysis was performed to determine the absolute configuration. Powder diffraction was used to confirm that the one crystal used for single-crystal X-ray diffraction was representative of the whole batch and to check the correctness of the single-crystal diffraction model. For powder diffraction analysis, crystals were taken from the vial and put into a mortar. The little

solvent present was left to evaporate before grinding. After grinding the sample was put into a 0.3 mm glass capillary and was measured on a Panalytical Empyrean diffractometer with Cu K $\alpha$  radiation in capillary mode.

**Protein Crystallization, Data Collection, and Structure Determination.** Crystal-grade protein was produced at Crelux GmbH. The MBP-MCL1 fusion construct used for crystallization was described previously.<sup>56</sup> MBP-MCL1 in complex with compound 1 was crystallized by sitting-drop vapor diffusion at 20 °C. MBP-MCL1 (10 mg/mL in 200 mM NaCl, 20 mM HEPES-NaOH pH 7.5, 1 mM TCEP and 1% v/v glycerol) was incubated with 1.5 mM of compound 1 and 2 mM maltose for 1 h at 4 °C. 0.2  $\mu$ L of the sample was mixed with 0.2  $\mu$ L of crystallization solution (1.94 M ammonium citrate pH 7.0) and equilibrated against a reservoir containing 0.06 mL of crystallization solution. The crystals were mounted after 7 days. Crystals were cryo-protected with Paratone-n and cooled in liquid nitrogen. Data were collected at beamline ID30A1 of the European Synchrotron Radiation Facility (Grenoble, France). Diffraction data were integrated, analyzed, and scaled with energy-dispersive X-ray spectrum (XDS), Pointless, Aimless in autoPROC<sup>57</sup> (data in Table S4). The structure was determined by molecular replacement with PHASER using a previously determined model of the complex (without any ligands) as a starting model (PDB entry 4WGI). The model was improved through manual rebuilding of the model in Coot and restrained refinement with Refmac5. Atomic displacement factors were modeled with a single isotropic B-factor per atom. The backbone geometry was analyzed with Molprobability. The restraints for the modeled compounds were generated with Libcheck. Protein–ligand pictures were prepared using PyMOL Molecular Graphics System, Version 2.0 Schrödinger, LLC.

## ■ ASSOCIATED CONTENT

### Supporting Information

The Supporting Information is available free of charge at <https://pubs.acs.org/doi/10.1021/acs.jmedchem.3c02206>.

Experimental details combinatorial array synthesis; assay results for all combinatorial compounds; NMR spectra and HPLC traces of key compounds; single-molecule crystallography data for compound 2, including Ortep-drawing; protein–ligand crystallography data for compound 1; and conformational analysis NMR data (PDF) Molecular formula strings for all final compounds (CSV)

### Accession Codes

Coordinates for compound 1 in complex with Mcl-1 have been deposited into the Protein Data Bank (PDB: 8QSO). The authors will release the atomic coordinates upon article publication.

## ■ AUTHOR INFORMATION

### Corresponding Authors

Koen F. W. Hekking — Symeres, 6546BB Nijmegen, The Netherlands; [orcid.org/0000-0003-0925-654X](https://orcid.org/0000-0003-0925-654X); Email: [koen.hekking@symeres.com](mailto:koen.hekking@symeres.com)

Anthony D. Keefe — X-Chem, Inc., Waltham, Massachusetts 02453, United States; Email: [akeefe@x-chemrx.com](mailto:akeefe@x-chemrx.com)

### Authors

Sergio Maroto — Symeres, 6546BB Nijmegen, The Netherlands; [orcid.org/0000-0002-3992-7466](https://orcid.org/0000-0002-3992-7466)

Kees van Kekem — Symeres, 6546BB Nijmegen, The Netherlands

Frank S. Haasjes — Symeres, 6546BB Nijmegen, The Netherlands

Jack C. Slootweg — Symeres, 6546BB Nijmegen, The Netherlands



Patrick G. B. Oude Alink – Symeres, 6546BB Nijmegen, The Netherlands  
Ron Dirks – Symeres, 6546BB Nijmegen, The Netherlands  
Malvika Sardana – Symeres, 6546BB Nijmegen, The Netherlands; [orcid.org/0000-0002-6838-4392](https://orcid.org/0000-0002-6838-4392)  
Marjon G. Bolster – Symeres, 6546BB Nijmegen, The Netherlands  
Brian Kuipers – Symeres, 6546BB Nijmegen, The Netherlands  
Dennis Smith – Symeres, 6546BB Nijmegen, The Netherlands  
Robin Doodeman – Symeres, 6546BB Nijmegen, The Netherlands  
Marcel Scheepstra – Symeres, 6546BB Nijmegen, The Netherlands  
Birgit Zech – X-Rx, Inc., New York, New York 10016, United States  
Mark Mulvihill – X-Rx, Inc., New York, New York 10016, United States  
Louis M. Renzetti – X-Rx, Inc., New York, New York 10016, United States  
Lee Babiss – X-Rx, Inc., New York, New York 10016, United States  
Paolo A. Centrella – X-Chem, Inc., Waltham, Massachusetts 02453, United States  
Matthew A. Clark – X-Chem, Inc., Waltham, Massachusetts 02453, United States  
John W. Cuozzo – X-Chem, Inc., Waltham, Massachusetts 02453, United States; [orcid.org/0000-0002-6229-0395](https://orcid.org/0000-0002-6229-0395)  
Marie-Aude Guie – X-Chem, Inc., Waltham, Massachusetts 02453, United States  
Eric Sigel – X-Chem, Inc., Waltham, Massachusetts 02453, United States  
Sevan Habeshian – X-Chem, Inc., Waltham, Massachusetts 02453, United States  
Christopher D. Hupp – X-Chem, Inc., Waltham, Massachusetts 02453, United States  
Julie Liu – X-Chem, Inc., Waltham, Massachusetts 02453, United States  
Heather A. Thomson – X-Chem, Inc., Waltham, Massachusetts 02453, United States  
Ying Zhang – X-Chem, Inc., Waltham, Massachusetts 02453, United States  
Gerhard Müller – Symeres, 6546BB Nijmegen, The Netherlands  
Stijn Gremmen – Symeres, 6546BB Nijmegen, The Netherlands

Complete contact information is available at:

<https://pubs.acs.org/10.1021/acs.jmedchem.3c02206>

## Author Contributions

The manuscript was written through contributions of all authors. All authors have given approval to the final version of the manuscript, with the exception of L.B. and H.A.T., who are deceased.

## Notes

The authors declare no competing financial interest.

## ACKNOWLEDGMENTS

The authors acknowledge Crelux GmbH (Martinsried, Germany) for X-ray crystallography services and the European Synchrotron Radiation Facility (ESRF) for provision of synchrotron radiation facilities. Eddy Damen and Giovanni

Bolcato (Symeres Nijmegen, The Netherlands) are acknowledged for computational support. Paula van der Aa, Marjolijn Beens, Guillermo Maassen, Katarzyna Borsuk, Ruud Titulaer, and Henk Regeling (Symeres Nijmegen, The Netherlands) are thanked for synthetic contributions to the project. Rutger Folmer (Symeres Nijmegen, The Netherlands) is thanked for useful discussions during manuscript preparation. René de Gelder (Radboud University Nijmegen) is acknowledged for performing single-compound X-ray diffraction. The people at Reaction Biology Europe (formerly ProQinase, Freiburg, Germany) are kindly acknowledged for performing the biological assays.

## ABBREVIATIONS USED

BAK, Bcl-2 antagonist/killer protein; Bcl-2, B-cell lymphoma 2 protein; BH3, Bcl-2 homology domain3; bRo5, beyond-rule-of-five; DEL, DNA-encoded chemical library; DIAD, diisopropyl azodicarboxylate; FBDD, fragment-based drug discovery; HRMS, high-resolution mass spectrometry; HTS, high-throughput screening; MBP, maltose binding protein; Mcl-1, myeloid leukemia cell differentiation protein; PAMPA, parallel artificial membrane permeability assay; PDB, Protein Data Bank; SBDD, structure-based drug discovery; TR-FRET, time-resolved fluorescence energy transfer

## REFERENCES

- (1) Green, D. R.; Llambi, F. Cell Death Signaling. *Cold Spring Harbor Perspect. Biol.* **2015**, 7 (12), No. a006080.
- (2) Taylor, R. C.; Cullen, S. P.; Martin, S. J. Apoptosis: Controlled Demolition at the Cellular Level. *Nat. Rev. Mol. Cell Biol.* **2008**, 9 (3), 231–241.
- (3) Singh, R.; Letai, A.; Sarosiek, K. Regulation of Apoptosis in Health and Disease: The Balancing Act of BCL-2 Family Proteins. *Nat. Rev. Mol. Cell Biol.* **2019**, 20 (3), 175–193.
- (4) Hanahan, D.; Weinberg, R. A. Hallmarks of Cancer: The Next Generation. *Cell* **2011**, 144 (5), 646–674.
- (5) Delbridge, A. R. D.; Strasser, A. The BCL-2 Protein Family, BH3-Mimetics and Cancer Therapy. *Cell Death Differ.* **2015**, 22 (7), 1071–1080.
- (6) Delbridge, A. R. D.; Grabow, S.; Strasser, A.; Vaux, D. L. Thirty Years of BCL-2: Translating Cell Death Discoveries into Novel Cancer Therapies. *Nat. Rev. Cancer* **2016**, 16 (2), 99–109.
- (7) Souers, A. J.; Levenson, J. D.; Boghaert, E. R.; Ackler, S. L.; Catron, N. D.; Chen, J.; Dayton, B. D.; Ding, H.; Enschede, S. H.; Fairbrother, W. J.; Huang, D. C. S.; Hymowitz, S. G.; Jin, S.; Khaw, S. L.; Kovar, P. J.; Lam, L. T.; Lee, J.; Maecker, H. L.; Marsh, K. C.; Mason, K. D.; Mitten, M. J.; Nimmer, P. M.; Oleksijew, A.; Park, C. H.; Park, C.-M.; Phillips, D. C.; Roberts, A. W.; Sampath, D.; Seymour, J. F.; Smith, M. L.; Sullivan, G. M.; Tahir, S. K.; Tse, C.; Wendt, M. D.; Xiao, Y.; Xue, J. C.; Zhang, H.; Humerickhouse, R. A.; Rosenberg, S. H.; Elmore, S. W. ABT-199, a Potent and Selective BCL-2 Inhibitor, Achieves Antitumor Activity While Sparing Platelets. *Nat. Med.* **2013**, 19 (2), 202–208.
- (8) Schieber, M.; Ma, S. The Expanding Role of Venetoclax in Chronic Lymphocytic Leukemia and Small Lymphocytic Lymphoma. *Blood Lymphat. Cancer Targets Ther.* **2019**, 9, 9–17.
- (9) Wang, H.; Guo, M.; Wei, H.; Chen, Y. Targeting MCL-1 in Cancer: Current Status and Perspectives. *J. Hematol. Oncol.* **2021**, 14 (1), No. 67.
- (10) Beroukhi, R.; Mermel, C. H.; Porter, D.; Wei, G.; Raychaudhuri, S.; Donovan, J.; Barretina, J.; Boehm, J. S.; Dobson, J.; Urashima, M.; Mc Henry, K. T.; Pinchback, R. M.; Ligon, A. H.; Cho, Y.-J.; Haery, L.; Greulich, H.; Reich, M.; Winckler, W.; Lawrence, M. S.; Weir, B. A.; Tanaka, K. E.; Chiang, D. Y.; Bass, A. J.; Loo, A.; Hoffman, C.; Prensner, J.; Liefeld, T.; Gao, Q.; Yecies, D.; Signoretti, S.; Maher, E.; Kaye, F. J.; Sasaki, H.; Tepper, J. E.

- Fletcher, J. A.; Tabernero, J.; Baselga, J.; Tsao, M.-S.; Demicheli, F.; Rubin, M. A.; Janne, P. A.; Daly, M. J.; Nucera, C.; Levine, R. L.; Ebert, B. L.; Gabriel, S.; Rustgi, A. K.; Antonescu, C. R.; Ladanyi, M.; Letai, A.; Garraway, L. A.; Loda, M.; Beer, D. G.; True, L. D.; Okamoto, A.; Pomeroy, S. L.; Singer, S.; Golub, T. R.; Lander, E. S.; Getz, G.; Sellers, W. R.; Meyerson, M. The Landscape of Somatic Copy-Number Alteration across Human Cancers. *Nature* **2010**, *463* (7283), 899–905.
- (11) Bolomsky, A.; Vogler, M.; Köse, M. C.; Heckman, C. A.; Ehx, G.; Ludwig, H.; Caers, J. MCL-1 Inhibitors, Fast-Lane Development of a New Class of Anti-Cancer Agents. *J. Hematol. Oncol.* **2020**, *13* (1), No. 173.
- (12) Glaser, S. P.; Lee, E. F.; Trounson, E.; Bouillet, P.; Wei, A.; Fairlie, W. D.; Izon, D. J.; Zuber, J.; Rappaport, A. R.; Herold, M. J.; Alexander, W. S.; Lowe, S. W.; Robb, L.; Strasser, A. Anti-Apoptotic Mcl-1 Is Essential for the Development and Sustained Growth of Acute Myeloid Leukemia. *Genes Dev.* **2012**, *26* (2), 120–125.
- (13) Aichberger, K. J.; Mayerhofer, M.; Krauth, M.-T.; Skvara, H.; Florian, S.; Sonneck, K.; Akgul, C.; Derdak, S.; Pickl, W. F.; Wacheck, V.; Selzer, E.; Monia, B. P.; Moriggl, R.; Valent, P.; Sillaber, C. Identification of Mcl-1 as a BCR/ABL-Dependent Target in Chronic Myeloid Leukemia (CML): Evidence for Cooperative Antileukemic Effects of Imatinib and Mcl-1 Antisense Oligonucleotides. *Blood* **2005**, *105* (8), 3303–3311.
- (14) Song, L.; Coppola, D.; Livingston, S.; Cress, W. D.; Haura, E. B. Mcl-1 Regulates Survival and Sensitivity to Diverse Apoptotic Stimuli in Human Non-Small Cell Lung Cancer Cells. *Cancer Biol. Ther.* **2005**, *4* (3), 267–276.
- (15) Campbell, K. J.; Dhayade, S.; Ferrari, N.; Sims, A. H.; Johnson, E.; Mason, S. M.; Dickson, A.; Ryan, K. M.; Kalna, G.; Edwards, J.; Tait, S. W. G.; Blyth, K. MCL-1 Is a Prognostic Indicator and Drug Target in Breast Cancer. *Cell Death Dis.* **2018**, *9* (2), No. 19.
- (16) Winder, M. L.; Campbell, K. J. MCL-1 Is a Clinically Targetable Vulnerability in Breast Cancer. *Cell Cycle* **2022**, *21* (14), 1439–1455.
- (17) Ramsey, H. E.; Fischer, M. A.; Lee, T.; Gorska, A. E.; Arrate, M. P.; Fuller, L.; Boyd, K. L.; Strickland, S. A.; Sensintaffar, J.; Hogdal, L. J.; Ayers, G. D.; Olejniczak, E. T.; Fesik, S. W.; Savona, M. R. A Novel MCL1 Inhibitor Combined with Venetoclax Rescues Venetoclax-Resistant Acute Myelogenous Leukemia. *Cancer Discovery* **2018**, *8* (12), 1566–1581.
- (18) Tausch, E.; Close, W.; Dolnik, A.; Bloehdorn, J.; Chyla, B.; Bullinger, L.; Döhner, H.; Mertens, D.; Stilgenbauer, S. Venetoclax Resistance and Acquired BCL2 Mutations in Chronic Lymphocytic Leukemia. *Haematologica* **2019**, *104* (9), e434–e437.
- (19) Negi, A.; Murphy, P. V. Development of Mcl-1 Inhibitors for Cancer Therapy. *Eur. J. Med. Chem.* **2021**, *210*, No. 113038.
- (20) Wan, Y.; Dai, N.; Tang, Z.; Fang, H. Small-Molecule Mcl-1 Inhibitors: Emerging Anti-Tumor Agents. *Eur. J. Med. Chem.* **2018**, *146*, 471–482.
- (21) Li, K. Interdiction at a Protein-Protein Interface: MCL-1 Inhibitors for Oncology. *Bioorg. Med. Chem. Lett.* **2021**, *32*, No. 127717.
- (22) Hird, A. W.; Tron, A. E. Recent Advances in the Development of Mcl-1 Inhibitors for Cancer Therapy. *Pharmacol. Ther.* **2019**, *198*, 59–67.
- (23) Yuda, J.; Will, C.; Phillips, D. C.; Abraham, L.; Alvey, C.; Avigdor, A.; Buck, W.; Besenhofer, L.; Boghaert, E.; Cheng, D.; Cojocari, D.; Doyle, K.; Hansen, T. M.; Huang, K.; Johnson, E. F.; Judd, A. S.; Judge, R. A.; Kalvass, J. C.; Kunzer, A.; Lam, L. T.; Li, R.; Martin, R. L.; Mastracchio, A.; Mitten, M.; Petrich, A.; Wang, J.; Ward, J. E.; Zhang, H.; Wang, X.; Wolff, J. E.; Bell-McGuinn, K. M.; Souers, A. J. Selective MCL-1 Inhibitor ABBV-467 Is Efficacious in Tumor Models but Is Associated with Cardiac Troponin Increases in Patients. *Commun. Med.* **2023**, *3* (1), No. 154.
- (24) Adams, B. Amid Amgen's Similar Struggles, AstraZeneca Slams the Brakes on MCL-1 Blood Cancer Drug. <https://www.fiercebiotech.com/biotech/amid-amgen-s-similar-struggles-astrazeneca-slams-brakes-mcl-1-blood-cancer-drug>. October 20, 2021.
- (25) Shultz, M. D. Two Decades under the Influence of the Rule of Five and the Changing Properties of Approved Oral Drugs. *J. Med. Chem.* **2019**, *62* (4), 1701–1714.
- (26) Doak, B. C.; Over, B.; Giordanetto, F.; Kihlberg, J. Oral Druggable Space beyond the Rule of 5: Insights from Drugs and Clinical Candidates. *Chem. Biol.* **2014**, *21* (9), 1115–1142.
- (27) Friberg, A.; Vigil, D.; Zhao, B.; Daniels, R. N.; Burke, J. P.; Garcia-Barrantes, P. M.; Camper, D.; Chauder, B. A.; Lee, T.; Olejniczak, E. T.; Fesik, S. W. Discovery of Potent Myeloid Cell Leukemia 1 (Mcl-1) Inhibitors Using Fragment-Based Methods and Structure-Based Design. *J. Med. Chem.* **2013**, *56* (1), 15–30.
- (28) Burke, J. P.; Bian, Z.; Shaw, S.; Zhao, B.; Goodwin, C. M.; Belmar, J.; Browning, C. F.; Vigil, D.; Friberg, A.; Camper, D. V.; Rossanese, O. W.; Lee, T.; Olejniczak, E. T.; Fesik, S. W. Discovery of Tricyclic Indoles That Potently Inhibit Mcl-1 Using Fragment-Based Methods and Structure-Based Design. *J. Med. Chem.* **2015**, *58* (9), 3794–3805.
- (29) Pelz, N. F.; Bian, Z.; Zhao, B.; Shaw, S.; Tarr, J. C.; Belmar, J.; Gregg, C.; Camper, D. V.; Goodwin, C. M.; Arnold, A. L.; Sensintaffar, J. L.; Friberg, A.; Rossanese, O. W.; Lee, T.; Olejniczak, E. T.; Fesik, S. W. Discovery of 2-Indole-Acylsulfonamide Myeloid Cell Leukemia 1 (Mcl-1) Inhibitors Using Fragment-Based Methods. *J. Med. Chem.* **2016**, *59* (5), 2054–2066.
- (30) Szlavik, Z.; Ondi, L.; Csékei, M.; Paczal, A.; Szabó, Z. B.; Radics, G.; Murray, J.; Davidson, J.; Chen, I.; Davis, B.; Hubbard, R. E.; Pedder, C.; Dokurno, P.; Surgenor, A.; Smith, J.; Robertson, A.; LeToumelin-Braizat, G.; Cauquil, N.; Zarka, M.; Demarles, D.; Perron-Sierra, F.; Claperon, A.; Colland, F.; Geneste, O.; Kotschy, A. Structure-Guided Discovery of a Selective Mcl-1 Inhibitor with Cellular Activity. *J. Med. Chem.* **2019**, *62* (15), 6913–6924.
- (31) Kotschy, A.; Szlavik, Z.; Murray, J.; Davidson, J.; Maragno, A. L.; LeToumelin-Braizat, G.; Chanrion, M.; Kelly, G. L.; Gong, J.-N.; Moujalled, D. M.; Bruno, A.; Csekei, M.; Paczal, A.; Szabo, Z. B.; Sipos, S.; Radics, G.; Prosznyak, A.; Balint, B.; Ondi, L.; Blasko, G.; Robertson, A.; Surgenor, A.; Dokurno, P.; Chen, I.; Matassova, N.; Smith, J.; Pedder, C.; Graham, C.; Studeny, A.; Lysiak-Auvity, G.; Girard, A.-M.; Gragé, F.; Segal, D.; Riffkin, C. D.; Pomilio, G.; Galbraith, L. C. A.; Aubrey, B. J.; Brennan, M. S.; Herold, M. J.; Chang, C.; Guasconi, G.; Cauquil, N.; Melchiorre, F.; Guigal-Stephan, N.; Lockhart, B.; Colland, F.; Hickman, J. A.; Roberts, A. W.; Huang, D. C. S.; Wei, A. H.; Strasser, A.; Lessene, G.; Geneste, O. The MCL1 Inhibitor S63845 Is Tolerable and Effective in Diverse Cancer Models. *Nature* **2016**, *538* (7626), 477–482.
- (32) Szlavik, Z.; Csekei, M.; Paczal, A.; Szabo, Z. B.; Sipos, S.; Radics, G.; Prosznyak, A.; Balint, B.; Murray, J.; Davidson, J.; Chen, I.; Dokurno, P.; Surgenor, A. E.; Daniels, Z. M.; Hubbard, R. E.; LeToumelin-Braizat, G.; Claperon, A.; Lysiak-Auvity, G.; Girard, A.-M.; Bruno, A.; Chanrion, M.; Colland, F.; Maragno, A.-L.; Demarles, D.; Geneste, O.; Kotschy, A. Discovery of S64315, a Potent and Selective Mcl-1 Inhibitor. *J. Med. Chem.* **2020**, *63* (22), 13762–13795.
- (33) Braje, W.; Doherty, G.; Jantos, K.; Ji, C.; Judd, A.; Kunzer, A.; Mastracchio, A.; Song, X.; Souers, A.; Sullivan, G.; Tao, Z.-F.; Teske, J.; Wang, X.; Wendt, M.; Penning, T.; Lai, C.; Kling, A.; Pohlki, F. Macrocyclic Mcl-1 Inhibitors and Methods of Use. WO2019/035911, February 21, 2019.
- (34) Tron, A. E.; Belmonte, M. A.; Adam, A.; Aquila, B. M.; Boise, L. H.; Chiarpin, E.; Cidado, J.; Embrey, K. J.; Gangl, E.; Gibbons, F. D.; Gregory, G. P.; Hargreaves, D.; Hendricks, J. A.; Johannes, J. W.; Johnstone, R. W.; Kazmirski, S. L.; Kettle, J. G.; Lamb, M. L.; Matulis, S. M.; Nooka, A. K.; Packer, M. J.; Peng, B.; Rawlins, P. B.; Robbins, D. W.; Schuller, A. G.; Su, N.; Yang, W.; Ye, Q.; Zheng, X.; Secrist, J. P.; Clark, E. A.; Wilson, D. M.; Fawell, S. E.; Hird, A. W. Discovery of Mcl-1-Specific Inhibitor AZD5991 and Preclinical Activity in Multiple Myeloma and Acute Myeloid Leukemia. *Nat. Commun.* **2018**, *9* (1), No. 5341.
- (35) Caenepeel, S.; Brown, S. P.; Belmontes, B.; Moody, G.; Keegan, K. S.; Chui, D.; Whittington, D. A.; Huang, X.; Poppe, L.; Cheng, A. C.; Cardozo, M.; Houze, J.; Li, Y.; Lucas, B.; Paras, N. A.; Wang, X.; Taygerly, J. P.; Vimolratana, M.; Zancanella, M.; Zhu, L.; Cajulis, E.

- Osgood, T.; Sun, J.; Damon, L.; Egan, R. K.; Greninger, P.; McClanaghan, J. D.; Gong, J.; Moujalled, D.; Pomilio, G.; Beltran, P.; Benes, C. H.; Roberts, A. W.; Huang, D. C.; Wei, A.; Canon, J.; Coxon, A.; Hughes, P. E. AMG 176, a Selective MCL1 Inhibitor, Is Effective in Hematologic Cancer Models Alone and in Combination with Established Therapies. *Cancer Discovery* **2018**, *8* (12), 1582–1597.
- (36) Caenepeel, S.; Karen, R.; Belmontes, B.; Verlinsky, A.; Tan, H.; Yang, Y.; Chen, X.; Li, K.; Allen, J.; Wahlstrom, J.; Canon, J.; Coxon, A.; Hughes, P. Discovery and Preclinical Evaluation of AMG 397, a Potent, Selective and Orally Bioavailable MCL1 Inhibitor [Abstract]. In *Proceedings of the Annual Meeting of the American Association for Cancer Research 2020*; AACR: Philadelphia (PA), 2020 DOI: 10.1158/1538-7445.AM2020-6218.
- (37) Chu, H.; Guerrero, J. A.; Hurtle, Anna, E.; Jiang, L.; Kato, D.; Kobayashi, T.; Lin, D. W.; Medley, J. W.; Naduthambi, D.; Tsui, V. H.; Venkataramani, C.; Watkins, W. J.; Yang, H.; Zhu, Q. Mcl-1 Inhibitors. WO2021/096860 A1, May 20, 2021.
- (38) Zhuo, J.; Combs, A. P. Spiro-Sulfonimidamide Derivatives as Inhibitors Of Myeloid Cell Leukemia-1 (MCL-1) Protein. WO2021/211922 A1, October 21, 2021.
- (39) Johannes, J. W.; Bates, S.; Beigie, C.; Belmonte, M. A.; Breen, J.; Cao, S.; Centrella, P. A.; Clark, M. A.; Cuozzo, J. W.; Dumelin, C. E.; Ferguson, A. D.; Habeshian, S.; Hargreaves, D.; Joubbran, C.; Kazmirski, S.; Keefe, A. D.; Lamb, M. L.; Lan, H.; Li, Y.; Ma, H.; Mlynarski, S.; Packer, M. J.; Rawlins, P. B.; Robbins, D. W.; Shen, H.; Sigel, E. A.; Soutter, H. H.; Su, N.; Troast, D. M.; Wang, H.; Wickson, K. F.; Wu, C.; Zhang, Y.; Zhao, Q.; Zheng, X.; Hird, A. W. Structure Based Design of Non-Natural Peptidic Macrocyclic Mcl-1 Inhibitors. *ACS Med. Chem. Lett.* **2017**, *8* (2), 239–244.
- (40) Demin, S.; Peschiulli, A.; Velter, A. I.; Vos, A.; Boeck, B. D.; Miller, B.; Rombouts, F. J. R.; Reuillon, T.; Lento, W.; Blanco, M. D.; Jouffroy, M.; Steyvers, H.; Bekkers, M.; Altrocchi, C.; Pietrak, B.; Koo, S. J.; Szweczk, L.; Attar, R.; Philipp, U. Macrocyclic Carbon-Linked Pyrazoles As Novel Inhibitors of MCL-1. *ACS Med. Chem. Lett.* **2023**, *14* (7), 955–961.
- (41) Rombouts, F. In Pursuit of MCL-1 Inhibitors with Improved Therapeutic Window for the Treatment of Hematological Malignancies: Discovery of JNJ-4355 [Abstract]. In *Proceedings of the American Association for Cancer Research Annual Meeting*; AACR: Philadelphia (PA), 2022 DOI: 10.1158/1538-7445.AM2022-2133.
- (42) Romanov-Michailidis, F.; Hsiao, C.-C.; Urner, L. M.; Jerhaoui, S.; Surkyn, M.; Miller, B.; Vos, A.; Dominguez Blanco, M.; Bueters, R.; Vinken, P.; Bekkers, M.; Walker, D.; Pietrak, B.; Eyckmans, W.; Dore-Sousa, J. L.; Joo Koo, S.; Lento, W.; Bauser, M.; Philipp, U.; Rombouts, F. J. R. Discovery of an Oral, Beyond-Rule-of-Five Mcl-1 Protein–Protein Interaction Modulator with the Potential of Treating Hematological Malignancies. *J. Med. Chem.* **2023**, *66* (9), 6122–6148.
- (43) Abdelraheem, E. M. M.; Shaabani, S.; Dömling, A. Macrocycles: MCR Synthesis and Applications in Drug Discovery. *Drug Discovery Today Technol.* **2018**, *29*, 11–17.
- (44) Amrhein, J. A.; Knapp, S.; Hanke, T. Synthetic Opportunities and Challenges for Macrocyclic Kinase Inhibitors. *J. Med. Chem.* **2021**, *64* (12), 7991–8009.
- (45) Peterson, A. A.; Liu, D. R. Small-Molecule Discovery through DNA-Encoded Libraries. *Nat. Rev. Drug Discovery* **2023**, *22*, 699–722.
- (46) Goodnow, R. A.; Dumelin, C. E.; Keefe, A. D. DNA-Encoded Chemistry: Enabling the Deeper Sampling of Chemical Space. *Nat. Rev. Drug Discovery* **2017**, *16* (2), 131–147.
- (47) Connors, W. H.; Hale, S. P.; Terrett, N. K. DNA-Encoded Chemical Libraries of Macrocycles. *Curr. Opin. Chem. Biol.* **2015**, *26*, 42–47.
- (48) Röhm, S.; Berger, B.-T.; Schröder, M.; Chaikuad, A.; Winkel, R.; Hekking, K. F. W.; Benninghof, J. J. C.; Müller, G.; Tesch, R.; Kudolo, M.; Forster, M.; Laufer, S.; Knapp, S. Fast Iterative Synthetic Approach toward Identification of Novel Highly Selective P38 MAP Kinase Inhibitors. *J. Med. Chem.* **2019**, *62* (23), 10757–10782.
- (49) Veerman, J. J. N.; Bruseker, Y. B.; Damen, E.; Heijne, E. H.; van Bruggen, W.; Hekking, K. F. W.; Winkel, R.; Hupp, C. D.; Keefe, A. D.; Liu, J.; Thomson, H. A.; Zhang, Y.; Cuozzo, J. W.; McRiner, A. J.; Mulvihill, M. J.; van Rijnsbergen, P.; Zech, B.; Renzetti, L. M.; Babiss, L.; Müller, G. Discovery of 2,4–1H-Imidazole Carboxamides as Potent and Selective TAK1 Inhibitors. *ACS Med. Chem. Lett.* **2021**, *12* (4), 555–562.
- (50) Al Toma, R. S.; Brieke, C.; Cryle, M. J.; Süßmuth, R. D. Structural Aspects of Phenylglycines, Their Biosynthesis and Occurrence in Peptide Natural Products. *Nat. Prod. Rep.* **2015**, *32* (8), 1207–1235.
- (51) Liang, C.; Behnam, M. A. M.; Sundermann, T. R.; Klein, C. D. Phenylglycine Racemization in Fmoc-Based Solid-Phase Peptide Synthesis: Stereochemical Stability Is Achieved by Choice of Reaction Conditions. *Tetrahedron Lett.* **2017**, *58* (24), 2325–2329.
- (52) Rezaei Araghi, R.; Bird, G. H.; Ryan, J. A.; Jenson, J. M.; Godes, M.; Pritz, J. R.; Grant, R. A.; Letai, A.; Walensky, L. D.; Keating, A. E. Iterative Optimization Yields Mcl-1–Targeting Stapled Peptides with Selective Cytotoxicity to Mcl-1–Dependent Cancer Cells. *Proc. Natl. Acad. Sci. U.S.A.* **2018**, *115* (5), E886–E895.
- (53) Stewart, M. L.; Fire, E.; Keating, A. E.; Walensky, L. D. The MCL-1 BH3 Helix Is an Exclusive MCL-1 Inhibitor and Apoptosis Sensitizer. *Nat. Chem. Biol.* **2010**, *6* (8), 595–601.
- (54) Garcia Jimenez, D.; Poongavanam, V.; Kihlberg, J. Macrocycles in Drug Discovery—Learning from the Past for the Future. *J. Med. Chem.* **2023**, *66* (8), 5377–5396.
- (55) Sander, T.; Freyss, J.; von Korff, M.; Rufener, C. DataWarrior: An Open-Source Program For Chemistry Aware Data Visualization And Analysis. *J. Chem. Inf. Model.* **2015**, *55* (2), 460–473.
- (56) Fang, C.; D'Souza, B.; Thompson, C. F.; Clifton, M. C.; Fairman, J. W.; Fulroth, B.; Leed, A.; McCarren, P.; Wang, L.; Wang, Y.; Feau, C.; Kaushik, V. K.; Palmer, M.; Wei, G.; Golub, T. R.; Hubbard, B. K.; Serrano-Wu, M. H. Single Diastereomer of a Macrolactam Core Binds Specifically to Myeloid Cell Leukemia 1 (MCL1). *ACS Med. Chem. Lett.* **2014**, *5* (12), 1308–1312.
- (57) Vonnrhein, C.; Flensburg, C.; Keller, P.; Sharff, A.; Smart, O.; Paciorek, W.; Womack, T.; Bricogne, G. Data Processing and Analysis with the AutoPROC Toolbox. *Acta Crystallogr., Sect. D: Biol. Crystallogr.* **2011**, *67* (4), 293–302.